27 November 2011

A Journey in Electrocatalysis *for* Green Energy

Aulice Scibioh Maria Joseph

NCSU, USA

A Few Challenging Avenues in Energy, Electrocatalysis, Materials…

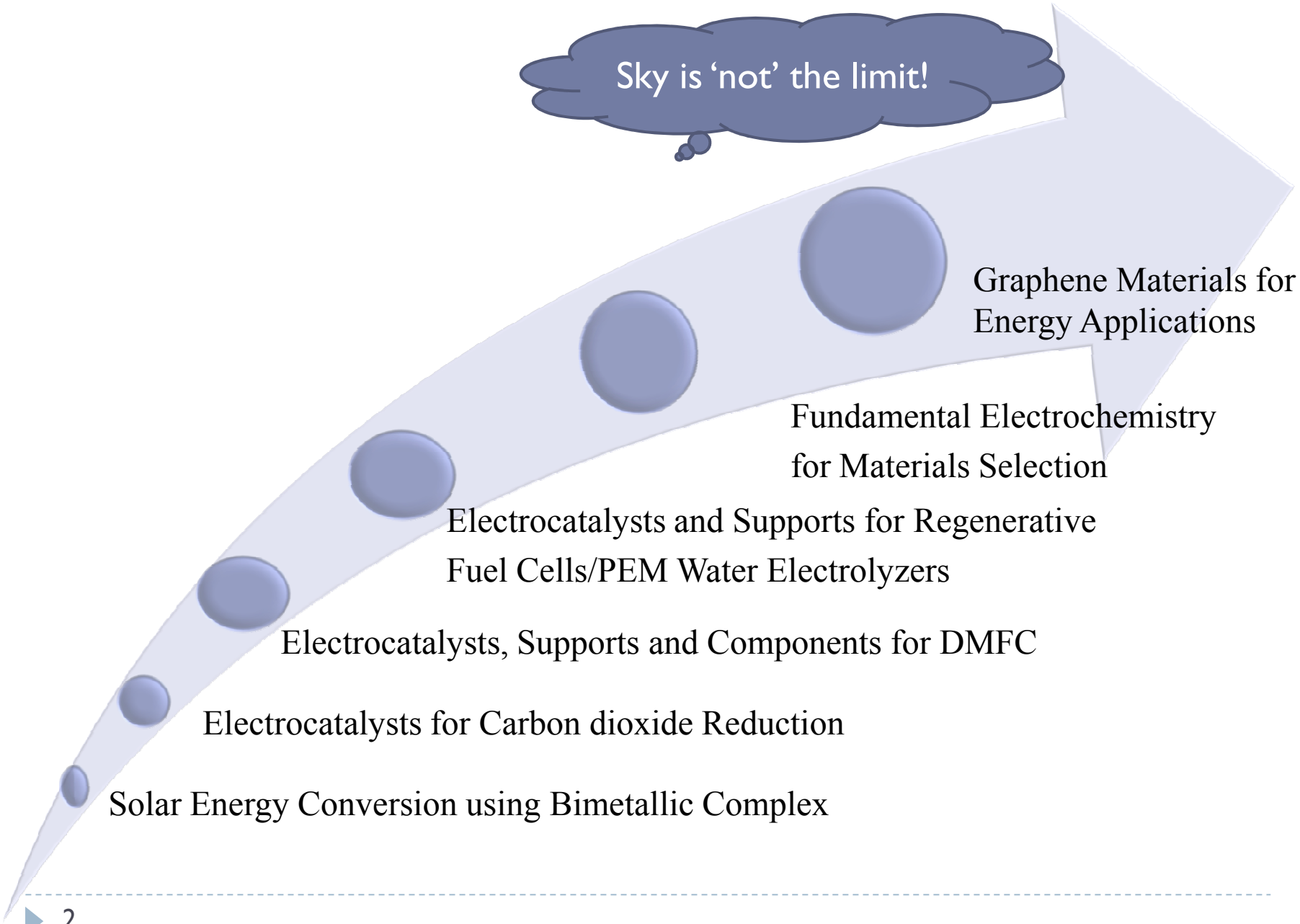

Energy Outlook

- **Energy is an important societal issue.**
  It impacts our way of life, economy, national security, environment & health
- **Energy production can not keep up with our energy needs**
- **Energy is the greatest challenge facing the mankind in 21st century**

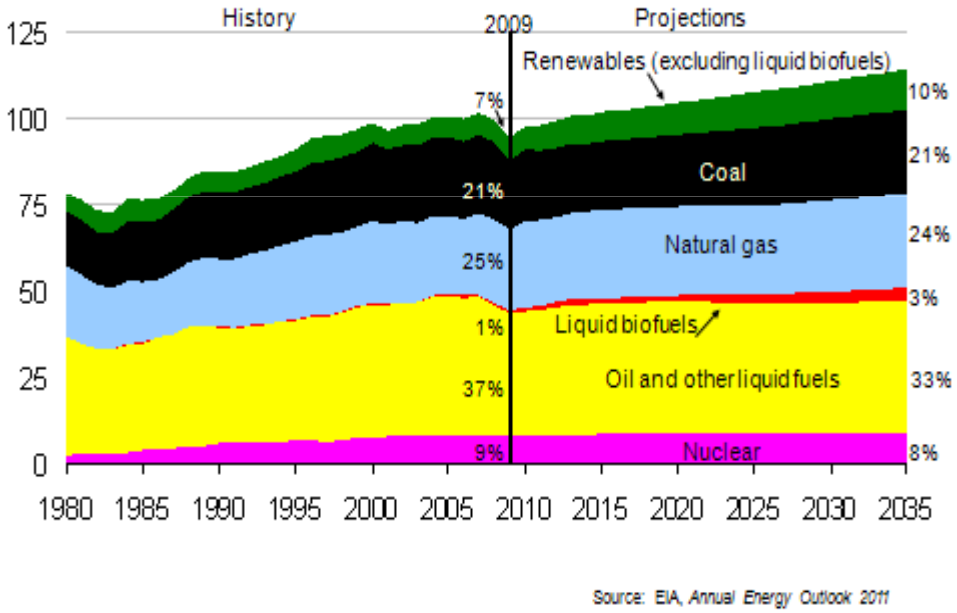

Source: EIA, *Annual Energy Outlook 2011*

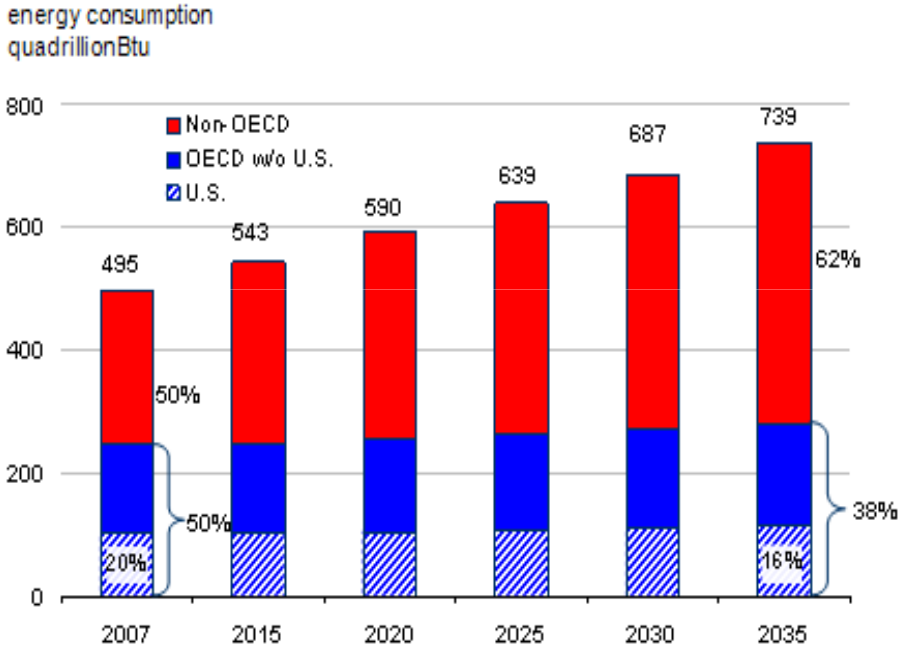

Source: EIA, *International Energy Outlook 2010*

Renewables grow rapidly, still fossil fuels provide 78% for energy use in 2035.

Non-OECD countries account for nearly 50% increase in global energy use by in 2035.

Energy *Vs* Emission

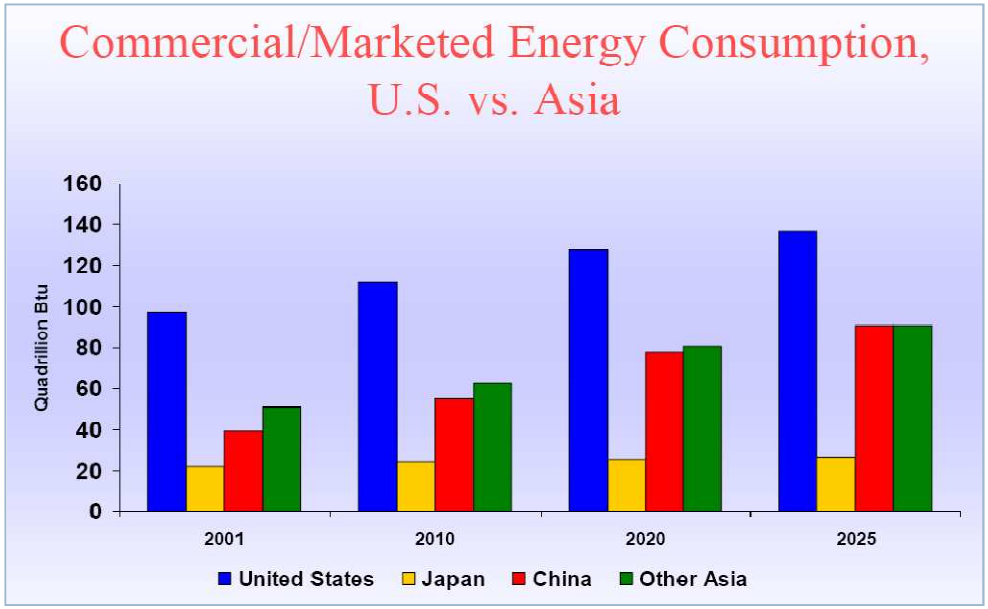

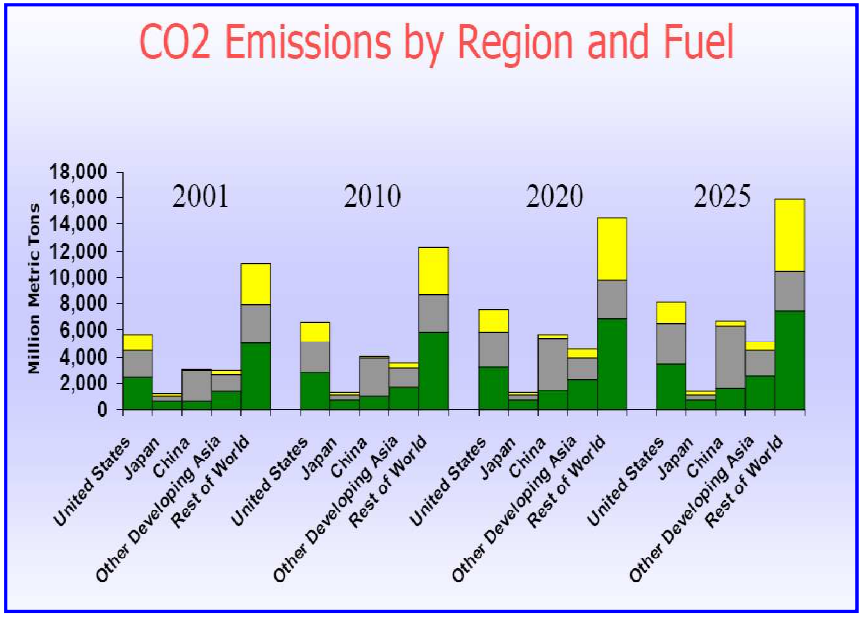

World population, energy & electricity demands are ever increasing and are directly related to emission levels

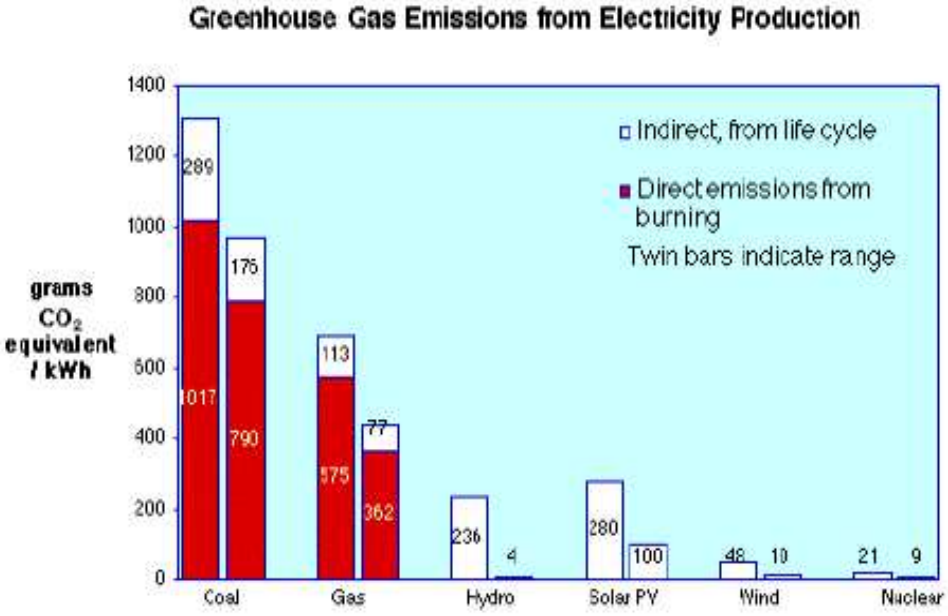

Carbon Cycle

Movement of carbon in its many forms, between the biosphere, atmosphere, oceans & geo-sphere

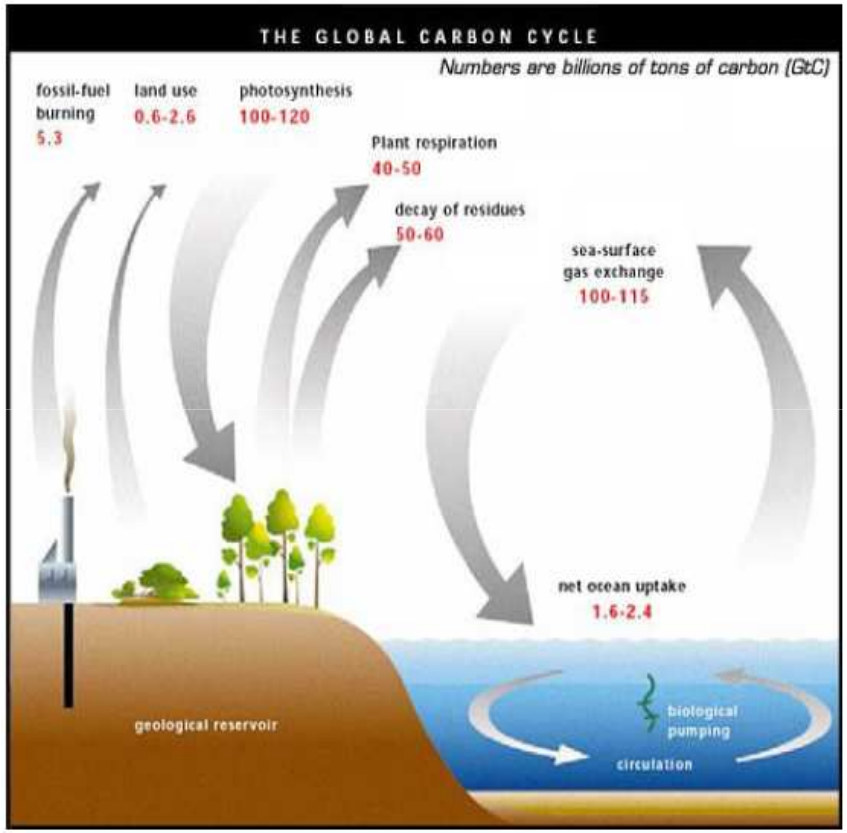

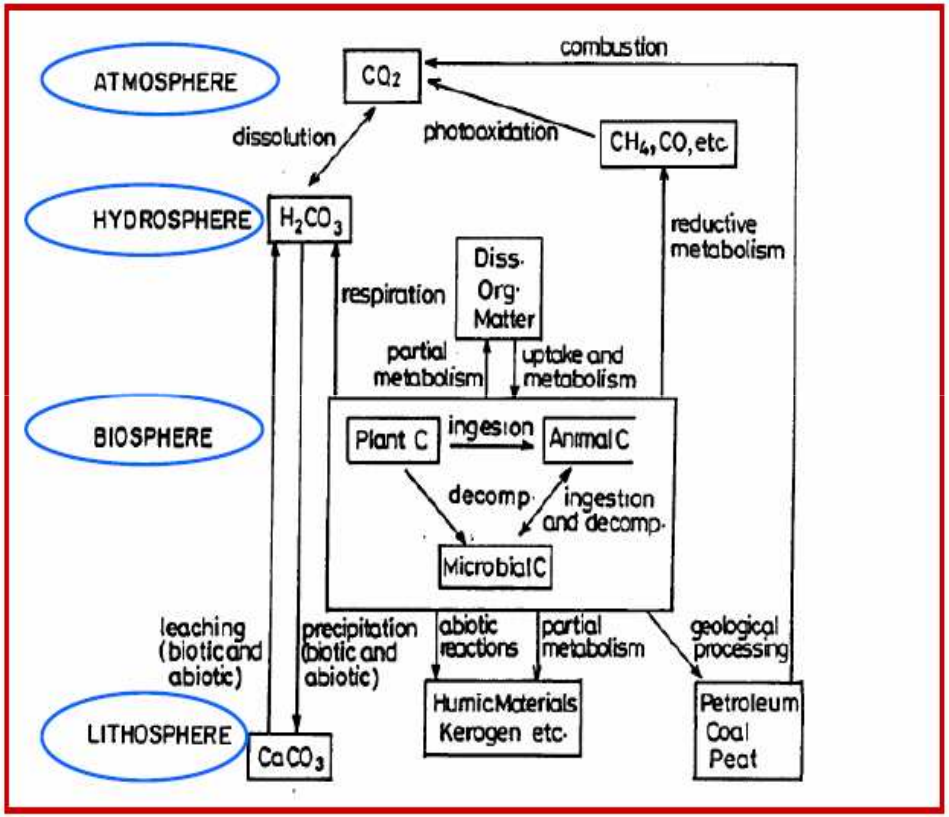

Natural flux of carbon would be imbalanced by anthropogenic additions from fossilized matters

Part 1. Solar Energy Conversion using Bimetallic Complex

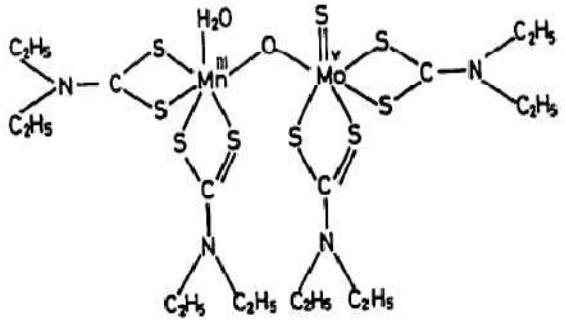

Fig.1:Structure of $[MnMoO_2(Et_2dtc)_4(H_2O)]$

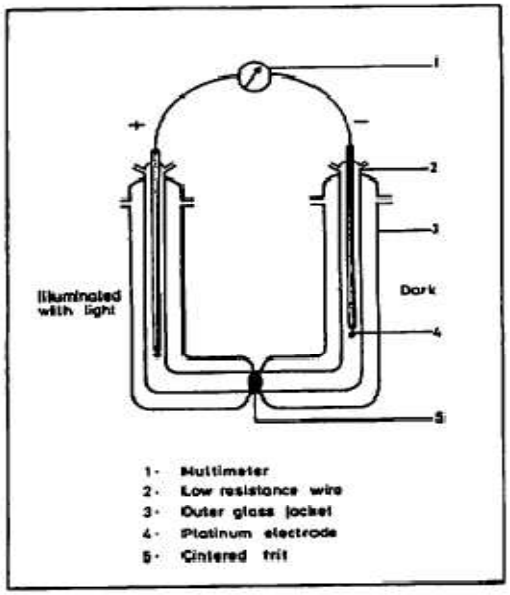

Fig.2: Honda Cell

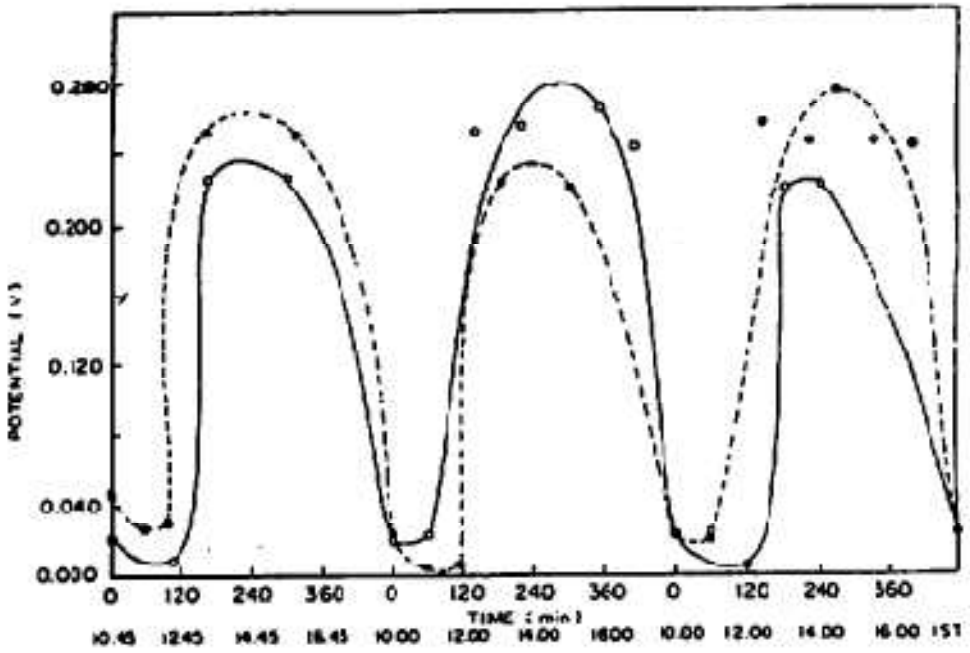

Fig.3:Photogalvanic behaviour of $[MnMoO_2(Et_2dtc)_4(H_2O)]$ *in DMF -* H_2O *(4:1 v/v)in sunlight (with-, without---- benzophenone*

Potential: 0.243 V/SCE; Current: 7.0 µA

Scibioh et al., Bull of Electrochemistry, 14(4-5), (1998), 164-167.

Solar Energy Conversion using Bimetallic Complex

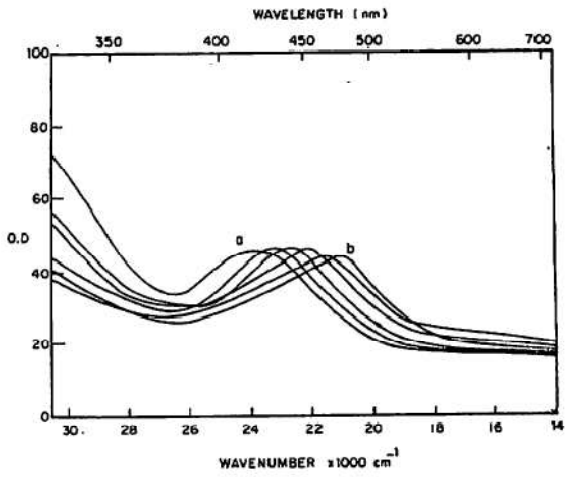

Fig.4:Visible spectrum of $[MnMoO_2(Et_2dtc)_4(H_2O)]$in DMF (a) Before Irradiation b. After Irradiation [The shift in λ_{max} during irradiation to sunlight for each one hour is recorded

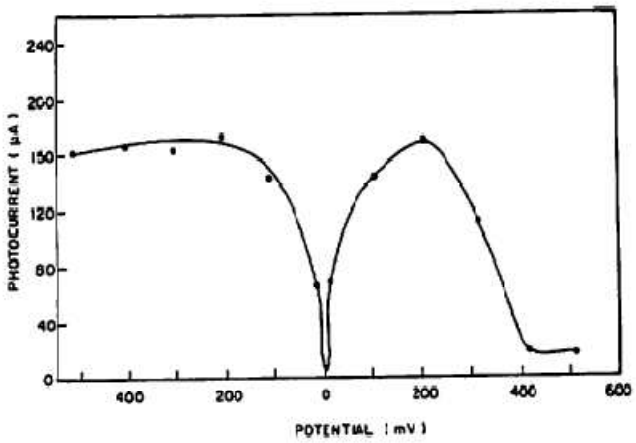

Fig.5:Applied potential vs photocurrent of $[MnMoO_2(Et_2dtc)_4(H_2O)]$in DMF in the presence of sunlight

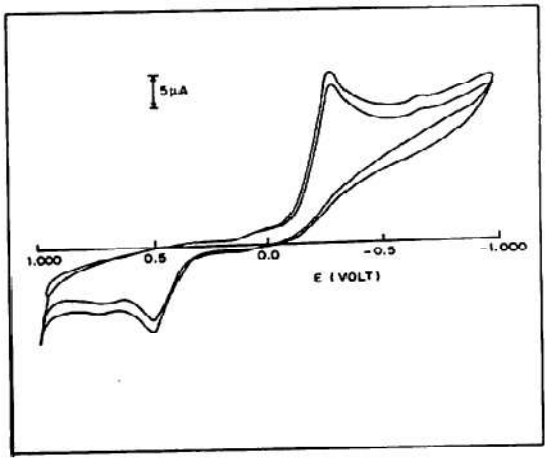

Fig.6:Cyclic voltammogram of $[MnMoO_2(Et_2dtc)_4(H_2O)]$ (1.0 mmol dm^{-3}) in 0.1 mol dm^{-3}TEAB in DMF at pt working electrode. scan rate = 100 mV s^{-1}

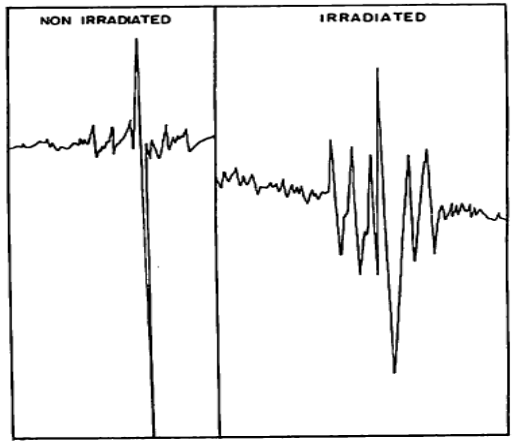

Fig.7:Electron paramagnetic resonance spectrum of $[MnMoO_2(Et_2dtc)_4(H_2O)]$ in DMF

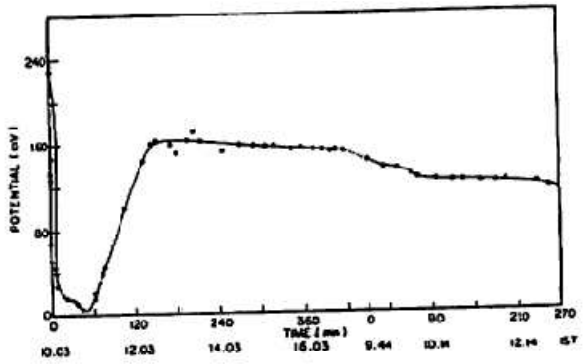

Fig.8:Photogalvanic behaviour of $[Mo_2O_3(Et_2dtc)_4]$ in DMF in sunlight

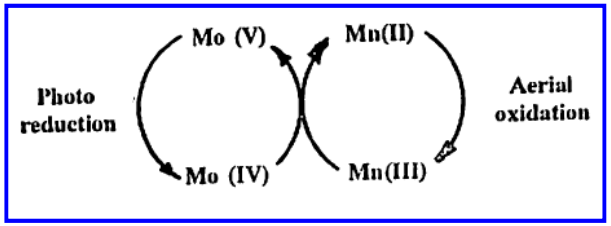

Scibioh et al., Bull of Electrochemistry, 14(4-5), (1998), 164-167.

Part 2. Development of Suitable Electrocatalysts for Reduction of CO_2

RELEVANCE & IMPORTANCE

CO_2 - Problem Matter or Inexpensive Raw Material?

Global Warming - Green House Gas

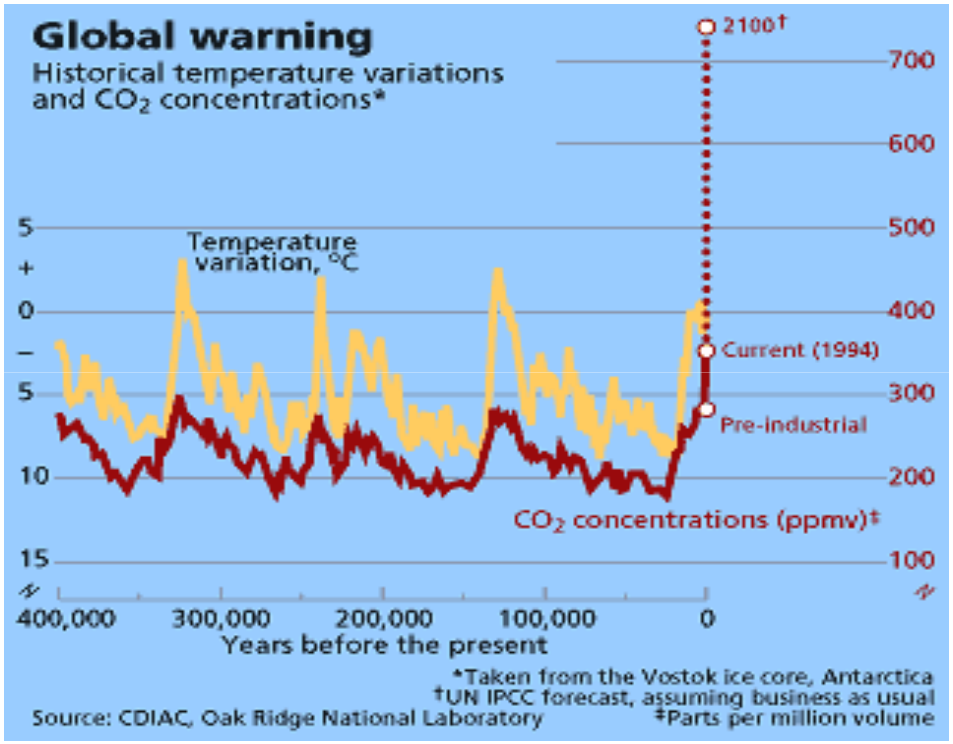

Raw Material in Chemical Processes

Fossil raw materials
Mineral Oil, Natural gas, Coal

3

↓

Basic products & Intermediates
CO, methanol, Arenes, Ethylene dioxide, Acrylic acid etc.,

300

↓

End products
Plastics, Pharmaceuticals, Fertilizers etc.,

30000

Small amount of anthropogenic additions exhibit a large effect on climate change

M. A. Scibioh & B. Viswanathan, Proc. Indn. Natl. Acad. Sci., 70 A (3), (2004) 407-462.

Comparison of the properties of various C_1 building blocks

Factors	CO	$COCl_2$	CO_2
MAK Value	30 ppm	0.1 ppm	5000 ppm
Toxicology	Affinity for Hemoglobin 210 times that of O_2	War gas	Danger of asphyxiation at 10 vol % in air
Environmental Hazard	Yes	High	Negative
Flammability	12 – 74 vol %	No	No
Boiling point	81 K	291 K	195 K (subl)
Storage	Only at < 3.5 Mpa	Very difficult	No problem
Transport	Gas bottles or tanks kg quantities	Possible	Gas bottles or tanks

M. A. Scibioh & B. Viswanathan, Proc. Indn. Natl. Acad. Sci., 70 A (3), (2004) 407-462.

Attempts at CO_2 reduction

- **Radiochemical**

$$CO_2 \xrightarrow{\gamma\text{-radiation}} HCOOH, HCHO$$

- **Chemical reduction**

$$2Mg + CO_2 \rightarrow 2MgO + C$$

$$Sn + 2CO_2 \rightarrow SnO_2 + 2CO$$

$$2Na + 2CO_2 \rightarrow Na_2C_2O_4$$

- **Thermo chemical**

$$CO_2 \xrightarrow{Ce4+} CO + \tfrac{1}{2}O_2$$

- **Photo chemical**

$$CO_2 \xrightarrow[T>900°C]{h\nu} CO, HCHO, HCOOH$$

- **Electrochemical**

$$CO_2 + xe^- + xH^+ \xrightarrow{eV} CO, HCOOH, (COOH)_2$$

- **Biochemical**

$$CO_2 + 4H_2 \xrightarrow{bacteria} CH_4 + 2H_2O$$

- **Biophotochemical**

$$CO_2 + \text{oxoglutaric acid} \xrightarrow{h\nu} \text{isocitric acid}$$

- **Photo electrochemical**

$$CO_2 + 2e^- + 2H^+ \xrightarrow{h\nu} CO + H_2O$$

- **Bioelectrochemical**

$$CO_2 + \text{oxoglutaric acid} \xrightarrow[eV, \text{ semicond}]{\text{enzyme}} \text{isocitric acid}$$

- **Biophotoelectrochemical**

$$CO_2 \xrightarrow[eV, \text{ methylviologen}]{h\nu.\ \text{enzyme, p-1nP}} HCOOH$$

M. A. Scibioh & B. Viswanathan, Proc. Indn. Natl. Acad. Sci., 70 A (3), (2004) 407-462.

Electrocatalytic Reduction of CO_2 – Why & How?

- Reducing atmospheric **CO_2** concentration

  (***A global environmental concern - Green house effect***)

- **Electrochemical approach** is already effective proven one (***energy-economic pathway***) – to minimize CO_2 concentration & conversion to valuable energy sources such as fuels or chemicals
- This subject has got **direct industrial relevance**. It deals with product formation such as HCHO, HCOOH, CH_3OH, CH_4 and other organic compounds that have assumed commercial importance & relevance

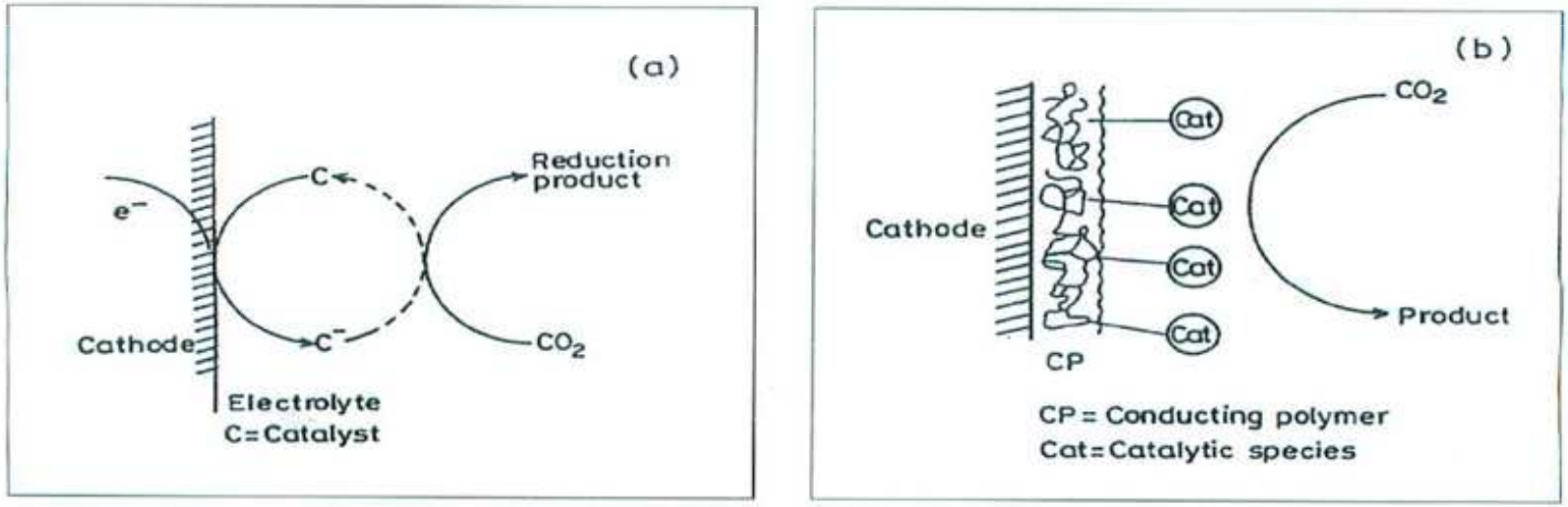

(a) Molecular electrocatalysts in solution; (b) Cathodic materials modified by surface deposition of molecular electrocatalysts

M. A. Scibioh & B. Viswanathan, Proc. Indn. Natl. Acad. Sci., 70 A (3), (2004) 407-462.

Electrochemical Reduction of CO_2

$CO_2/CO_2^{\cdot-}$ redox potential is -2.21V /(SCE)

$CO_2 + 2H^+ + 2e^- \rightarrow CO + H_2O$	$E^{\circ\prime} = -0.52$ V
$CO_2 + 2H^+ + 2e^- \rightarrow HCOOH$	$E^{\circ\prime} = -0.61$ V
$CO_2 + 4H^+ + 4e^- \rightarrow HCHO + H_2O$	$E^{\circ\prime} = -0.48$ V
$CO_2 + 6H^+ + 6e^- \rightarrow CH_3OH + H_2O$	$E^{\circ\prime} = -0.38$ V
$CO_2 + 8H^+ + 8e^- \rightarrow CH_4 + 2H_2O$	$E^{\circ\prime} = -0.24$ V

Influence of the Solvent and Electrode on the Reaction Mechanism

Reaction	Cathode	Solution
$CO_2 + e^- \rightarrow CO_2^{\cdot-}$	All	All
$CO_2^{\cdot-} + H^+ + e^- \rightarrow HCOO^-$	In, Pb, Hg	H_2O
$CO_2^{\cdot-} \rightarrow CO + O^-$		
$CO + O^- + H^+ + e^- \rightarrow CO + OH^-$	Zn, Au, Ag	H_2O
$CO_2^{\cdot-} + CO_2^{\cdot-} \rightarrow (COO)_2^{2-}$	Pb, Tl, Hg	Non-aqueous
$CO_2^{\cdot-} + CO_2 + e^- \rightarrow CO + CO_3^{2-}$	In, Zn, Sn, Au	Non-aqueous

M. A. Scibioh & B. Viswanathan
Proc. Indn. Natl. Acad. Sci., 70 A (3), 2004.

Reduction of CO_2 under Protic, Aprotic & Partially aprotic conditions

Protic

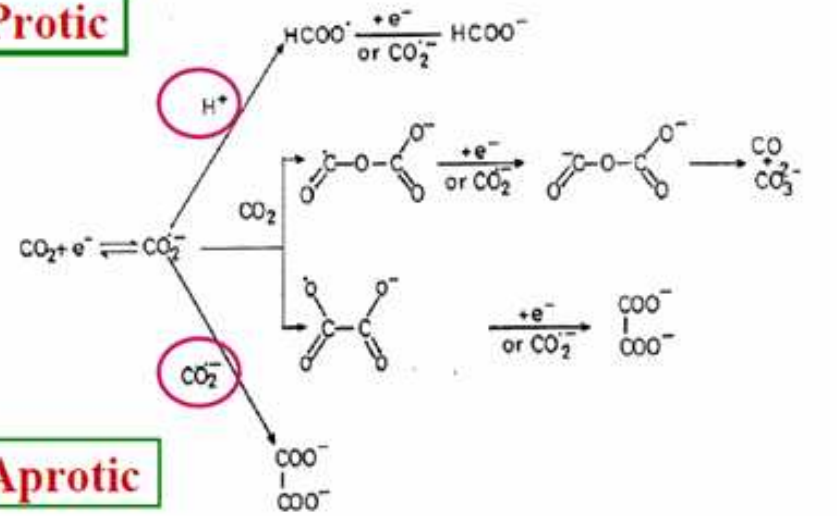

Aprotic

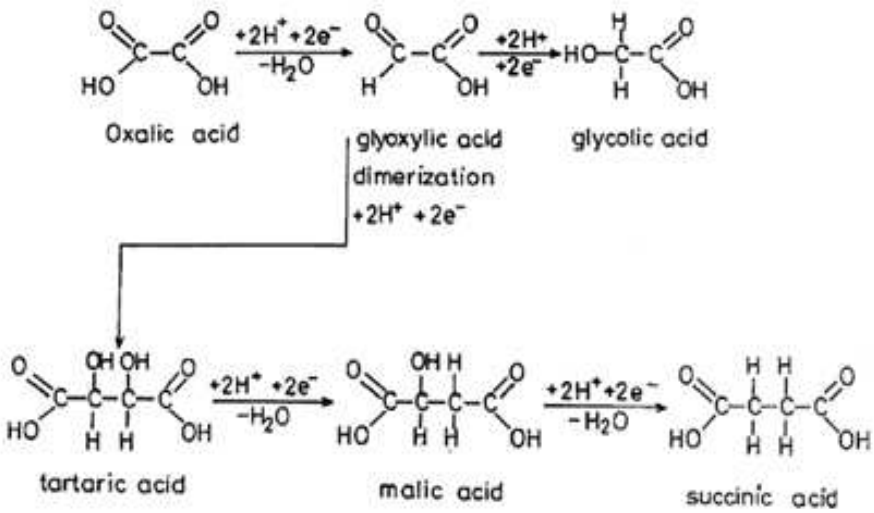

Partially Aprotic

Aq. solutions leads to formic acid production (C_1 products)
Aprotic solvents favor dimerization of CO_2 leading to C_n products

M. A. Scibioh & B. Viswanathan
Proc. Indn. Natl. Acad. Sci., 70 A (3), 2004.

Periodic table for CO_2 reduction products

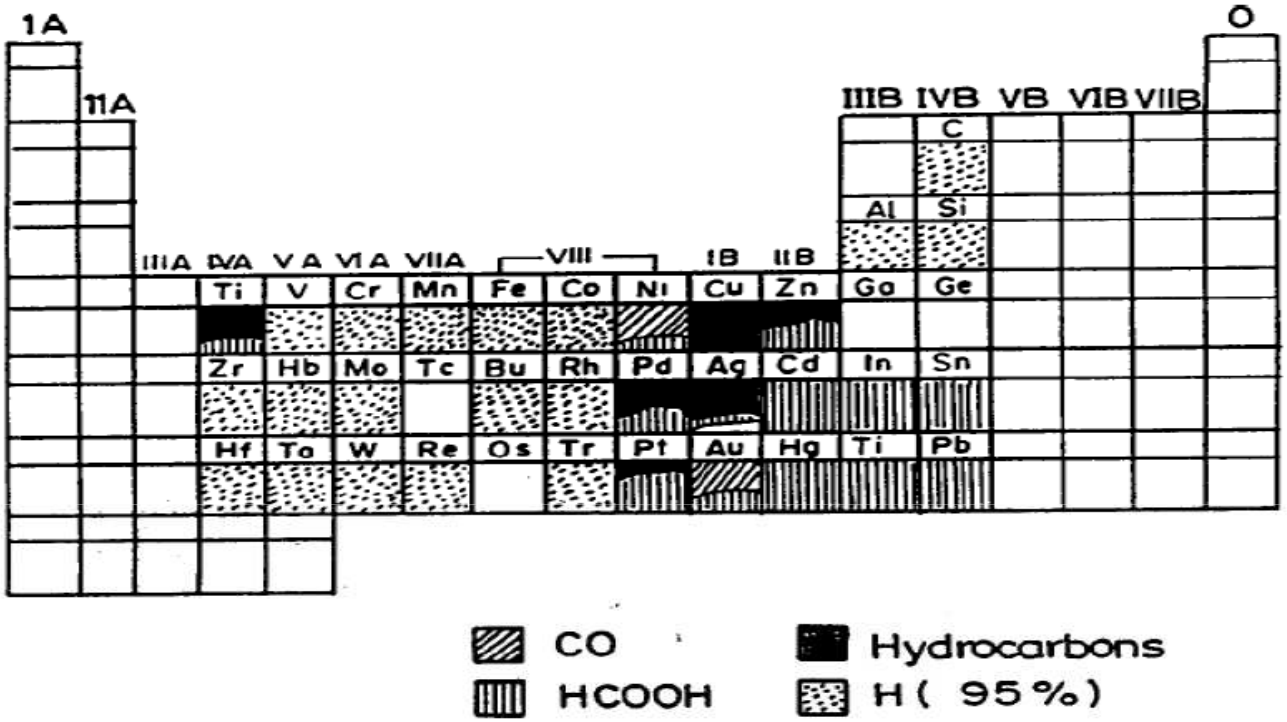

At –2.2 V /SCE in low temperature, 0.05 M $KHCO_3$ solution

Y Hori et al.,
J Chem Soc Chem Commun (1987) 728

Summary of Metal Cathodes Employed for Electroreduction of CO_2

Metals	Products	
	Aqueous medium	Non-aqueous medium
	sp group metals	
Cu, Zn, Sn	HCOOH	-
In, C, Si, Sn, Pb, Bi, Cu, Zn, Cd, Hg	HCOOH, CO, hydrocarbon	-
In, Sn, Pb, Cu, Au, Zn, Cd	-	Hydrocarbon, CO, CO_3^{2-}
In, Sn, Au, Hg	-	CO
In, Tl, Sn, Pd, Pd, Zn, Hg	-	Oxalic acid
	d group metals	
Ni, Pt	-	CO, CO_3^{2-}
Ni, Pd, Rh, Ir	HCOOH, CO	-
Fe, Ru, Ni, Pd, Pt	Hydrocarbon	-
Ti, Nb, Cr, Mo, Fe, Pd	-	Oxalic acid
Mo, W, Ru, Os, Pd, Pt	MeOH	-
Zr, Cr, Mn, Fe, Co, Rh, Ir	CO	-

M. A. Scibioh & B. Viswanathan
Proc. Indn. Natl. Acad. Sci., 70 A (3), 2004.

CO_2 electroreduction on sp group metal electrodes

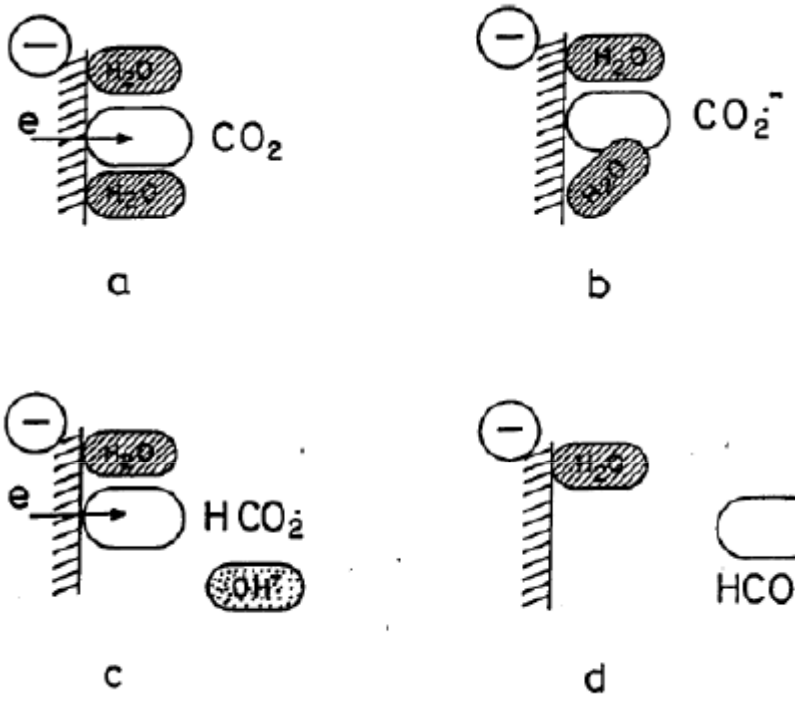

Influence of Pressure on Mechanism – An Example

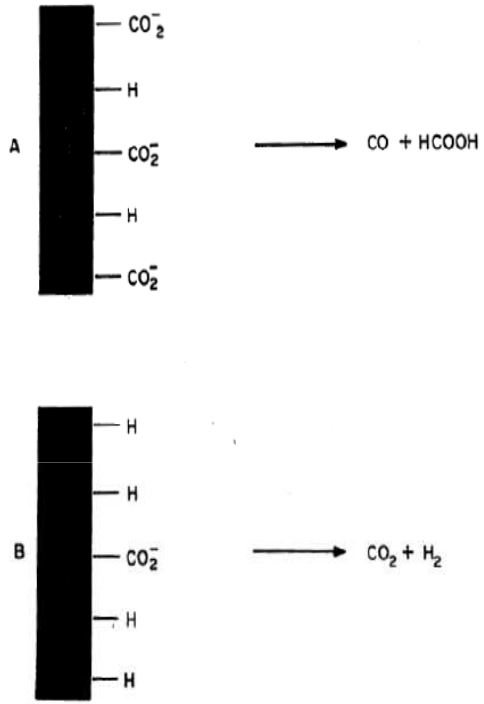

Comparative mechanism of high-pressure CO_2 electroreduction (A) & Electroreduction of CO_2 at atmospheric pressure (B) on Ni cathode

M. Jitaru
J. Appl. Elec.Chem 27 (1997) 875

Electrocatalytic Reduction of CO_2 by Ni (II) Macrocycles at HMDE

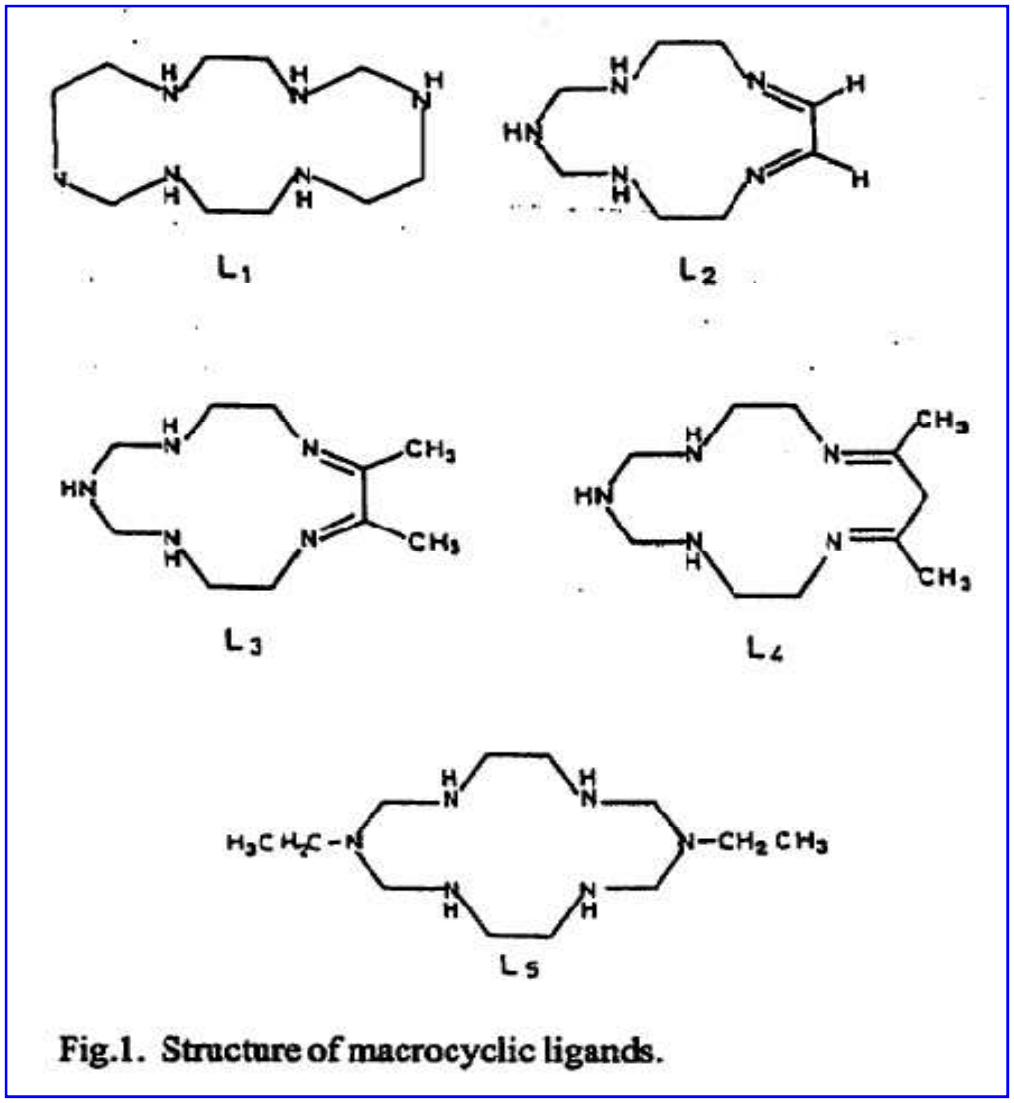

Fig.1. Structure of macrocyclic ligands.

1. **Synthesis**
2. **Characterization**
- Elemental Analysis
- UV – Visible
- IR
- ^{1}H NMR
3. **Electrochemical Study**
(At HMDE)
- CV, CPE

Influence of:

- Macrocyclic Ring Size
- Substituent
- Solvent
- Supporting Electrolyte
- pH

4. **Product Analysis**
- GC & Chemical Analysis

5. **Mechanism**

In-situ, Spectro-electrochemical
- UV-Vis, EPR

M. A. Scibioh, PhD Thesis, University of Madras, India, 1998.

An Example

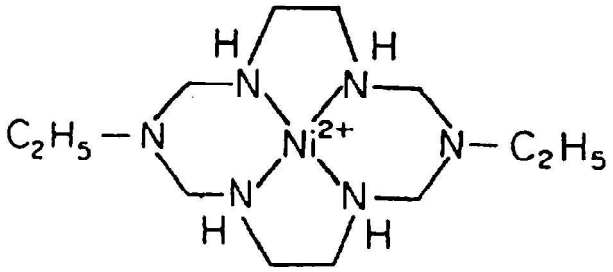

Fig. 1: Structure of [Ni(L)] $(ClO_4)_2$
where L = 1,8-diethyl-1,3,6,8,10,13-hexaazacyclotetradecane

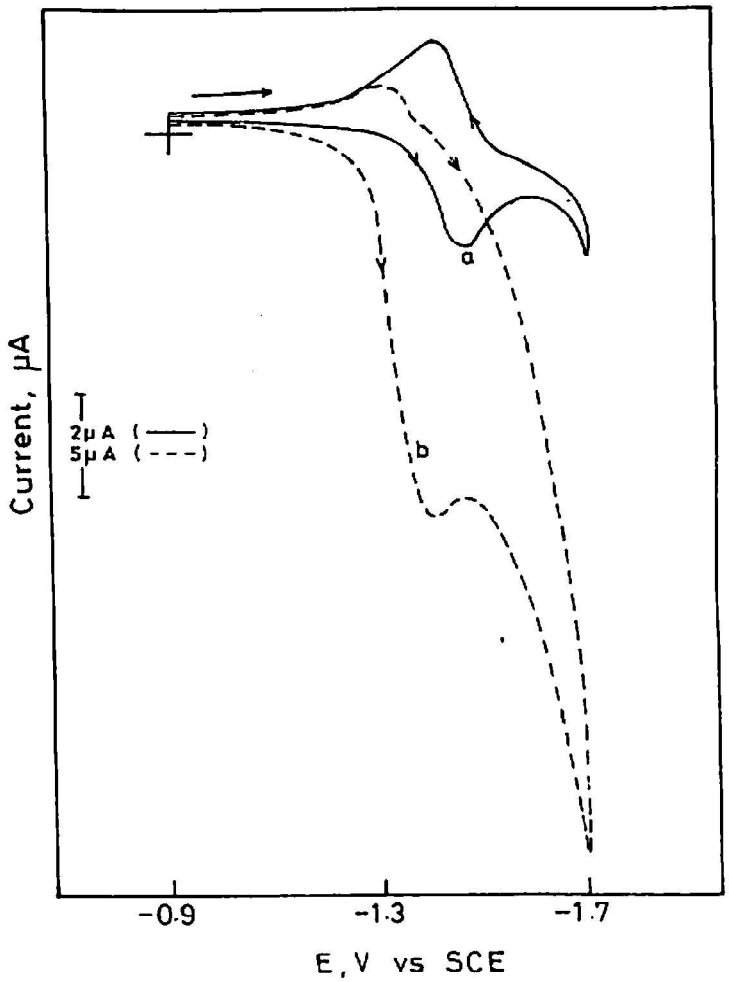

Fig. 2: Cyclic voltammogram of $[NiL]^{2+}$ (0.1 mM) in 0.1 M $LiClO_4$ in water at HMDE (0.0310 cm^2). Scan rate: 200 mVs^{-1} under N_2 (curve a); under CO_2 (curve b)

M. A. Scibioh & V.R. Vijayaraghavan, Bull of Electrochemistry, 16(8), 2000, 376-381.

Electrochemical Study

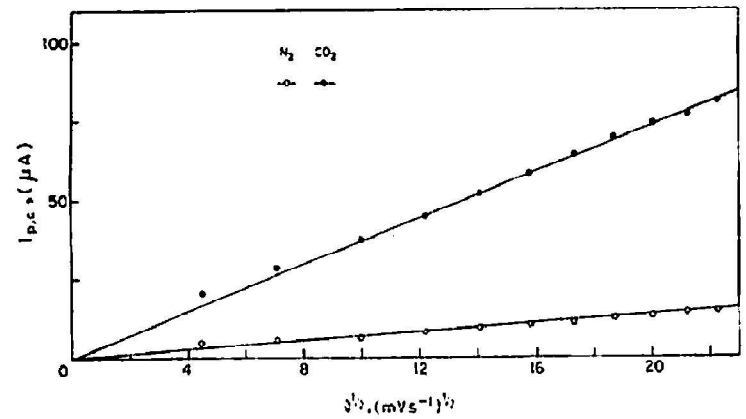

Fig. 3: Plot of $I_{p,c}$ vs $\sqrt{\nu}$
$[NiL]^{2+}$ = 0.5 mM; $[LiClO_4]$ = 0.1 M; Solvent = H_2O
Temp = 298 ± 2 K; Pressure: 1 atm
(1) N_2 (2) CO_2

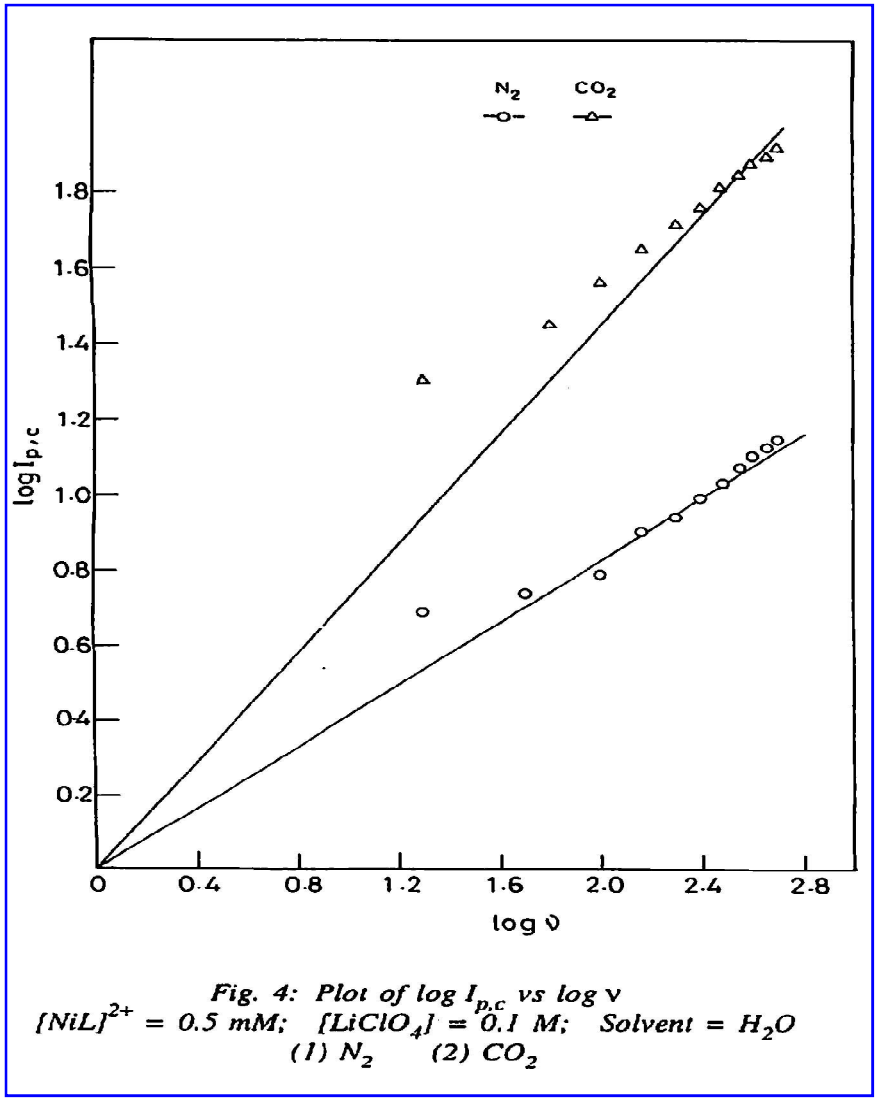

Fig. 4: Plot of log $I_{p,c}$ vs log ν
$[NiL]^{2+}$ = 0.5 mM; $[LiClO_4]$ = 0.1 M; Solvent = H_2O
(1) N_2 (2) CO_2

M. A. Scibioh & V.R. Vijayaraghavan, Bull of Electrochemistry, 16(8), 2000, 376-381.

Electrochemical Study

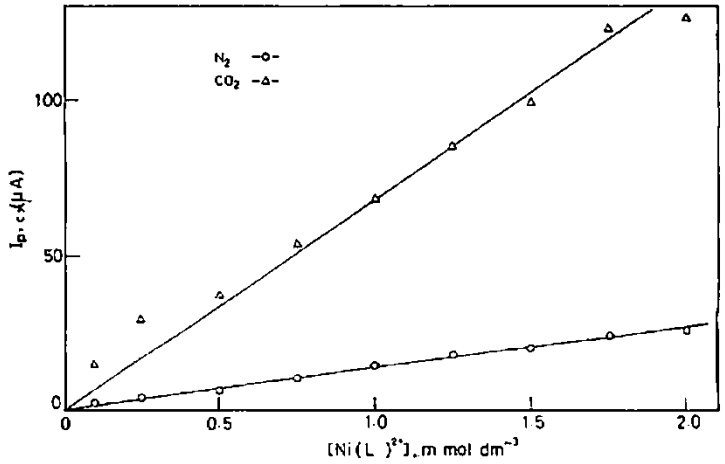

Fig. 5: Plot of $I_{p,c}$ vs complex
Scan rate = 100 mVs^{-1}; $[LiClO_4]$ = 0.1 M
(1) N_2 (2) CO_2

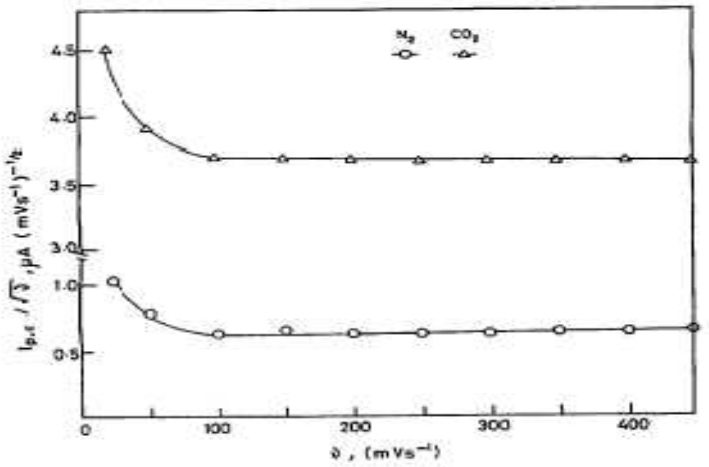

Fig. 6: Plot of $I_{p,c}/\sqrt{v}$
$[NiL]^{2+}$ = 0.1 mM; $[LiClO_4]$ = 0.1 M; Solvent = H_2O
(1) N_2 (2) CO_2

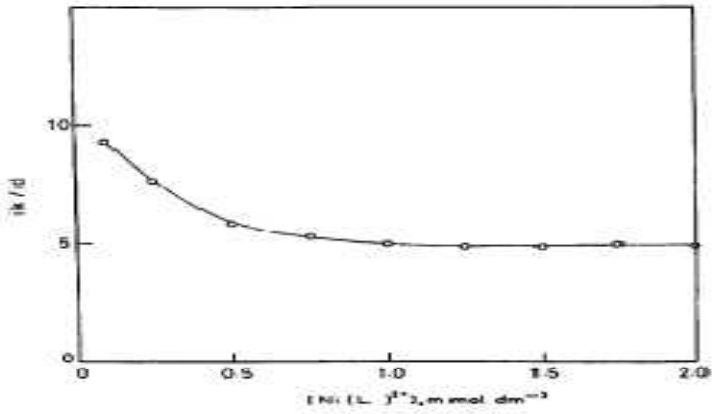

Fig. 7: Plot of i_k/i_d vs [copmplex]
$[LiClO_4]$ = 0.1 M; Solvent = H_2O; Scan rate = 100 mVs^{-1}
i_k = kineric current; i_d = diffusion current

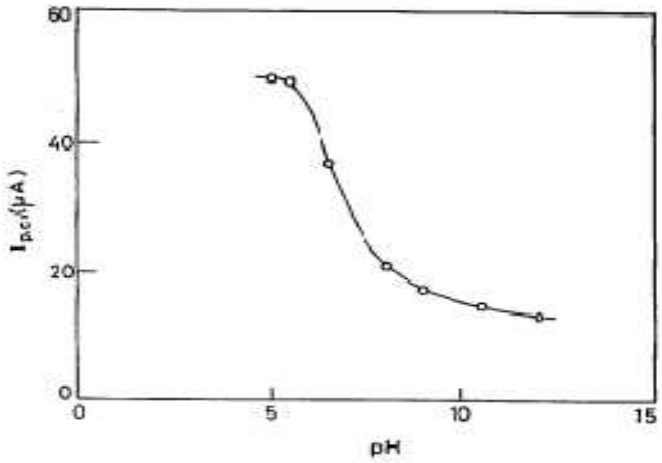

Fig. 8: Plot of $I_{p,c}$ vs pH
$[NiL)]^{2+}$ = 0.5 mM under CO_2 atmosphere
Scan rate = 100 mVs^{-1}

M. A. Scibioh & V.R. Vijayaraghavan, Bull of Electrochemistry, 16(8), 2000, 376-381.

Insitu – Spectroelectrochemical Study

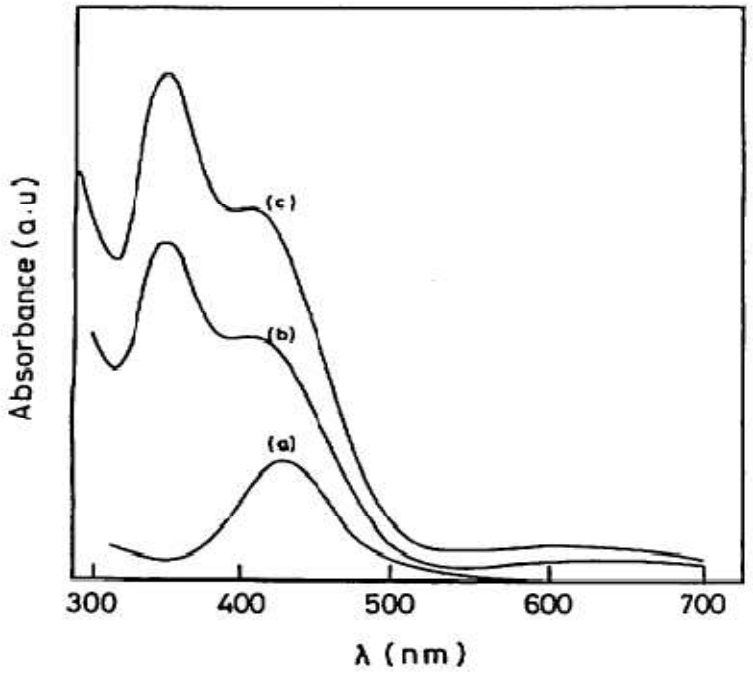

Fig. 5: UV-visible spectroscopy study in aqueous solution
(a) Electronic spectrum of $[NiL]^{2+}$ before electrolysis
(b) Electronic spectrum of $[NiL]^{2+}$ electrolysed under 1 atm CO_2
(c) Electronic spectrum of $[NiL]^{2+}$ electrolysed under 1 atm CO
$[NiL]^{2+}$ = 6 x 10^{-3} M in 0.1 mol dm^{-3} $LiClO_4$
aqueous solution at 298 ± 2K
Electrolysis: Hg pool at -1.60 V vs SCE

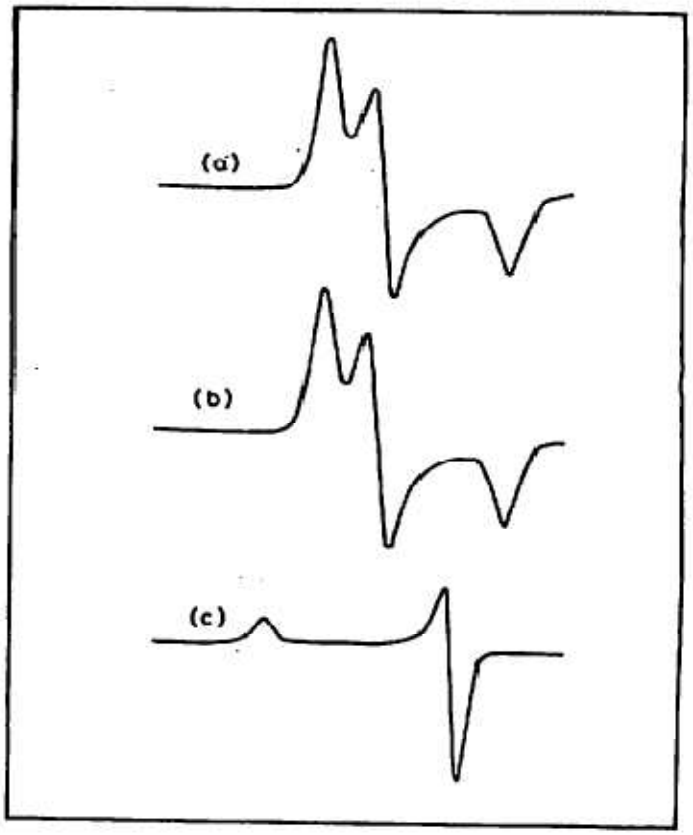

Fig. 6: EPR spectrum of frozen (77 K) electrolysed solutions of $[NiL]^{2+}$ in DMF at -1.60 V vs SCE at mercury cathode (0.1 M TEAB)
a) under CO_2 b) under CO c) under N_2

M. A. Scibioh & V.R. Vijayaraghavan, Bull of Electrochemistry, 13(6), 1997, 275-279.

Carbon dioxide Reduction Mechanism

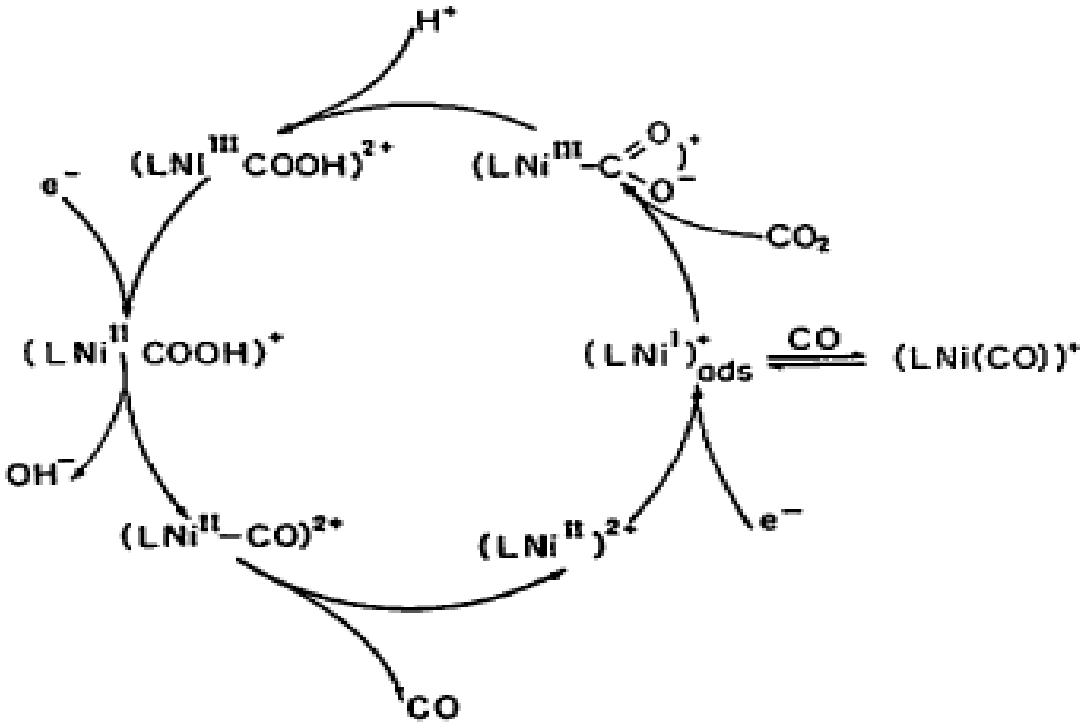

Scheme I: Postulated mechanistic cycle for the electrocatalytic reduction of CO_2 into CO by $[NiL]^{2+}$ in water

Scibioh et al., Proc. Indian. Acad. Sci (Chem. Sci) 113(4), 2001, 343-350.

Electrochemical Study

Table .1 Cathodic peak potentials and peak current values of complexes. The reaction conditions are $[LiClO_4] = 0.1$ mol dm^{-3}, temp. $= 298 \pm 2K$, scan rate $= 200$ mVs^{-1}, solvent $= H_2O$, area of HMDE $= 0.031$ cm^2

Complex	$-E_p$, vs SCE (V)		Peak current, (mA)	
	N_2	CO_2	N_2	CO_2
$[Ni(L_1)] (ClO_4)_2H_2O$	1.36	1.43	1.2	7.0
$[Ni(L_2)] (ClO_4)_2$	1.22	1 13	1.6	5.4
$[Ni(L_3)] (ClO_4)_2$	1.255	1.20	2.7	5.0
$[Ni(L_4)] (ClO_4)_2$	1.21	1.16	2.5	14.6
$[Ni(L_5)] (ClO_4)_2$	1.47	1.41	4.5	36.0

Table.2. The data of product using controlled potential electrolysis-gas chromatorgraphy (CPE-GC). The reaction conditions are $[LiClO_4] = 0.1$ mol dm^{-3}, [complex] $= 1.0$ mmol dm^{-3} temp. $= 298 \pm 2K$, solvent $= H_2O$.

Complex	-E, (V)	Time of electro-lysis, h (L)	Total volume of CO produced (ml)	Turnover Frequ-ency, (h^{-1})
[Ni(L1)](ClO4) 2H2O	1.6	3	20	6.6
[Ni(L2)](ClO4)2	1.6	3	11	3.6
[Ni(L3)](ClO4)2	1.6	3	13	4.3
[Ni(L4)](ClO4)2	1.6	3	23	7.6
[Ni(L5)](ClO4)2	1.6	3	28	9.2

The order of catalytic activity of the chosen systems towards CO_2 reduction in water may be represented as:

$[Ni(L_5)]^{2+} > [[Ni(L_4)]^{2+} > [Ni(L_1)]^{2+} > [Ni(L_3)]^{2+} \sim [Ni(L_1)]^{2+}$

Scibioh et al., Transcation of SAEST., 36 (3 & 4), (2002), 97 – 101.

Electrochemical Study

Table 3—Studies of scan rate variation in solvents of various compositions. $[NiL]^{2+}$ = 1.0 mmol.dm^{-3}; $[LiClO_4]$ = 1.0 mmol.dm^{-3}; Temp.= 298±2 K

Solvent	H_2O (vol%)	I_k/I_d Scan rate, v (mVs^{-1})			
		400	200	100	50
DMF	50	3.2	3.2	3.25	3.45
	60	3.35	3.4	3.5	3.7
	70	3.5	3.6	3.8	4.1
	80	3.45	3.5	3.7	4.2
	90	3.40	3.45	3.5	3.9
	100	3.0	2.92	2.95	3.1
DMSO	20	3.25	3.30	3.25	3.60
	40	3.32	3.35	3.40	3.70
	60	3.40	3.45	3.65	3.90
	80	3.45	3.50	3.70	4.0
	100	3.00	2.92	2.95	3.1
CH_3CN	20	1.9	2.43	2.5	4.2
	40	2.2	2.50	2.6	5.45
	60	2.3	2.55	2.65	6.7
	80	2.9	2.85	2.8	7.0
	100	3.0	2.92	2.95	3.1

Table 1—Studies on the effect of supporting electrolyte on current for the reduction of CO_2

Supporting Electrolyte, 0.1M	Solvent	I_k/I_d Scan rate, v(mVs^{-1})		
		200	100	50
TBAP	80%CH_3CN	5.65	5.7	7.5
	80% DMF	6.75	6.8	8.0
	70%DMSO	4.3	4.4	6.5
TEAP	100% CH_3CN	3.4	3.5	4.2
	80%CH_3CN	6.45	6.5	8.3
	70% DMF	7.0	7.2	8.5
$KClO_4$	100% H_2O	2.6	2.7	2.9
	70%DMSO	3.0	3.1	4.0
$NaClO_4$	100% H_2O	2.55	2.6	2.85
	80% DMF	2.8	2.9	3.8

Scibioh et al., Indian. J. Chem., Sec.A , 41A, (2002) 472 – 477.

Part 3. Research in Fuel Cells

Introduction to Fuel Cells

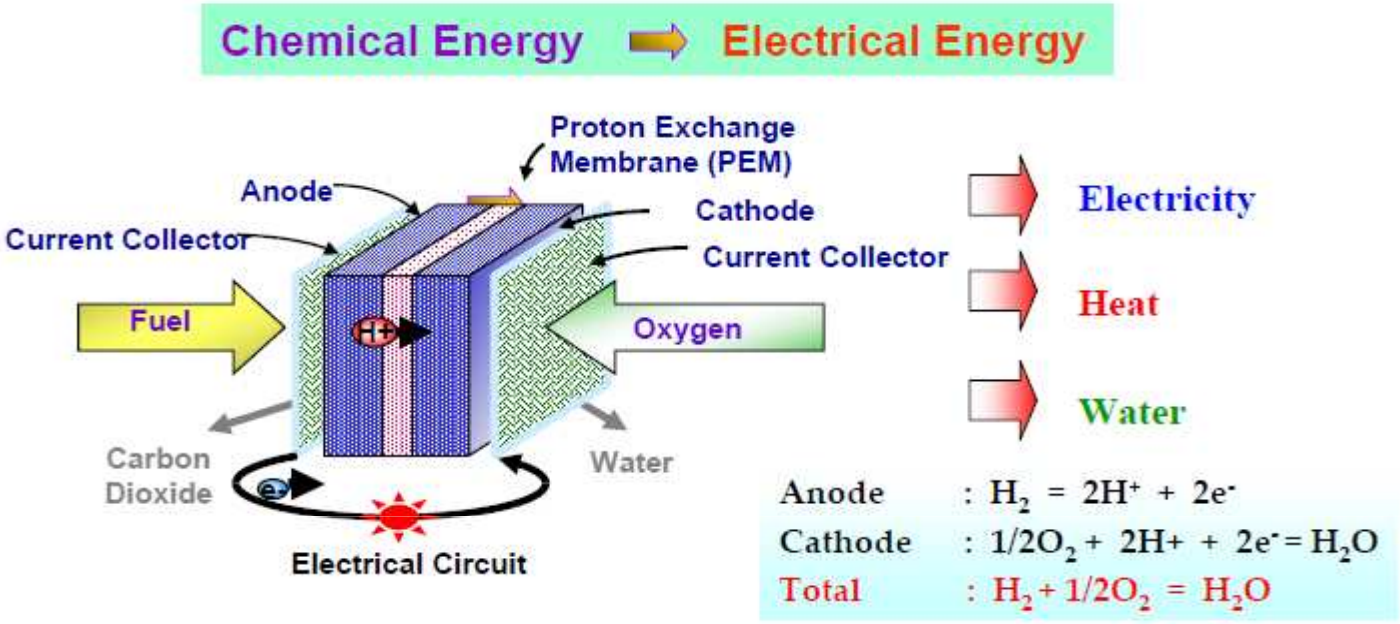

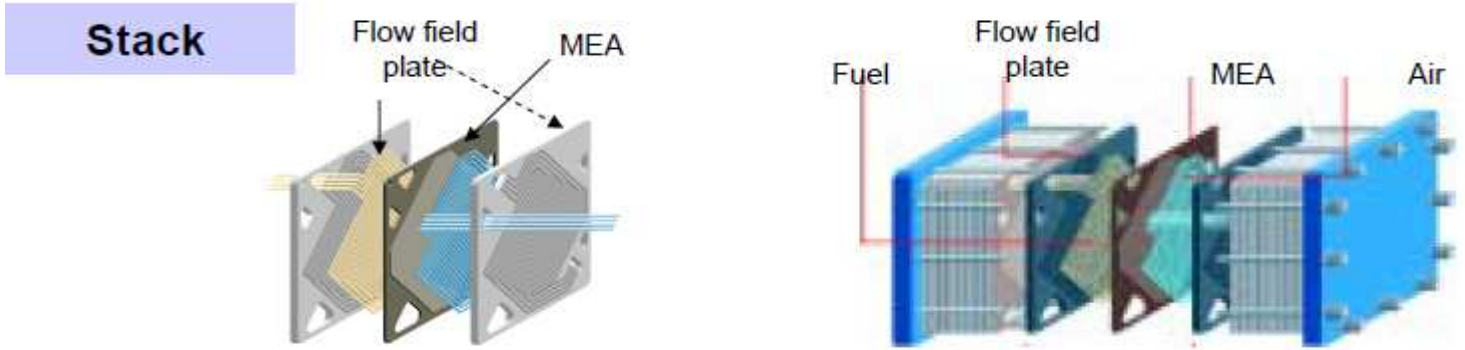

B. Viswanathan & M. A. Scibioh, *Fuel Cells-Principles and Applications*., CRC Press, Taylor & Francis Group, USA, 2007)

Applications

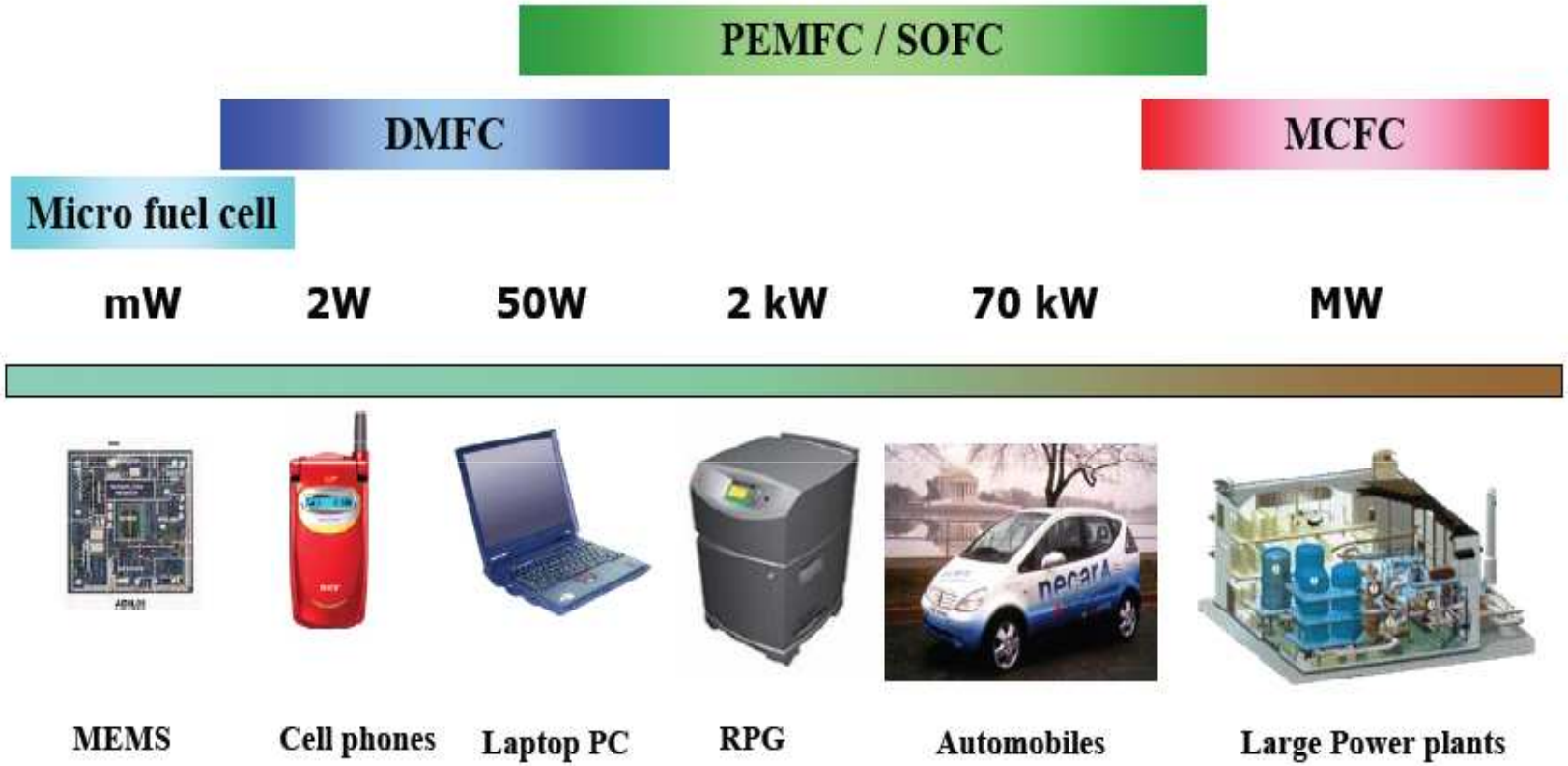

Others : military purposes, robots, portable power generators

KIST – Fuel Cell Research Center - Laboratories

MCFC Lab

PEMFC Lab

DMFC Lab

SOFC Lab

SiFC Lab

Reformer Lab

Cooperation

- **Foreign Organizations**
  - CEA (France)
  - AIST-KANSAI (Japan)
  - DICP (China)
  - ENEA (Italy)
  - Kurchatov Institute (Russia)
  - NRC (Canada)
  - IEA

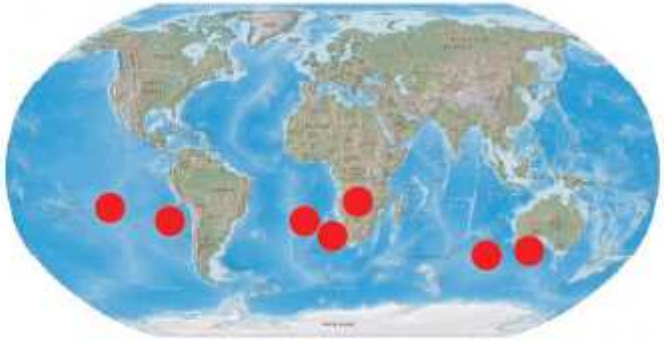

- **Domestic Companies**
  - Korea Electric Power Corporation
  - Hyundai Motor Company
  - LG Chemicals
  - Samsung Advanced Institute of Technology

Direct Methanol Fuel Cell

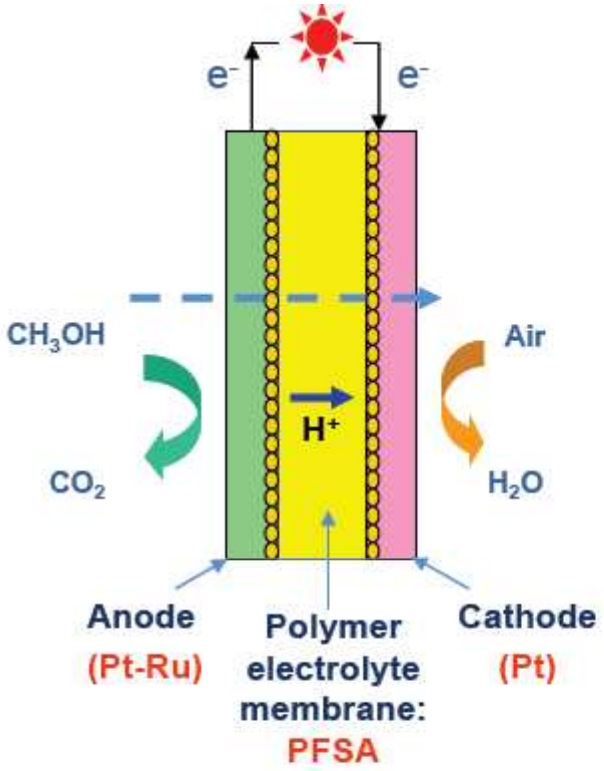

- high energy density
- longer use time
- enhanced functionality
- instant refueling
- environmentally friendly

Anode	:	$CH_3OH + H_2O$	$= CO_2 + 6H^+ + 6e^-$
Cathode	:	$1.5\ O_2 + 6H^+ + 6e^-$	$= 3H_2O$
Overall	:	$CH_3OH + 1.5O_2$	$= CO_2 + 2H_2O,$
		$E^o = 1.18$ V	

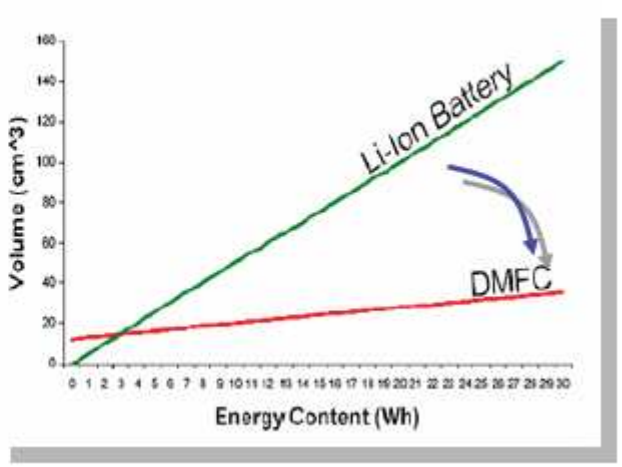

B. Viswanathan & M. A. Scibioh, *Fuel Cells-Principles and Applications*., CRC Press, Taylor & Francis Group, USA, 2007)

DMFC Technology

Efforts toward Commercialization

Manufactures	Power	Volume	Fuel volume	Target year	Prototypes
NTT DoCoMO and Fujitsu	9 wh (Battery charger)	160 cc	18 cc	2007	
Toshiba	100 mW (Flash) 300 mW (HDD)	80 cc 220 cc	10 cc 3.5 cc	2007	
Hitachi	1.0 W 5 hr	126 cc	3 cc	2006	
LG Chem	25 W 10 hr	1 liter	200 cc	2006	
Sanyo and IBM Japan	12~72 W 8 hr (Battery hybrid)	1.2 liter	130 cc	2007	
Samsung SDI	20 W 15 hr	1 liter	200 cc	2007	

Technical Barriers to Commercialization

- Catalyst - Activity and Cost
- Membrane - Methanol Crossover
- Fuel cell stack – Power Density
- Durability/reliability
- BOP Issues (thermal & water management)
- System & Component –Miniaturization
- Cost (based on technical impact)
- Conversion efficiency
- Consumer safety and Effluents
- Operating/storage envelope
- Manufacturing/Mass production
- Consumer acceptance/education/perception
- Codes & standards/Infrastructure

What Really Matters for Fuel Cell Commercialization?

Grand Challenges & Needed Breakthroughs for Fuel Cells

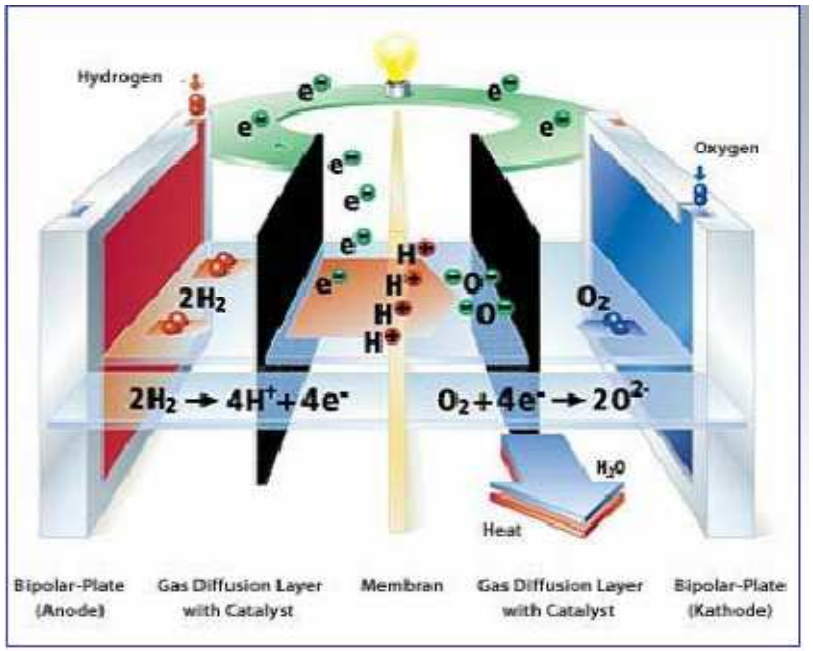

Grand Challenges

- Affordability ($/kW)
- Durability (performance loss ~ time)

Needed Breakthroughs

- Adv. Catalysts
- Adv. PEM Material
- Innovative CCM/MEA mft.

Cost breakdown for Automobile PEMFC Engine System

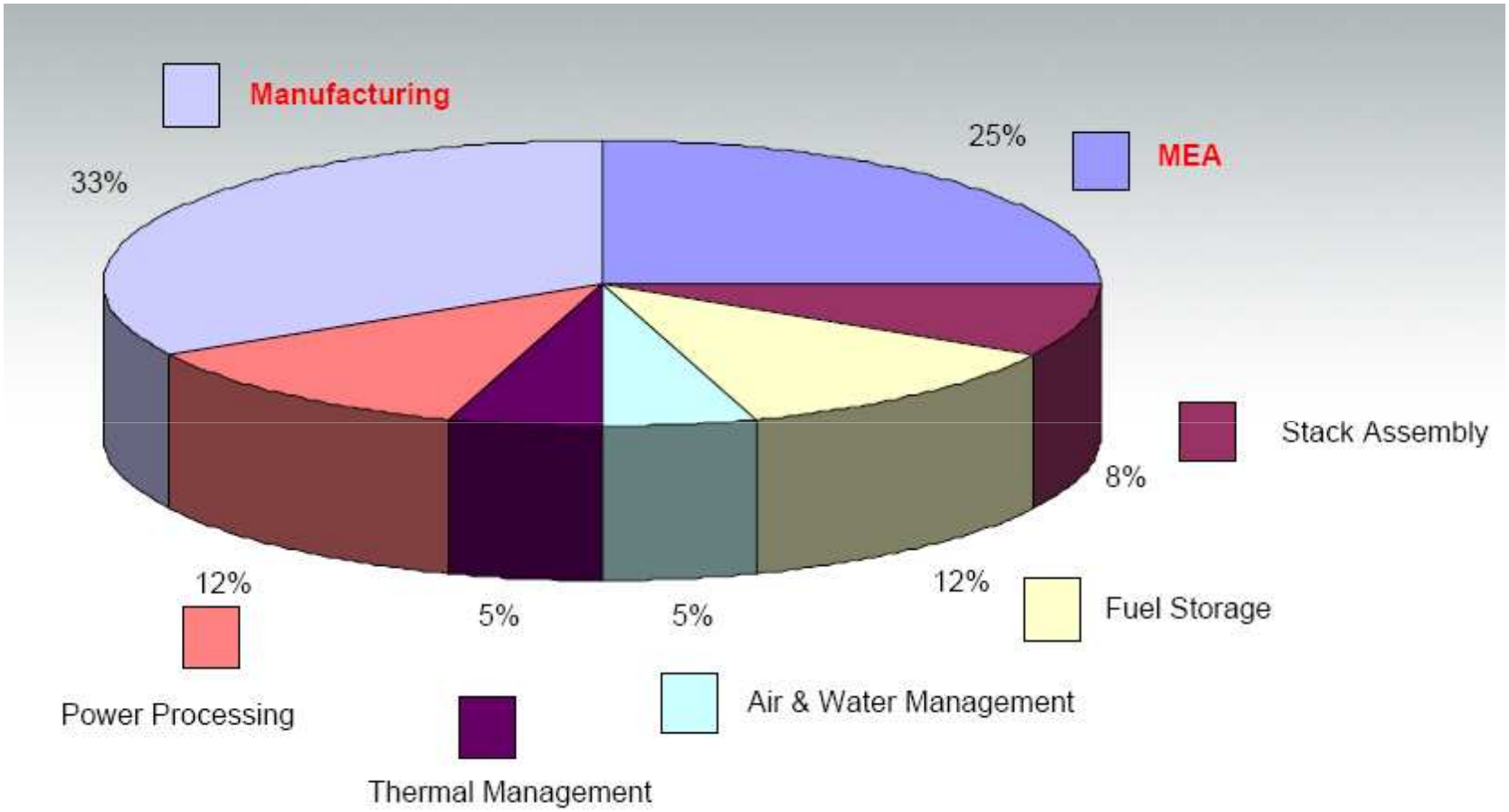

DMFC MEA Raw Materials Cost Analysis

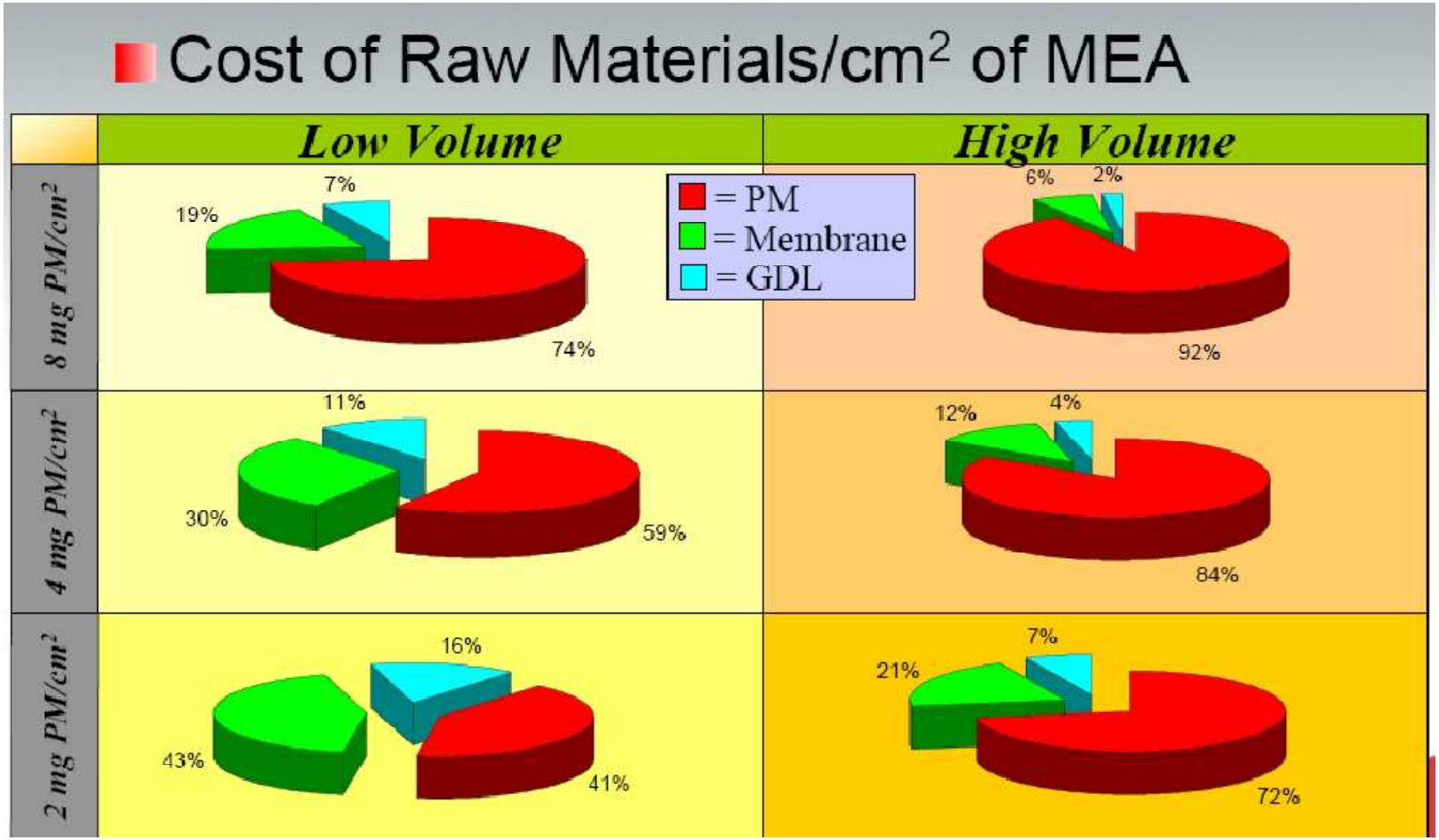

- *Current loadings of noble metals need to be reduced*
- *How to extract the best possible performance?*

Research Topics at KIST DMFC Lab

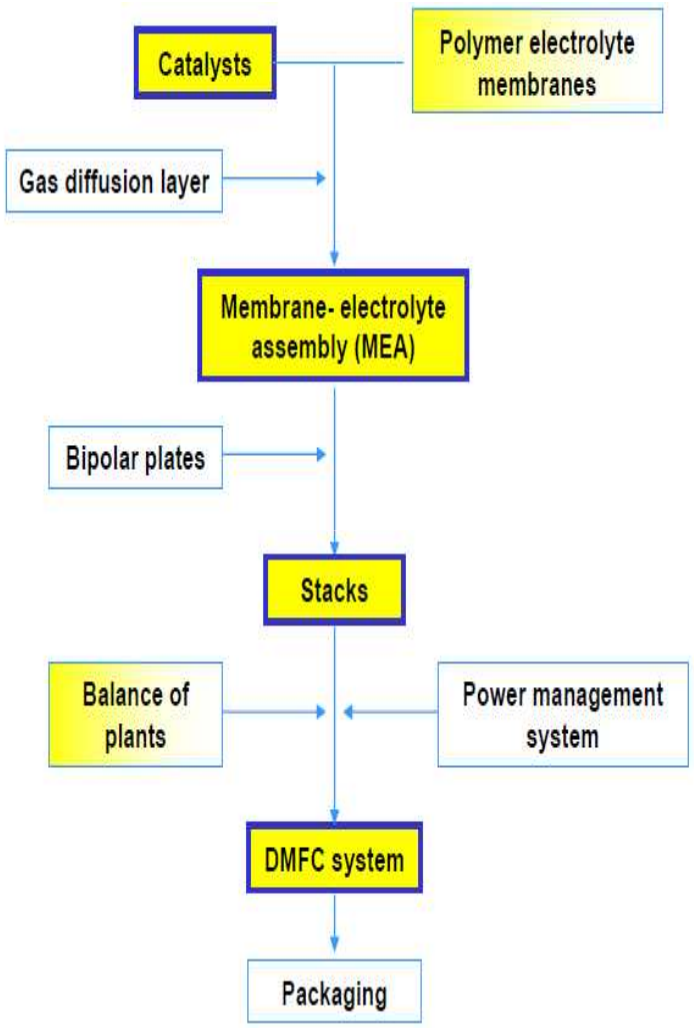

1. **Catalysts**
   - Modification of carbon supports with ionomer
   - Anode catalyst - Pt-CeO_2 - Activity/Durability/Cost
   - Cathode catalyst – Pt-CeO_2 - Air Utilization
2. **Membrane**
   - Surface modification by Silica layers
3. **Membrane Electrode Assembly**
   - Optimization of electrode structure
   - Durability test and Recovery measures
   - Simulation of flow fields
4. **Stacks**
   - Passive monopolar stacks
   - Active bipolar stacks: 20, 50, 500W stacks

Development of Catalysts

- Requirements
  - Higher active surface area
  - Smaller particle size
  - Porosity
  - Tolerant against corrosion and intermediates
  - Cost

- Approaches at KIST
  - To increase three phase boundary
    - ✓ Ionomer coated carbon
  - To increase air utilization at the cathode
    - ✓ Pt-Ceria + α
  - To replace Ru from the Pt-Ru anode catalysts
    - ✓ Pt-Ceria + β

Improve the utilization of methanol oxidation catalysts

Preparation of ionomer- coated carbon supports

(i) To reduce the micropore volume in carbon black particles
(ii) To extend the area of the three-phase boundary

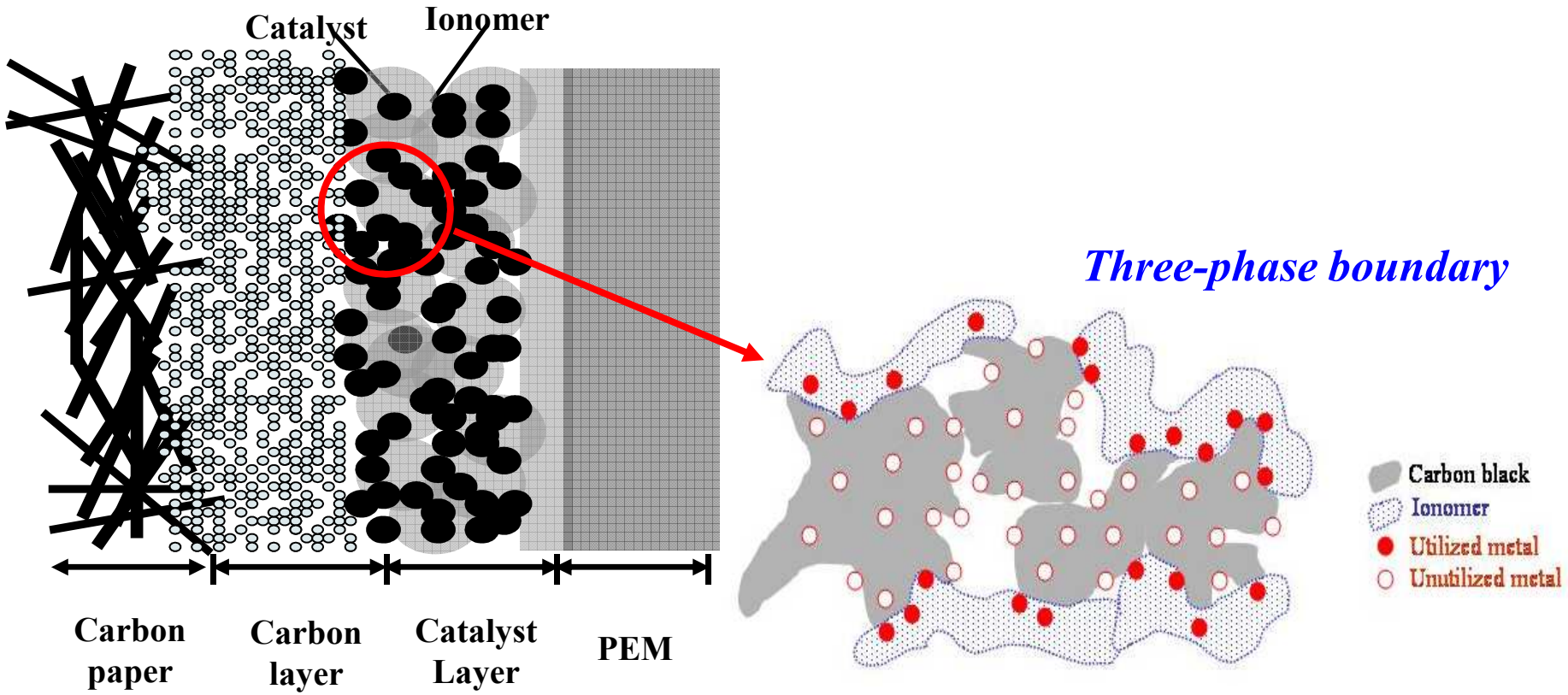

Ionomer Coated Carbon Supports

Conventional Pt / C catalyst

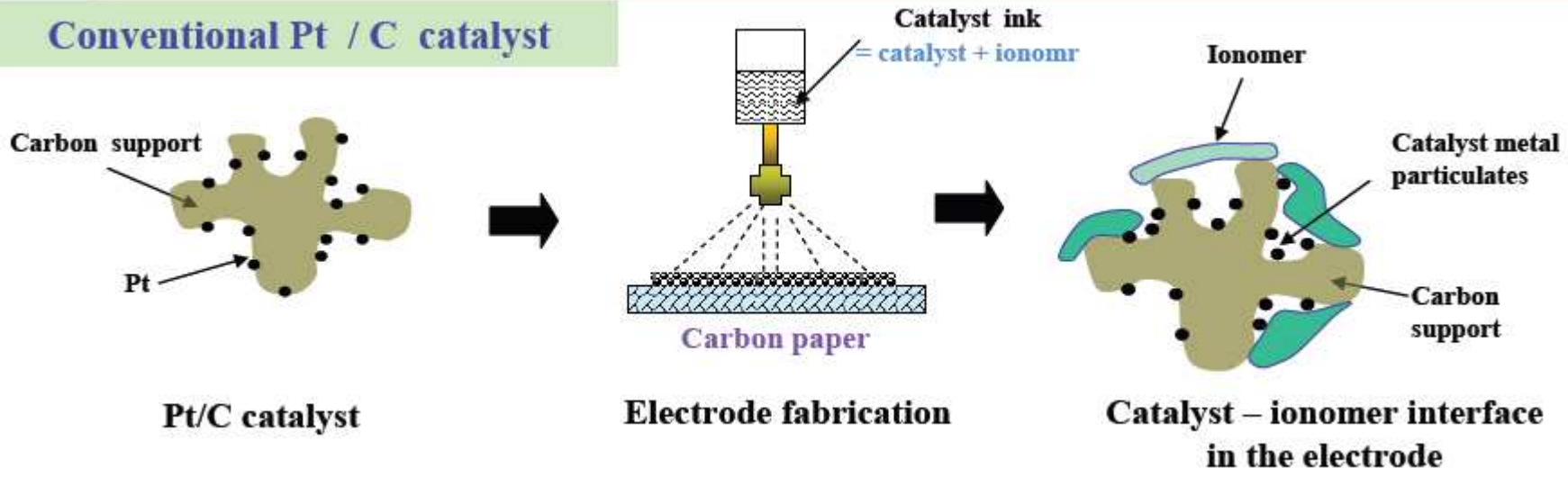

Pt/C catalyst | Electrode fabrication | Catalyst – ionomer interface in the electrode

Pt on ionomer-coated carbon

- Strategies & objective
  - To increase the interfacial area btn Pt and ionomer
- Experimental
  - Ionomer is first coated on the carbon support followed by Pt deposition

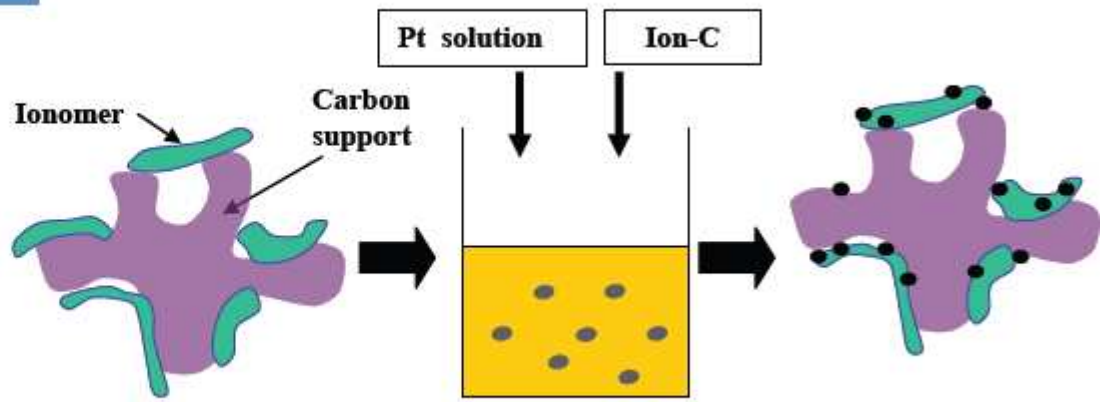

Ionomer / Carbon | Pt / Ionomer / Carbon

Catalyst Preparation – Colloidal Method

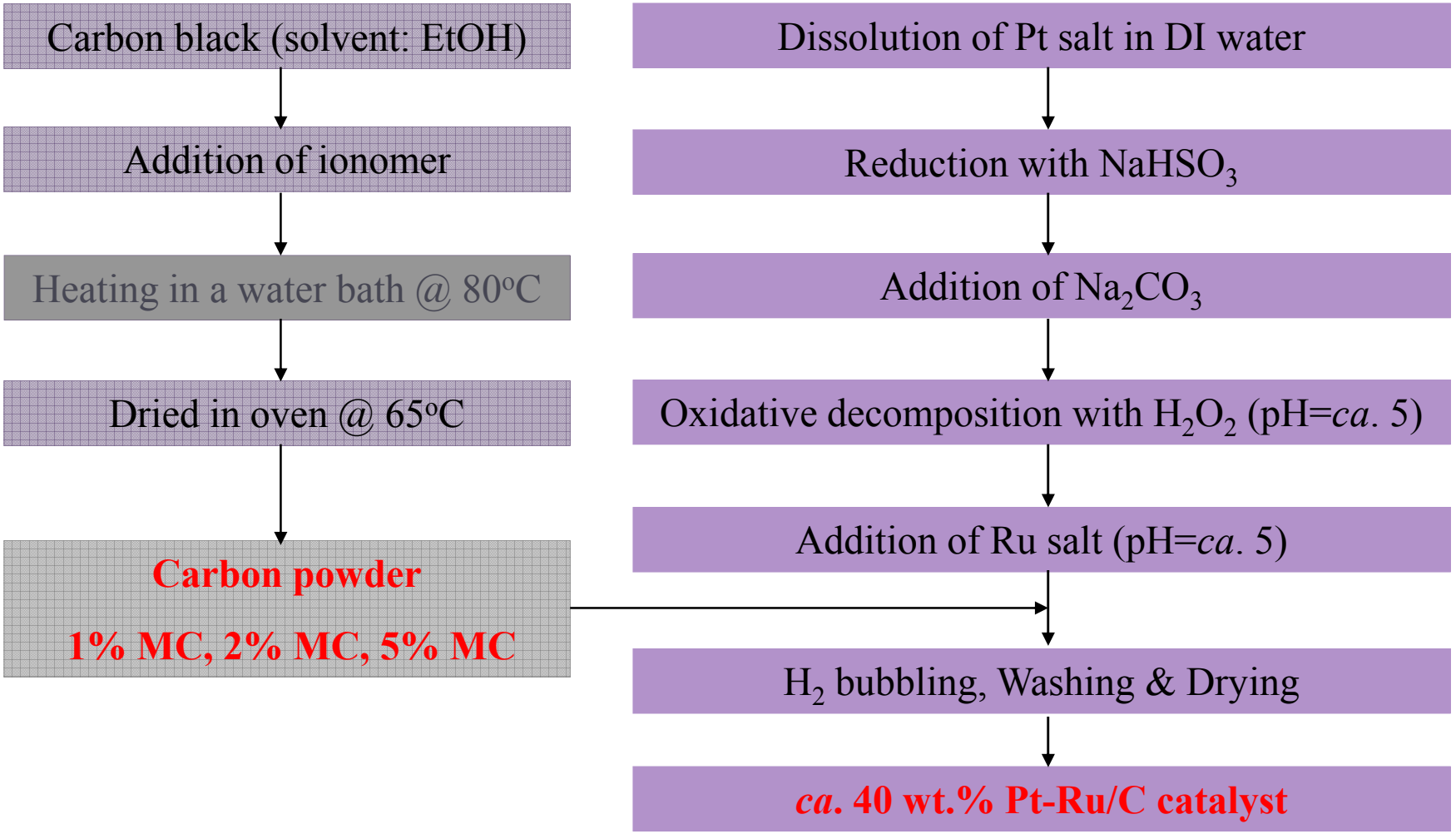

Fabrication of MEA (Electrode area = 10.89 cm^2)

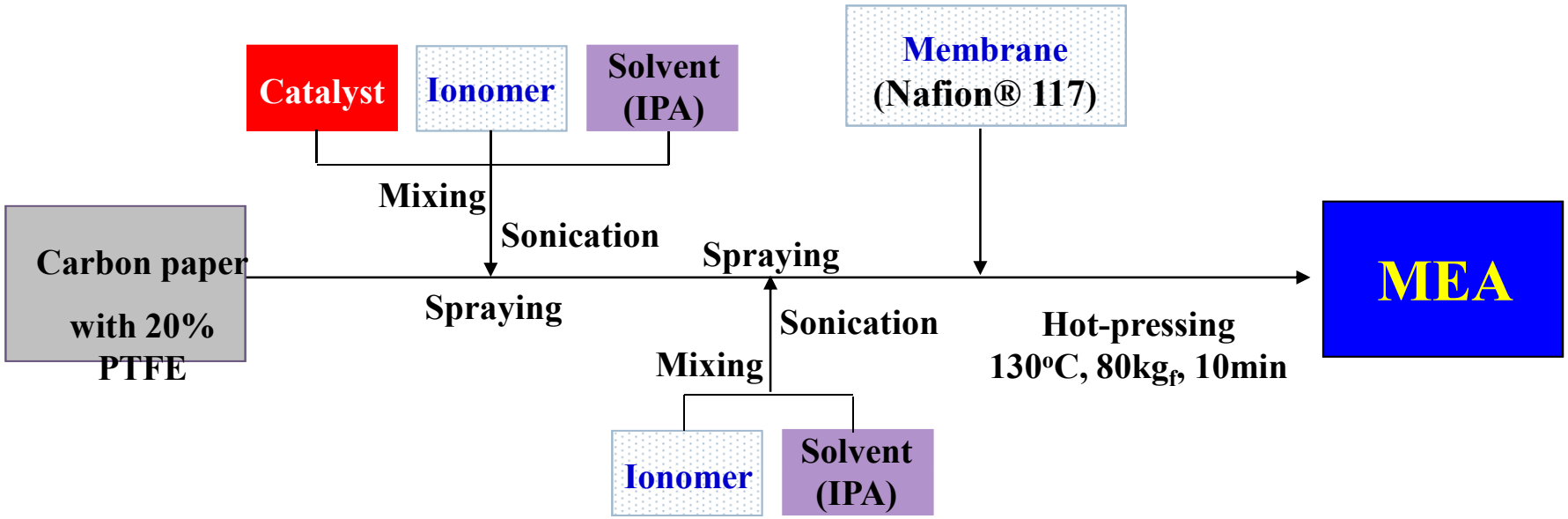

Electrode	Catalyst	Metal Loading	Ionomer/Catalyst
Cathode	46.5 wt.% Pt/C (Tanaka)	3 mg Pt/cm^2	0.3 (inner: 1/4, outer: 3/4)
Anode	*ca.* 40 wt.% Pt-Ru/C (Home-made & E-TEK)	3 mg Pt-Ru/cm^2	0.15, 0.3, and 0.6 (inner: 1/4, outer: 3/4)

Ionomer Coated Carbon Supports

To increase the utilization of catalyst

Use the ionomer-coated carbon as a catalyst support

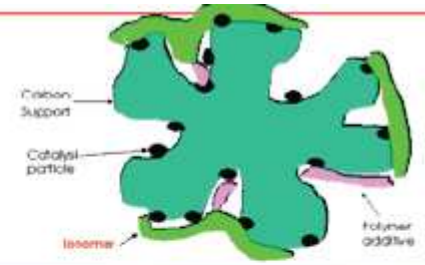

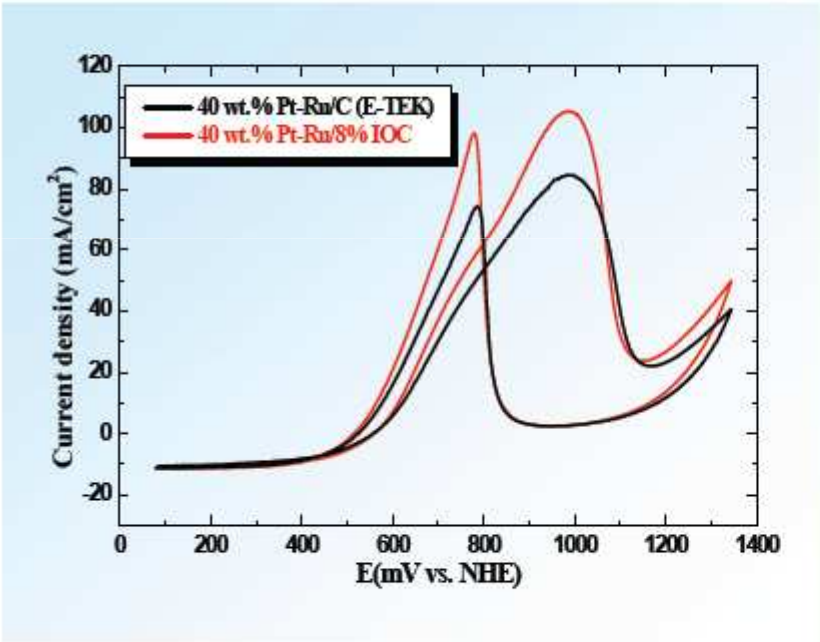

Fig. 1. Cyclic voltammetries of carbon-supported Pt-Ru catalysts for methanol oxidation in 0.5M H_2SO_4 + 2M MeOH.

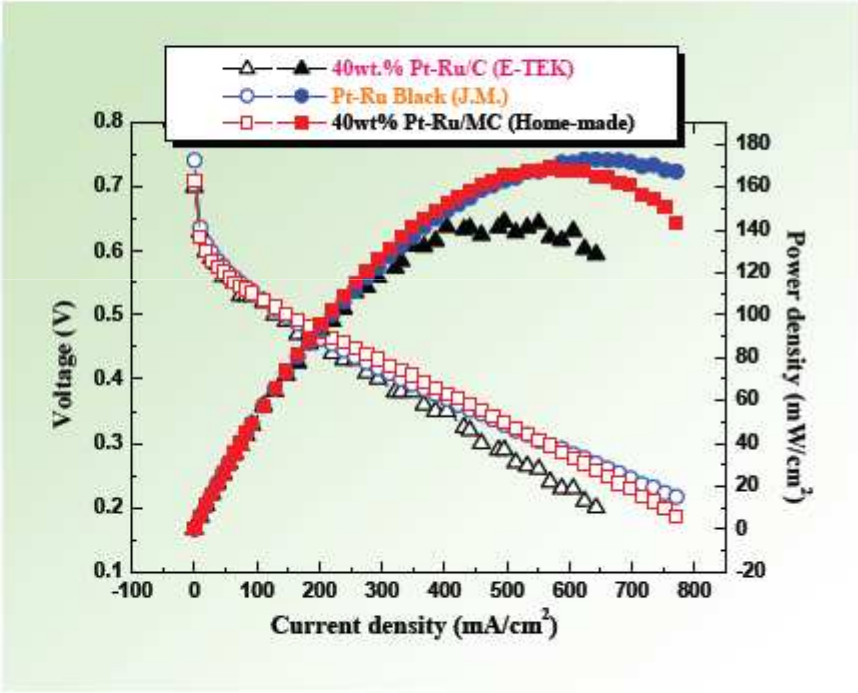

Fig. 2. DMFC performance at 90 °C, 2.0M CH_3OH 5 cc/min, humidified O_2 250 sccm. Cathode, 46.5 wt.% Pt/C (Tanaka, catalyst loading 3.0 mg Pt/cm²); membrane, Nafion-117

Ionomer Coated Carbon Supports

Pore-Size Distribution of carbon blacks

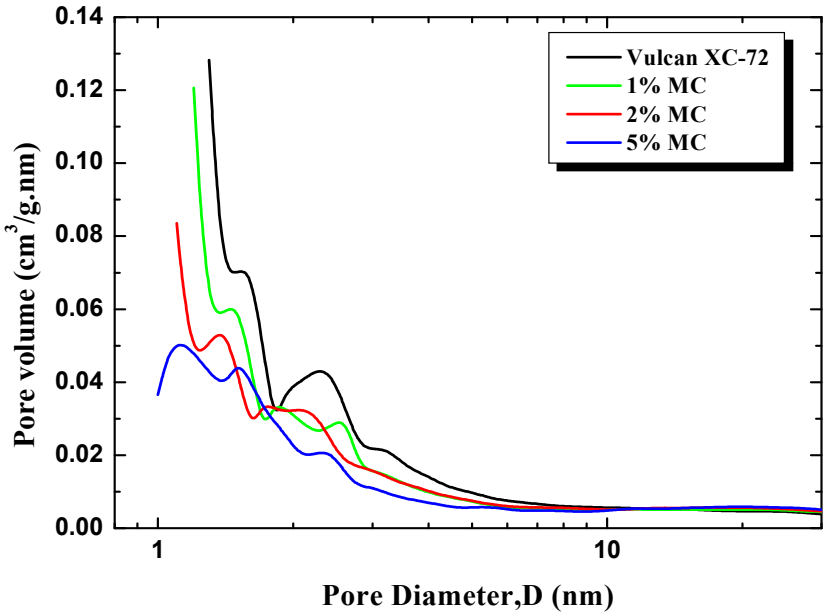

The micropore volume of the modified carbons decreased compared to unmodified VC XC-72

BET surface area (m^2/g):

VC XC-72 (217), 1% MC (189), 2% MC (178), 5% MC (161)

XRD Patterns of ca. 40wt.% Pt-Ru/C

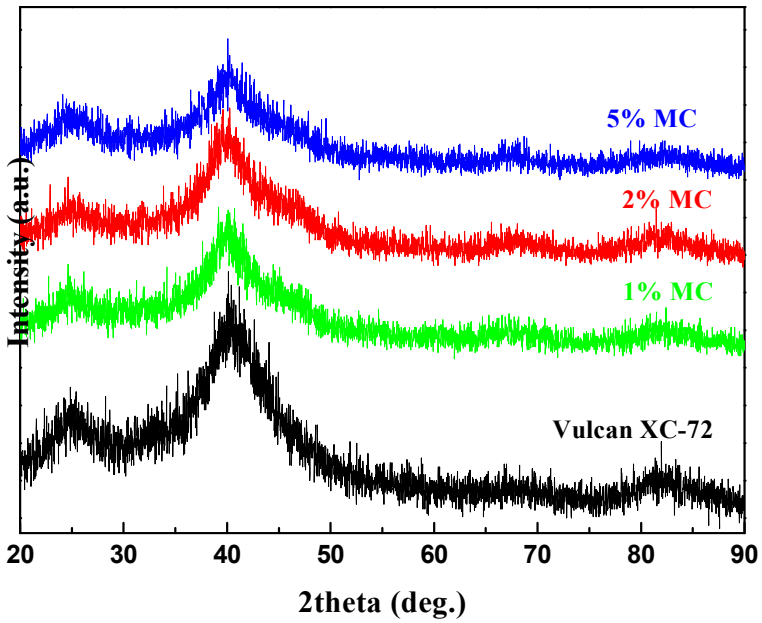

Diffraction peaks of the Pt-Ru/C slightly shift to higher 2θ values with respect to Pt reflections – Evidence for the formation of Pt-Ru alloy catalyst.

Various Ionomer Coated Carbon Supports for DMFC Applications

Preparation: Colloidal Route
Characterization: BET-PSD, FTIR, XRD, TEM, CO-Stripping, CV, CA

Table 1
Physical properties of the carbon black powders

Brand name	BET surface area (m^2/g) by this work	BET surface area (m^2/g) in catalogues	Primary particle size (nm) in catalogues	Maker
Vulcan XC-72R	217	254	30	Cabot
Ketjen Black (EC 300JD)	958	950	15	Ketjen Black International Company, Japan
Black Pearls (BP 2000C)	1477	1475	12	Cabot

Scibioh et al., Appl. Catal. B. Environ. 77 (2008) 373-385

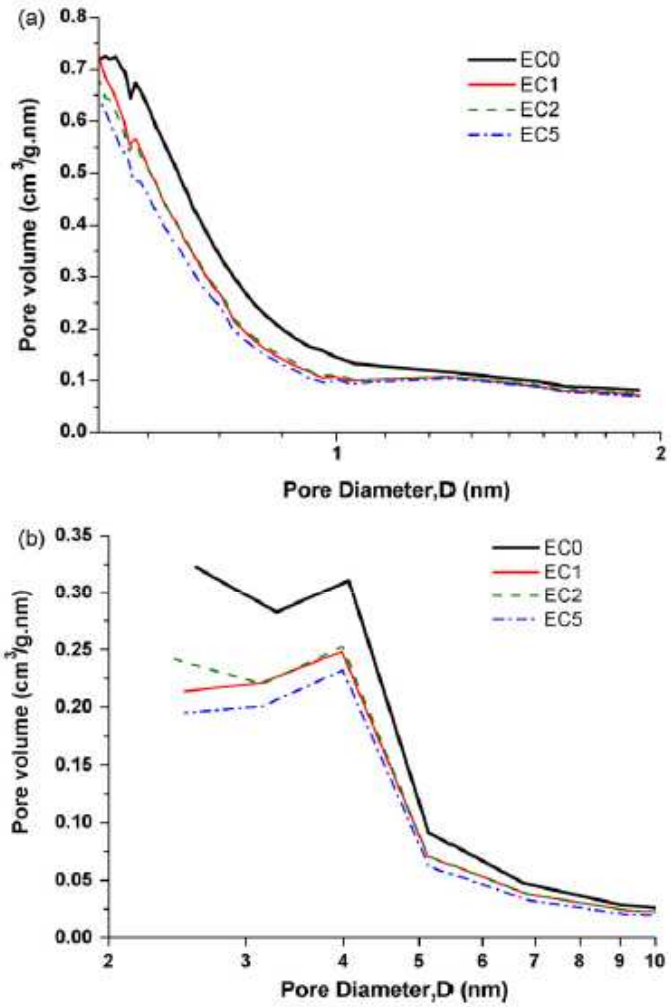

Fig. 1. Pore size distribution curves of EC 300JD plain and ionomer-coated carbon black powders. (a) Micropore region (<2 nm) made with Horvath–Kawazoe measurement. (b) Mesopore region (~2–100 nm) made with BJH method.

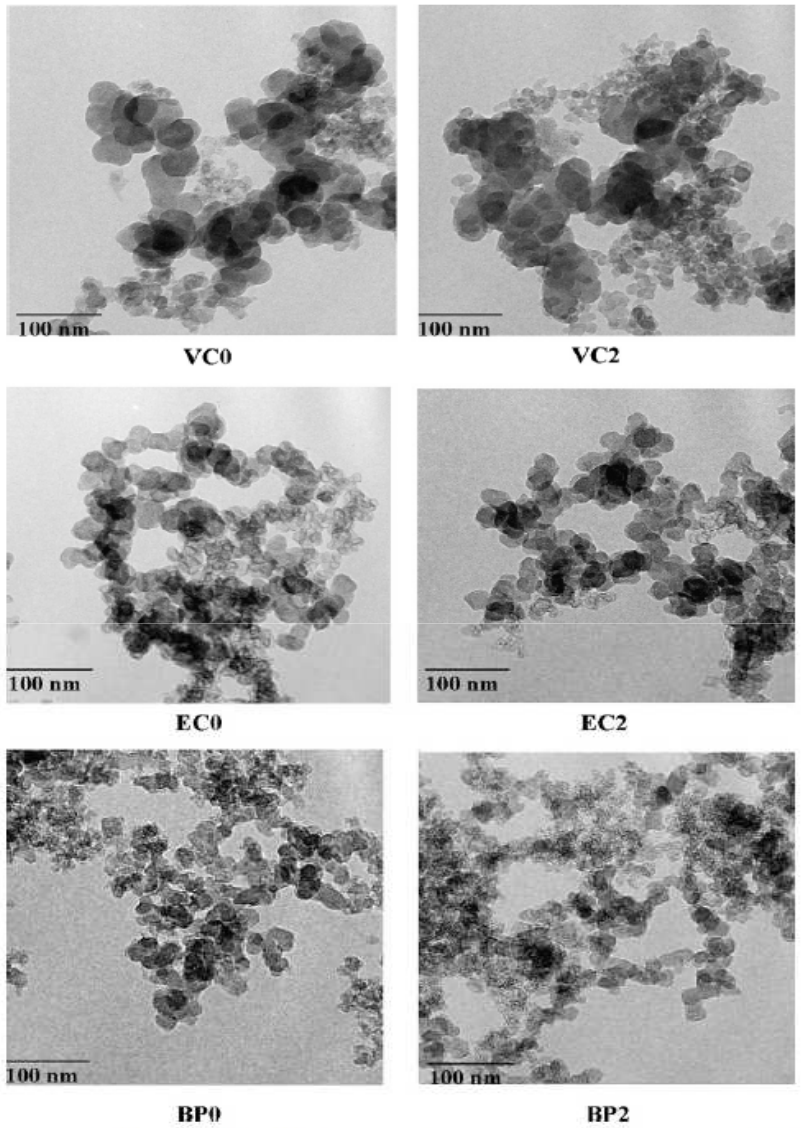

Fig. 2. TEM pictures of plain (VC0, EC0, BP0) and ionomer-coated (VC2, EC2, BP2) carbons.

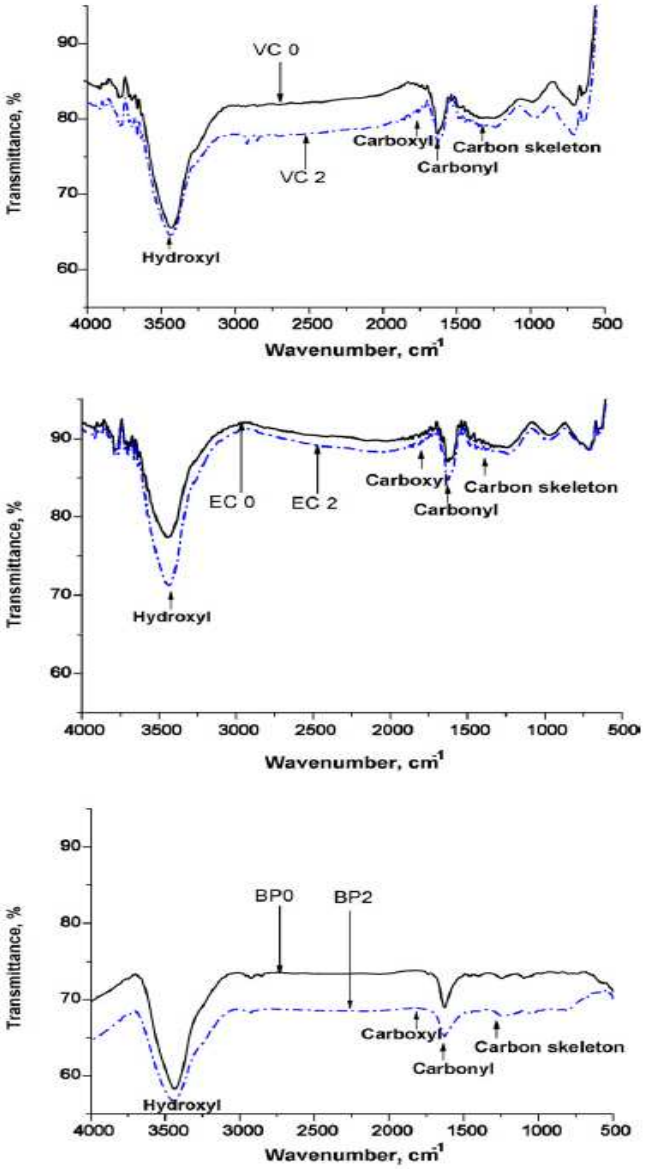

Fig. 3. IR spectra of plain (VC0, EC0, BP0) and ionomer-coated (VC2, EC2, BP2) carbon powders.

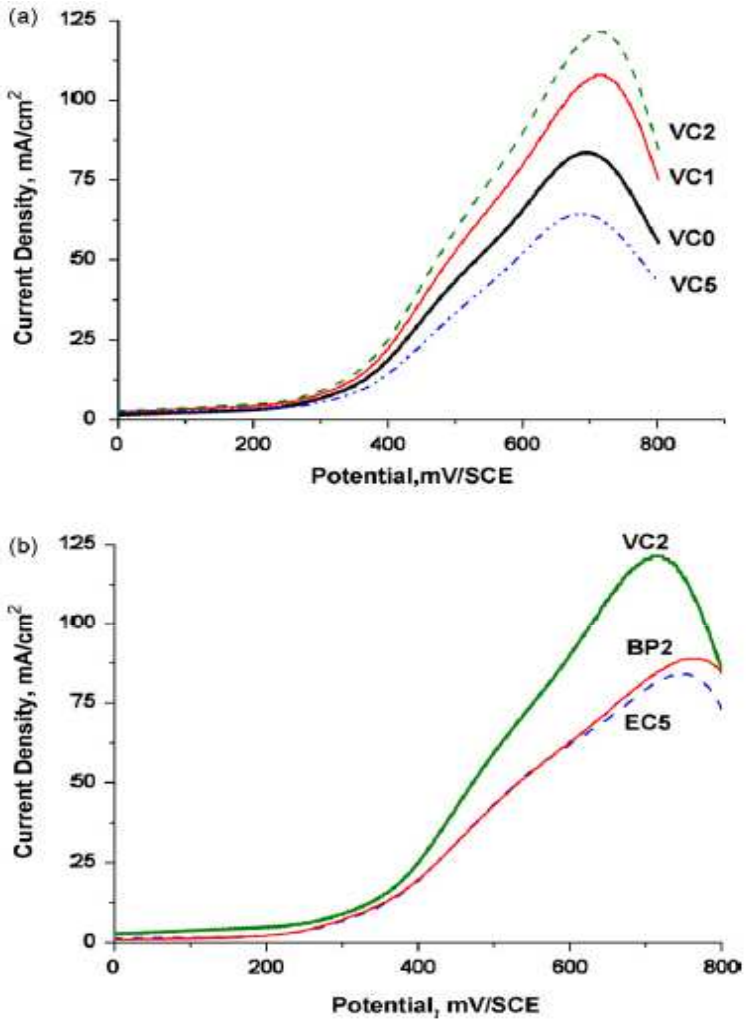

Fig. 4. (a) The forward sweep of the cyclic voltammograms of Pt–Ru/MC (MC = VC0, VC1, VC2, VC5). (b) A comparison among best performed catalyst systems with various modified carbon supports in electrolyte solution (0.5 M H_2SO_4 and 1.0 M MeOH) at 25 °C, Sweep rate = 50 mV/s.

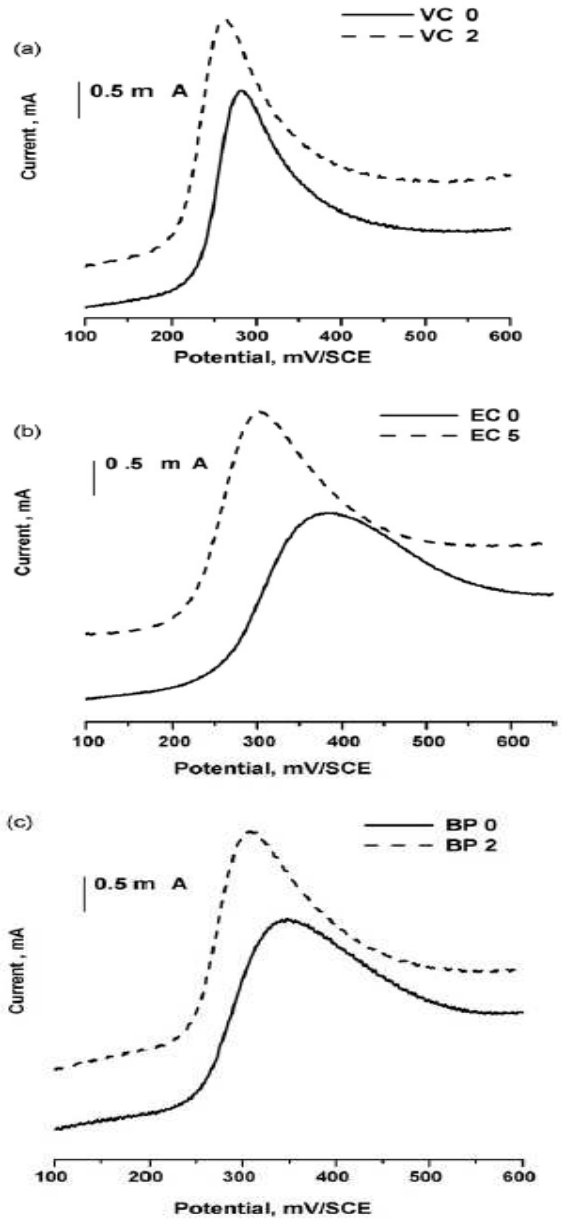

Fig. 7. CO_{ad} stripping voltammograms for the Pt–Ru/MC prepared with plain and best performed ionomer composition coated on carbon in each case. (a) VC0, VC2; (b) EC0, EC5; (c) BP0, BP2. Electrolyte: 0.5 M H_2SO_4 at 25 °C. Sweep rate = 50 mV/s.

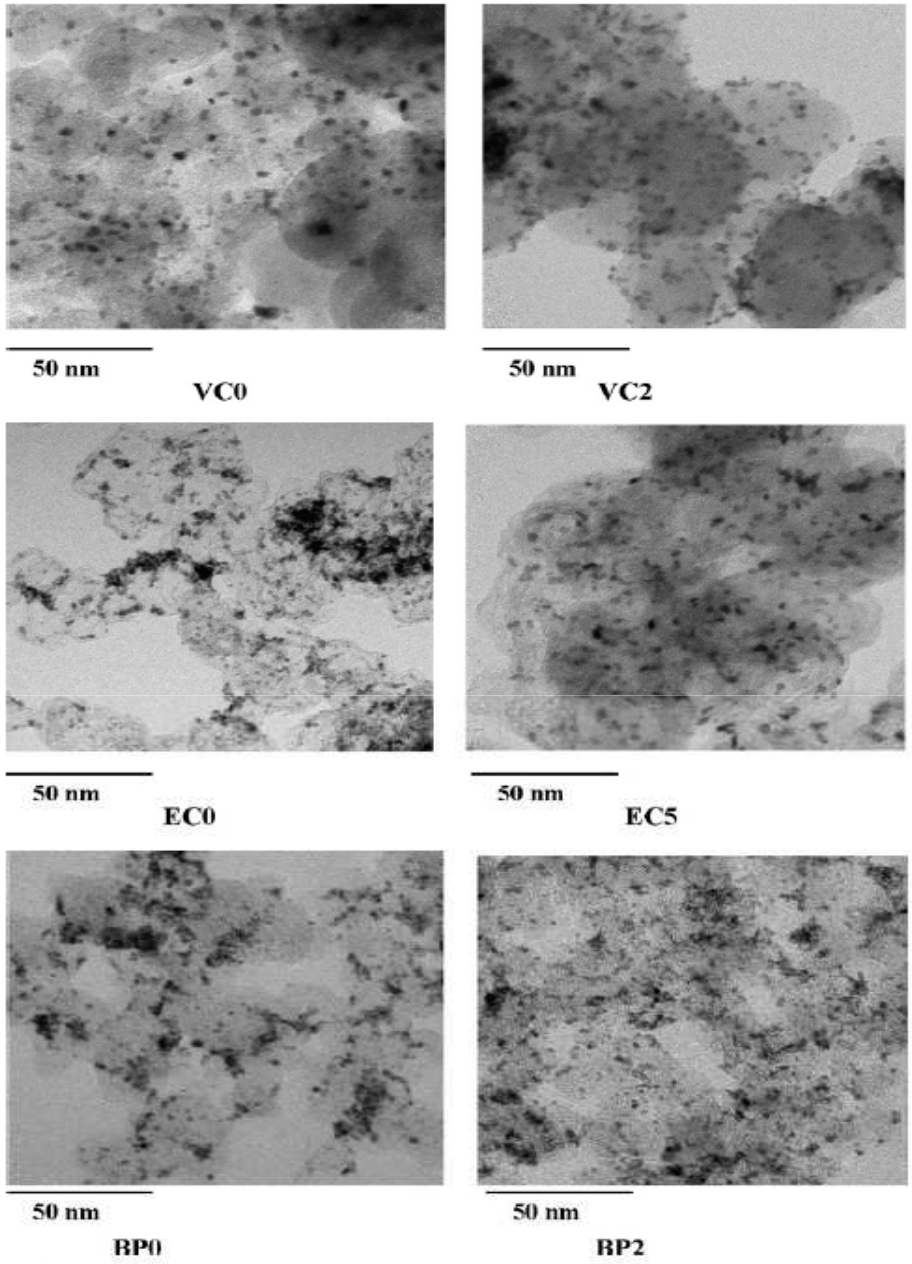

Fig. 9. TEM pictures of Pt–Ru/MC catalysts prepared with various carbon black supports.

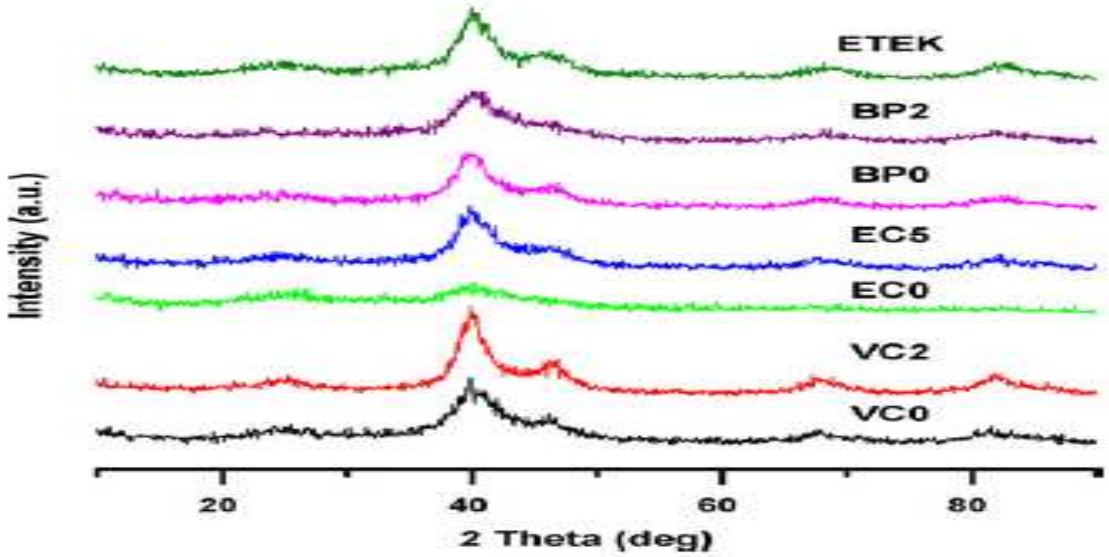

Fig. 8. X- ray diffraction patterns of Pt–Ru/MC catalysts prepared with various kinds of carbon black supports.

Microstructural characterization data of Pt–Ru/MC catalysts

Catalyst 40 wt.% Pt–Ru/MC	Particle size (nm)		Particle area[a] (m^2/g)	% Metal utilization
	TEM	XRD		
PR-ET[b]	2.6	2.75	107	53
VC0	3.0	3.0	93	60
VC2	3.5	3.5	79	73
EC0	1.5	1.4	186	32
EC5	2.5	2.5	111	56
BP0	1.5–3.5	3.0	186	29
BP2	2.0	1.9	144	35

[a] Particle area was calculated from TEM analysis by assuming spherical metal particles.
[b] PR-ET, commercial 40 wt.% Pt–Ru/C obtained from ETek.

Scibioh et al., Appl. Catal. B. Environ. 77 (2008) 373-385

Ceria to Replace Ru in Pt-Ru Anode Catalyst

Preparation: Impregnation /Co-precipitation Method
Characterization: BET-PSD, XRD, TEM, CO-Stripping, CV, CA, EIS

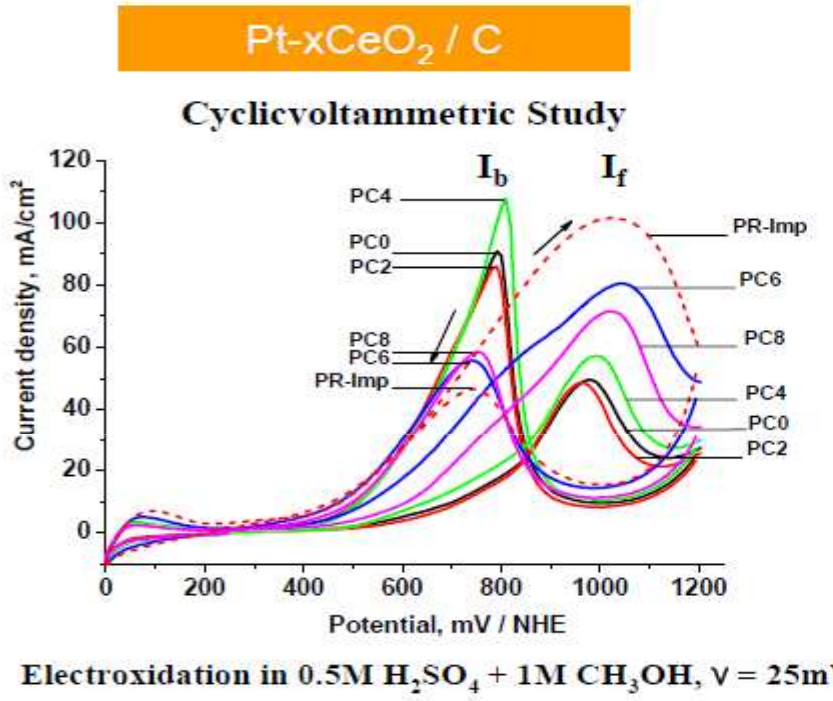

Electroxidation in 0.5M H_2SO_4 + 1M CH_3OH, v = 25mV/s

Catalyst	On-set Potential (mV/NHE)	Peak Current Density (mA/cm^2)	I_f/I_b
P-ET	480	49	0.54
PC0*	478	49	0.54
PC2	476	48	0.55
PC4	475	56	0.53
PC6	412	80	1.45
PC8	415	71	1.23
PR-Imp	375	102	2.17
PR-ET	378	101	2.16

* The number 0 – 8 denote the ceria percentage to Pt: PC0 = pure Pt, PC2 = 2%Ceria to Pt

- PC6- Better activity than Pt only system
  - ✓Shift in onset potential & better I_f/I_b ratio
- Non-noble metal oxide in the place of noble metal Ru

Scibioh et al., Appl. Catal. B. Environ. 84 (2008) 773-783

Pt-Ceria Anode Catalyst

Performance test: Nyquist plots

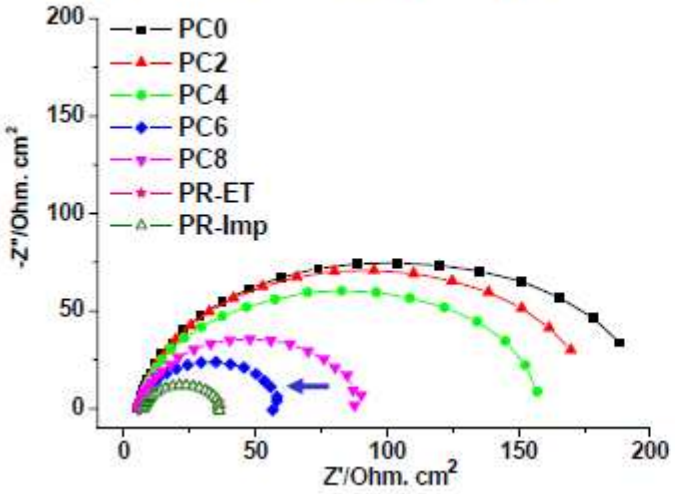

Stability Test: Chronoamperometry

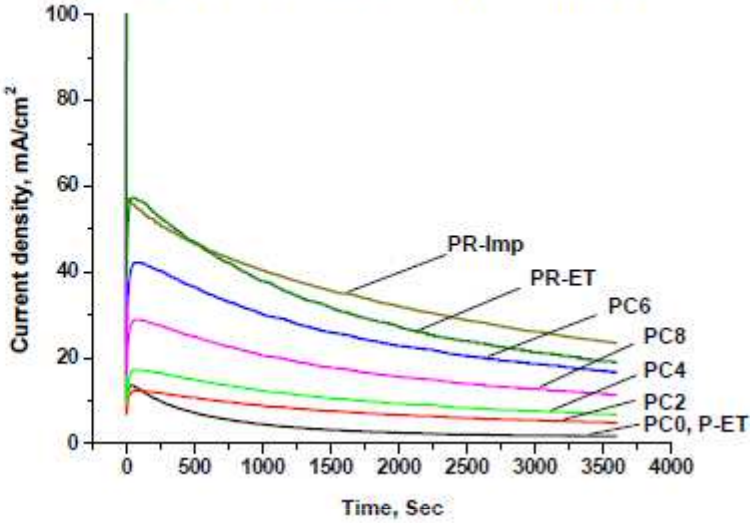

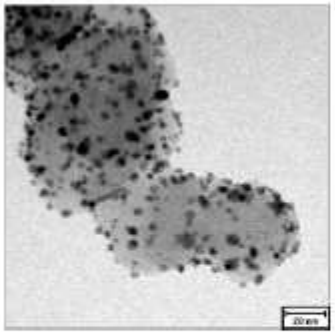

PC0

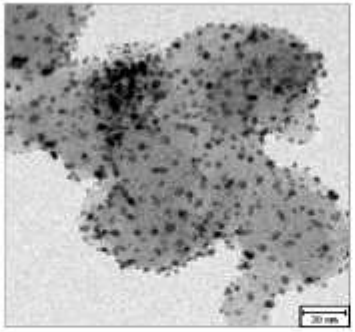

PC6

Catalyst	Particle Size, n m (TEM)	ESA (m^2/g)
P-ET	4.0	48
PC0	3.7	50
PC2	3.5	53
PC4	3.5	55
PC6	3.0	60
PC8	3.0	57
PR-Imp	3.5	61
PR-ET	2.6	63

- **Enhanced Electrochemical Active Surface Area (ESA)**

Scibioh et al., Appl. Catal. B. Environ. 84 (2008) 773-783

CATHODE RESEARCH – MAIN FOCUS

- Selective cathode catalyst and/or
- methanol-tolerant catalyst for oxygen reduction

ORR: $O_2 + 4H^+ + 4e^- \rightarrow 2H_2O$ E_r=1.229 V

ORR- At Fuel Cell Electrodes- Associated Issues

Acid Electrolyte Conditions

- Reaction takes place at high, positive potentials – hence most metals dissolve
- Only noble metals and some of their alloys

Even with Pt!

- Formation of surface oxide
- Complications - PtO_2 is a catalyst for H_2O_2 reduction
- Involvement of high potentials - sintering

Essentially, Metal dissolution & oxide formation

Catalysts for oxygen electro-reduction

Noble metal catalysts

Pt & certain Pt alloys
Amounts allowable (for the air electrode) would not produce currents required for commercial success at the desired cell terminal voltage

Attempts

(i) Improve the activity at high positive potentials
(ii) Develop non-noble metal complex catalysts – macrocyclic organometallic chelates

State of the art cathode catalysts

Methanol tolerant catalyst

Metal phthalocynines, porphyrins, metal oxides,
metal carbides & chalcogenides

ORR activity & methanol tolerant capability, but the life-time still need to improve

To improve ORR activity

Pt-Alloy catalysts

Pt–Co/C, Pt–Cr/C, Pt–Ni/C, Pt–Fe/C and Pt–Cr–Co/C

Our Directions

Pt-Ceria Cathode Catalyst

Our Focus

Increasing air utilization in the cathode

Incorporation of oxygen storage materials

Why Ceria?

The ability of ceria to store, transport and release oxygen

$$CeO_2 \leftrightarrow CeO_{2-x} + (x/2)\, O_2 \qquad (0 \leq x \leq 0.5)$$

Unique & delicate balance between structural (phase formation), kinetic (rate of shift between reduced & oxidized states ($Ce^{3+} \leftrightarrow Ce^{4+}$), and textural (presence of surface cerium sites) factors

Ceria functions as an oxygen buffer

Pt-Ceria Cathode Catalyst

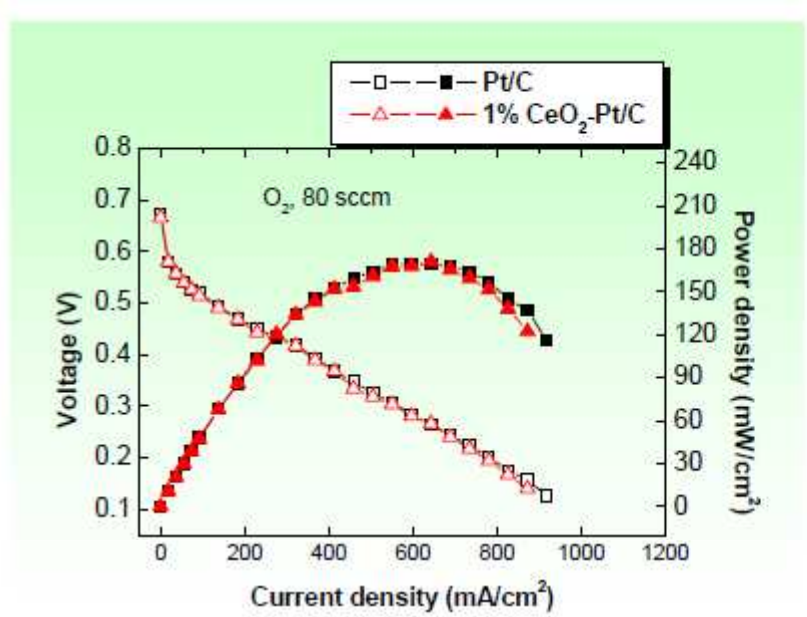

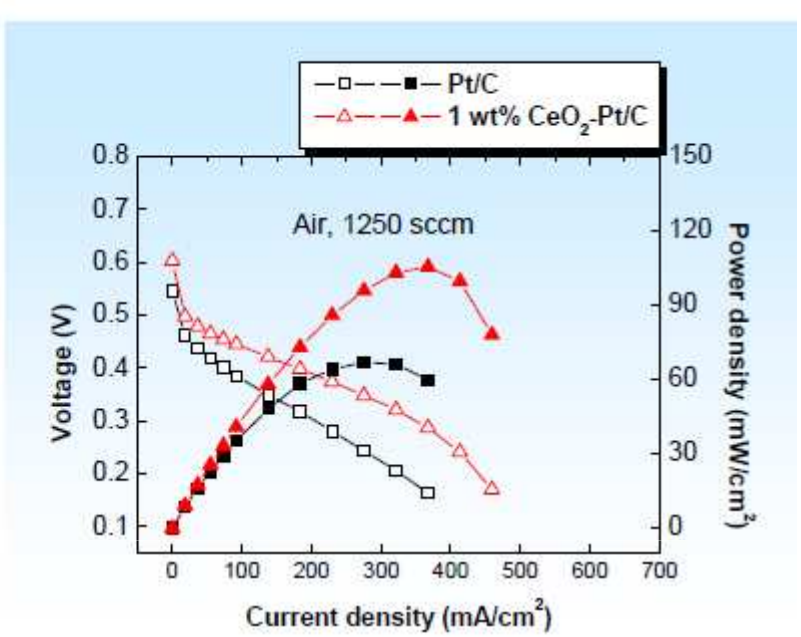

TEM image

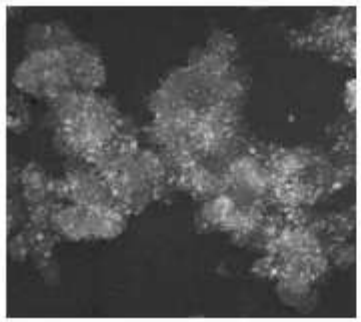

Incorporation of nanophase ceria (CeO_2) into the cathode catalyst Pt/C increases the local oxygen concentration at air atmosphere leading to enhanced single-cell performance of DMFC.

Role of Ceria in ORR at Air

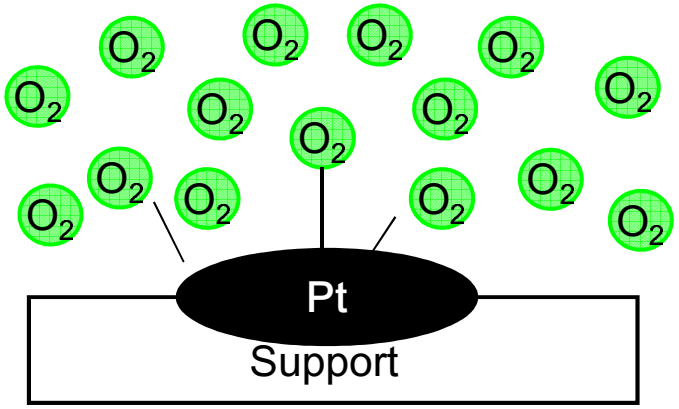

(a) Oxygen

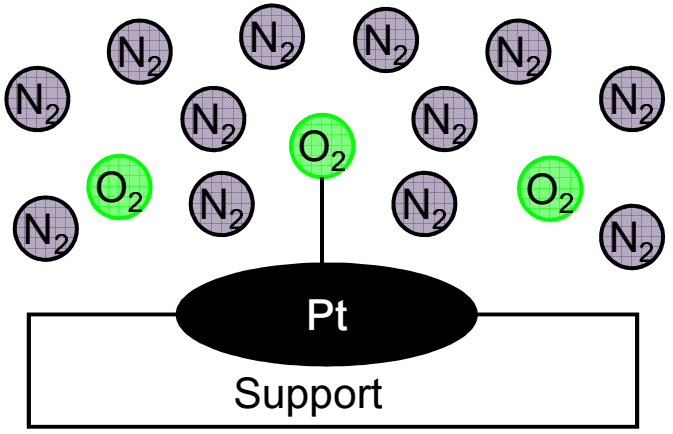

(b) Air

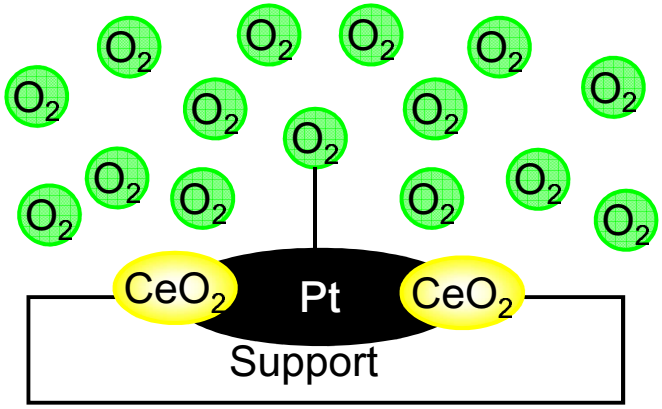

(a) Oxygen

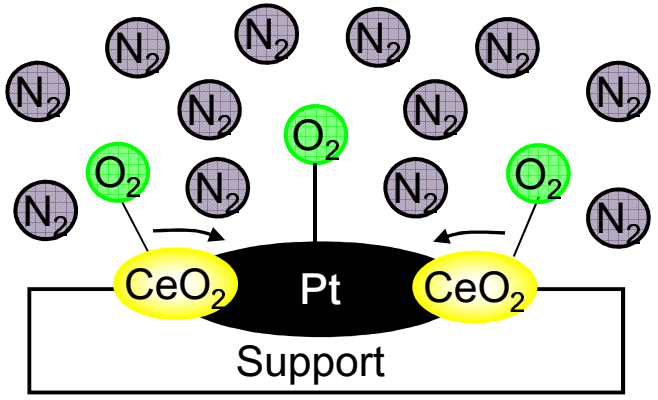

(b) Air

CeO_2- and $Ce_{0.8}Sm_{0.2}O_2$-Modified Pt/C Catalysts for Cathode of a DMFC

Catalyst Preparation – Impregnation Method

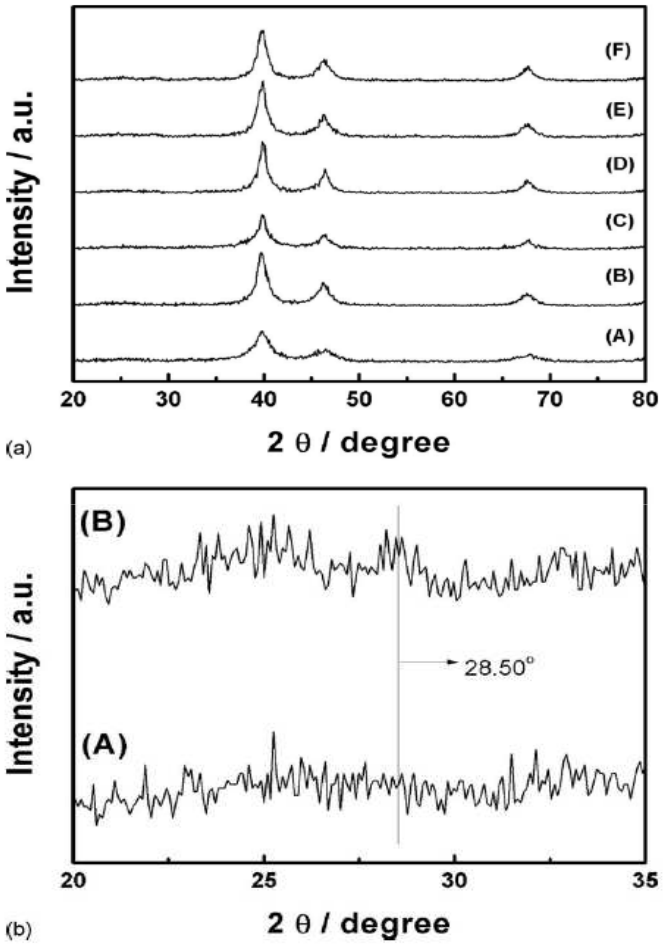

Figure 1. (a) XRD pattern of (A) Pt/C, (B) 1 wt % CeO_2, (C) 1 wt % $Ce_{0.8}Sm_{0.2}O_2$, (D) 2 wt % $Ce_{0.8}Sm_{0.2}O_2$, (E) 5 wt % $Ce_{0.8}Sm_{0.2}O_2$, and (F) 7 wt % $Ce_{0.8}Sm_{0.2}O_2$-modified Pt/C. (b) XRD pattern of (A) 1 wt % $Ce_{0.8}Sm_{0.2}O_2$ and (B) 7 wt % $Ce_{0.8}Sm_{0.2}O_2$-modified Pt/C in the 2θ range from 20 to 35°.

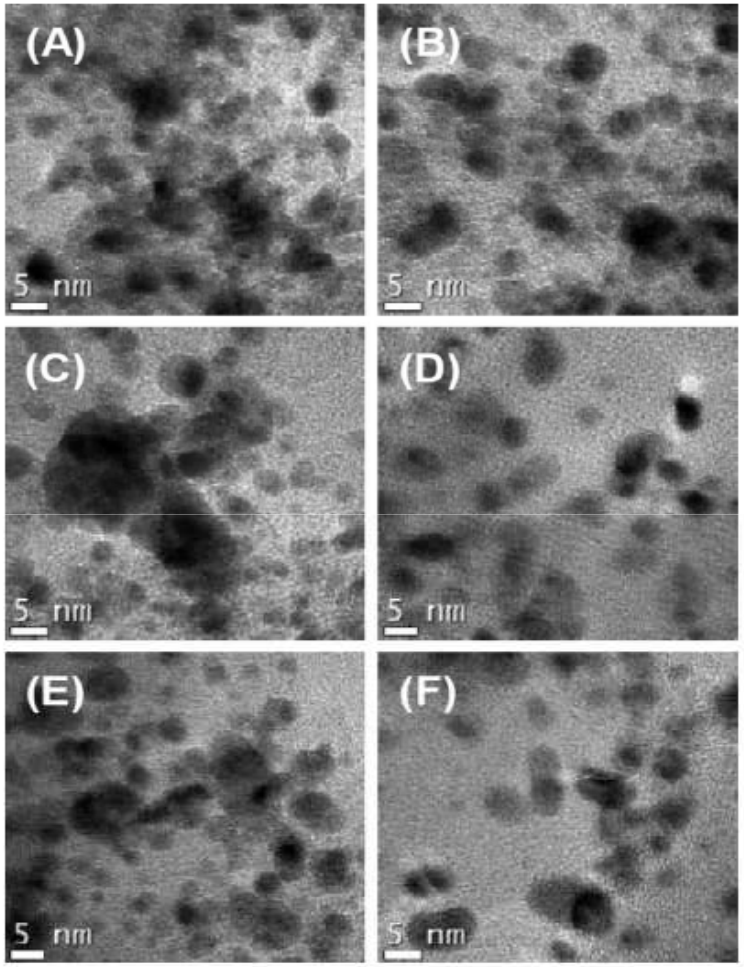

Figure 2. HRTEM images of (A) Pt/C, (B) 1 wt % CeO_2, (C) 1 wt % $Ce_{0.8}Sm_{0.2}O_2$, (D) 2 wt % $Ce_{0.8}Sm_{0.2}O_2$, (E) 5 wt % $Ce_{0.8}Sm_{0.2}O_2$, and (F) 7 wt % $Ce_{0.8}Sm_{0.2}O_2$-modified Pt/C.

J. Electrochem. Soc., 156 7 B801-B805 2009

CeO_2- and $Ce_{0.8}Sm_{0.2}O_2$-Modified Pt/C Catalysts

Ability of Methanol Tolerance

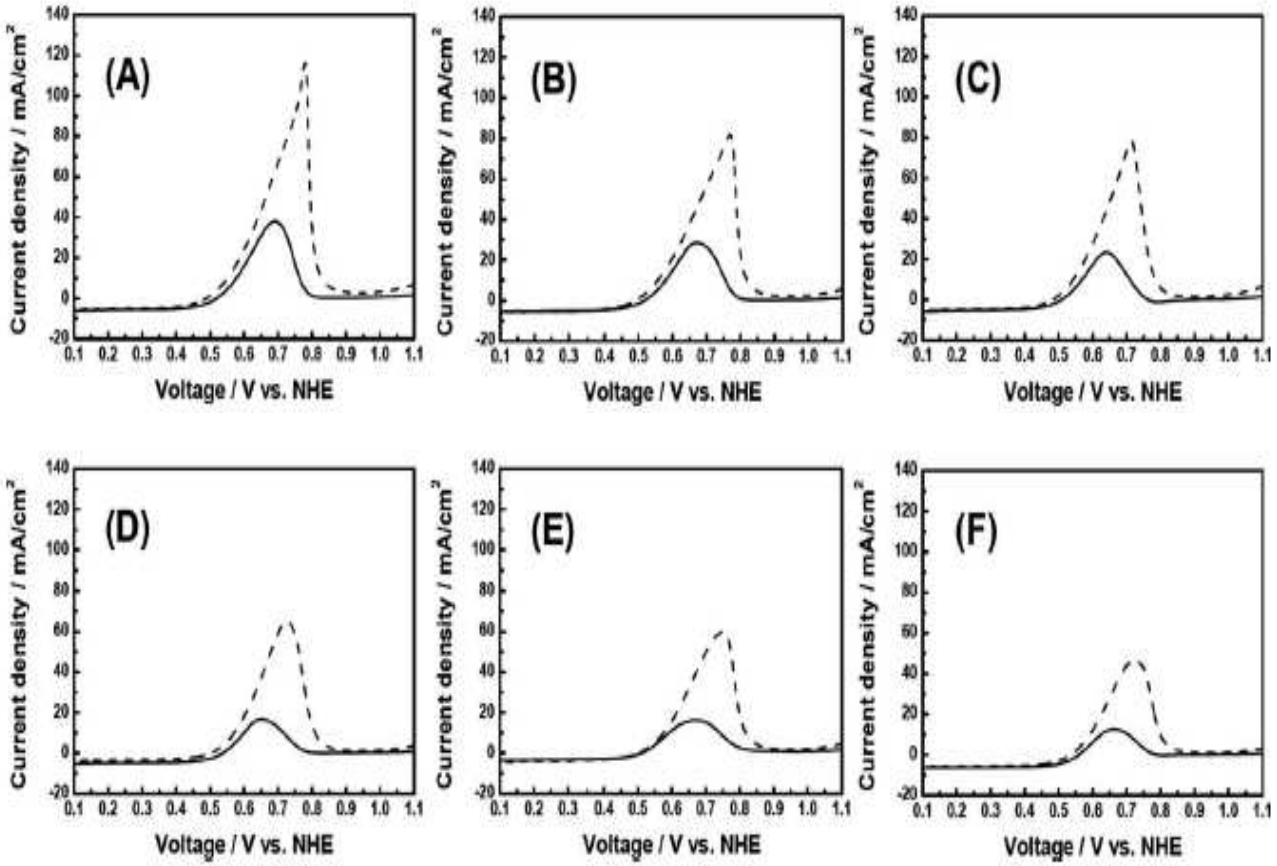

Figure 4. LSV curves for (A) Pt/C, (B) 1 wt % CeO_2, (C) 1 wt % $Ce_{0.8}Sm_{0.2}O_2$, (D) 2 wt % $Ce_{0.8}Sm_{0.2}O_2$, (E) 5 wt % $Ce_{0.8}Sm_{0.2}O_2$, and (F) 7 wt % $Ce_{0.8}Sm_{0.2}O_2$-modified Pt/C on the RDE in oxygen-saturated 0.5 M H_2SO_4 + 0.1 M CH_3OH (—, solid line) and 0.5 M H_2SO_4 + 0.5 M CH_3OH (– – –, dashed line) mixture at a scan rate of 5 mV s^{-1}.

J. Electrochem. Soc., 156 7 B801-B805 2009

CeO_2- and $Ce_{0.8}Sm_{0.2}O_2$-Modified Pt/C Catalysts for Cathode of a DMFC

ORR Activity

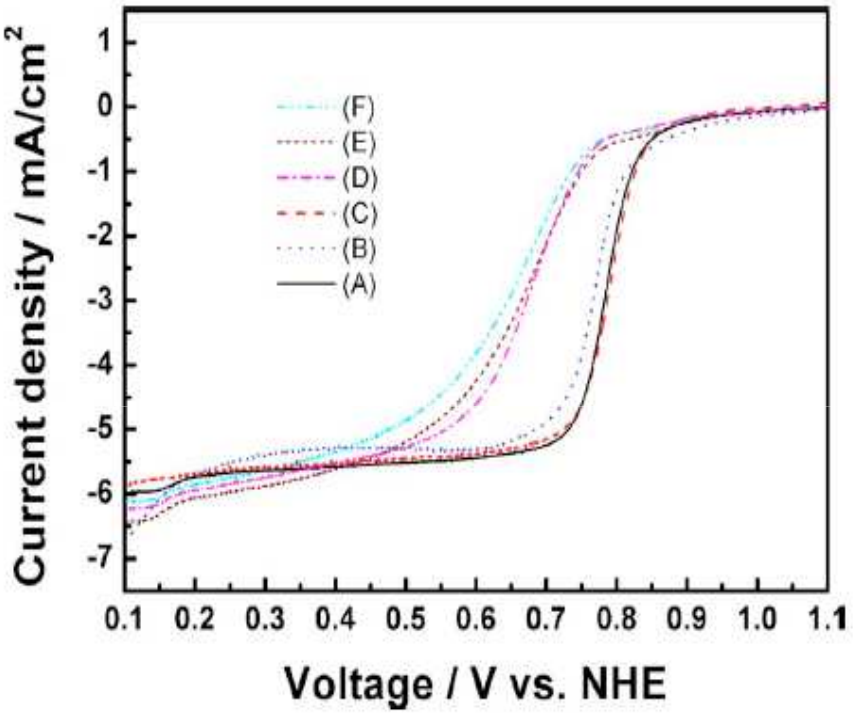

Figure 5. (Color online) LSV curves for (A) Pt/C, (B) 1 wt % CeO_2, (C) 1 wt % $Ce_{0.8}Sm_{0.2}O_2$, (D) 2 wt % $Ce_{0.8}Sm_{0.2}O_2$, (E) 5 wt % $Ce_{0.8}Sm_{0.2}O_2$, and (F) 7 wt % $Ce_{0.8}Sm_{0.2}O_2$-modified Pt/C on the RDE in oxygen-saturated 0.5 M H_2SO_4 solution at a scan rate of 5 mV s^{-1}.

DMFC Performance

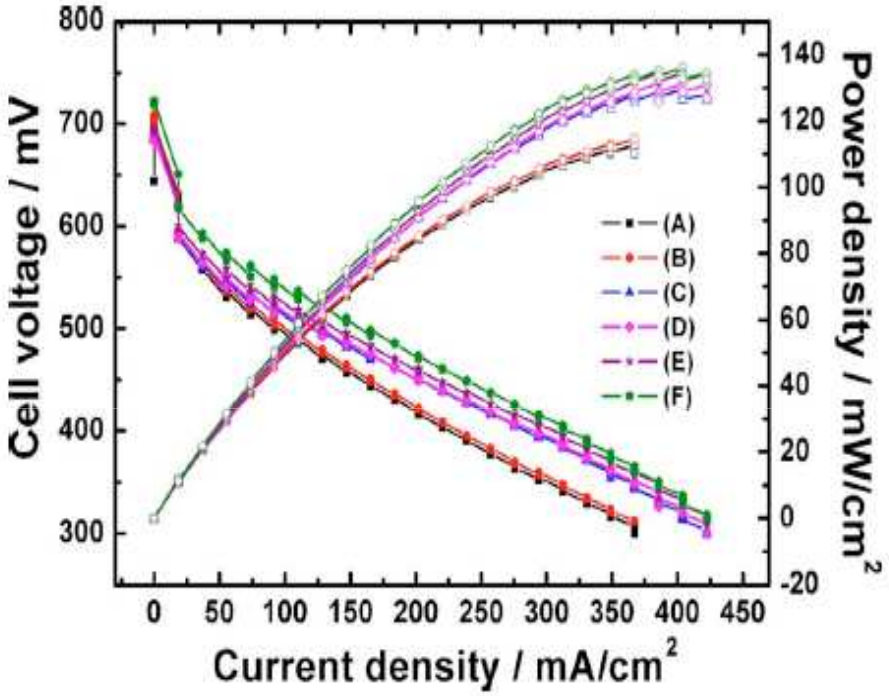

Figure 6. (Color online) The DMFC polarization curves for (A) Pt/C and (B) 1 wt % CeO_2, (C) 1 wt % $Ce_{0.8}Sm_{0.2}O_2$, (D) 2 wt % $Ce_{0.8}Sm_{0.2}O_2$, (E) 5 wt % $Ce_{0.8}Sm_{0.2}O_2$, and (F) 7 wt % $Ce_{0.8}Sm_{0.2}O_2$-modified Pt/C with 1.0 M CH_3OH fed to anode and dry air fed to cathode at 80°C.

Optimizations of MEAs

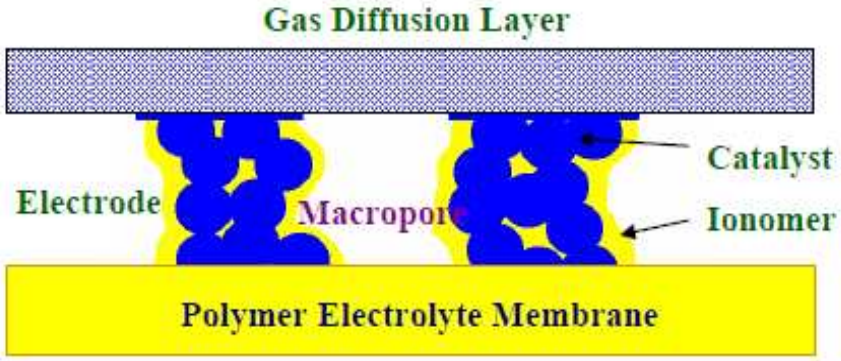

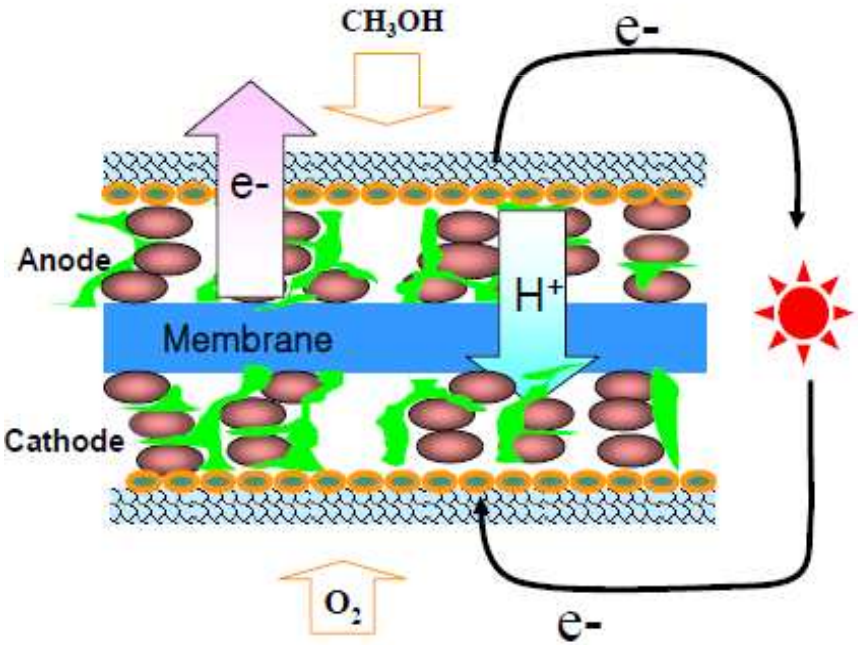

- Optimize ionomer content of catalyst layer
- Reduce thickness of catalyst layer
- Increase porosity of electrode
- Reduce charge and mass transfer resistance
- Increase hydrophobicity of catalyst layer to facilitate water removal from the cathode

Effect of Ionomer Content (Supported Catalyst)

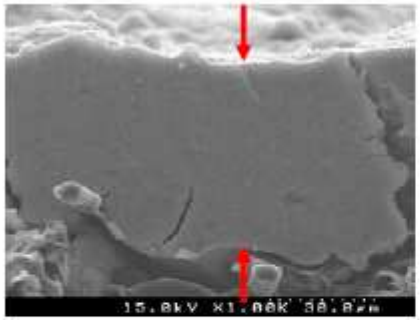

Thickness of the catalyst layer = 55 μm

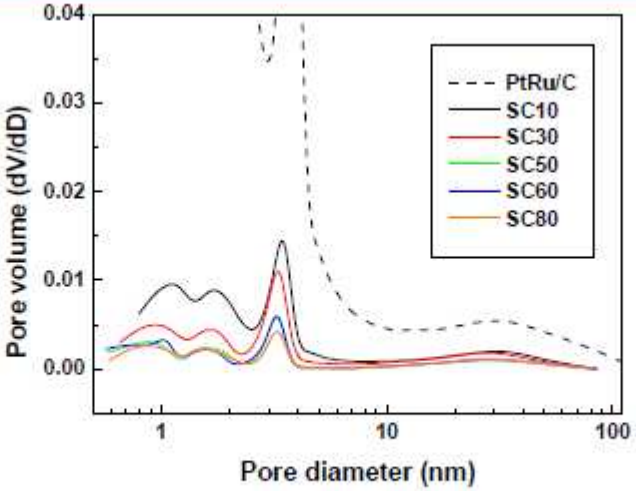

Electrode	Electrochemical active surface area (m^2/g)
SC10	1.9
SC30	3.1
SC50	7.9
SC60	10.1
SC80	10.6

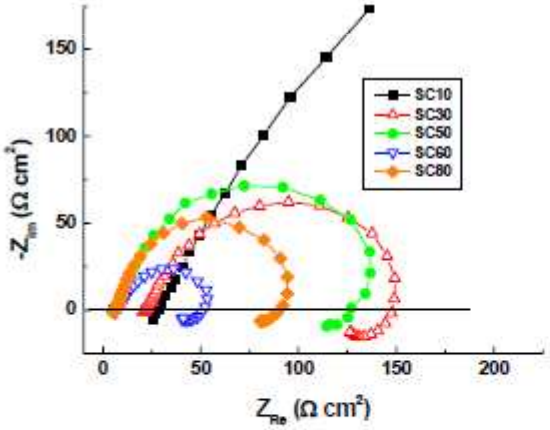

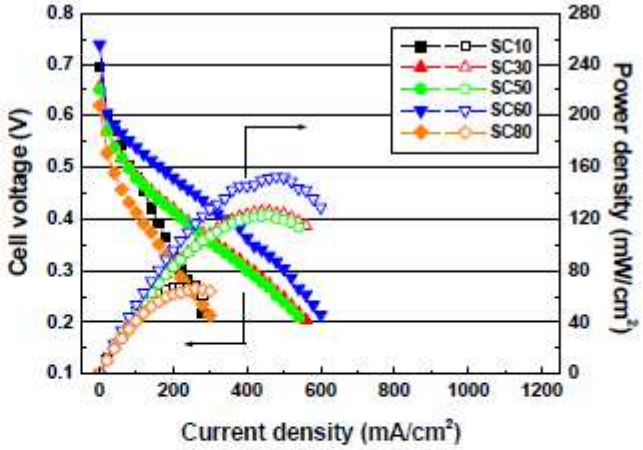

- Pore volume decreases with increasing the ionomer content
- Ionomer content affects pore active surface area and charge and mass transport resistances
- Maximum performance was observed at SC60

Effect of Ionomer Content (Black Catalyst)

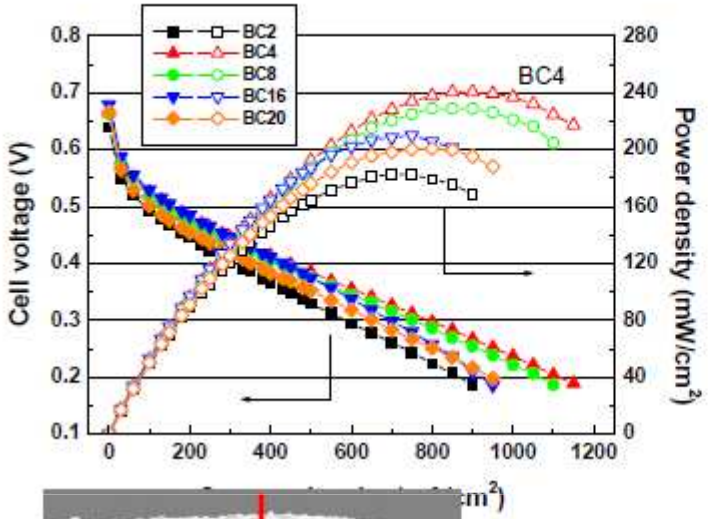

Electrode	Relative area of H_2 oxidation peak*
BC2	2.00 (21.3 m^2/g)
BC4	2.96 (31.5 m^2/g)
BC8	3.00 (31.9 m^2/g)
BC16	1.91 (20.3 m^2/g)
BC20	1.90 (20.2 m^2/g)

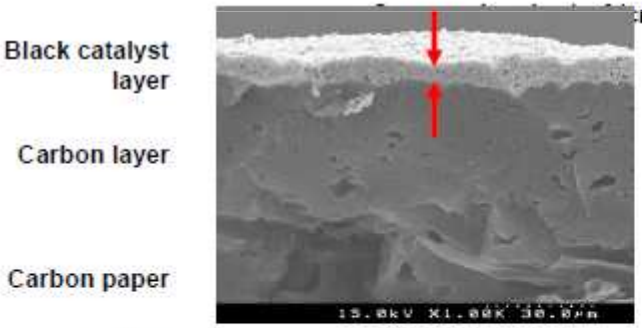

Thickness of the catalyst layer = 5.6 μm

- Maximum performance at around 4 and 8 wt.% of ionomer for the black catalyst
- Higher performance due to the smaller thickness of the black catalyst layer (1.6 ~ 6.5 μm) than that of the supported catalyst layer (55 μm)

Proton Exchange Membranes

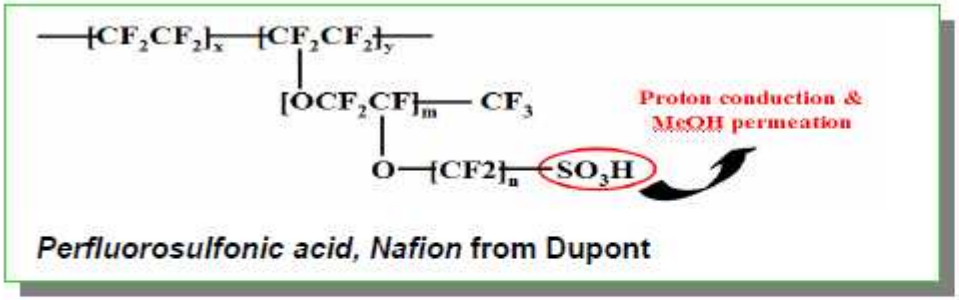

Perfluorosulfonic acid, Nafion from Dupont

- MeOH crossover from anode to cathode

  - Mixed potential
  - Poisoning of Pt catalyst
  - Loss of fuel
  - Increase air demand in cathode
  - Reduction of efficiency

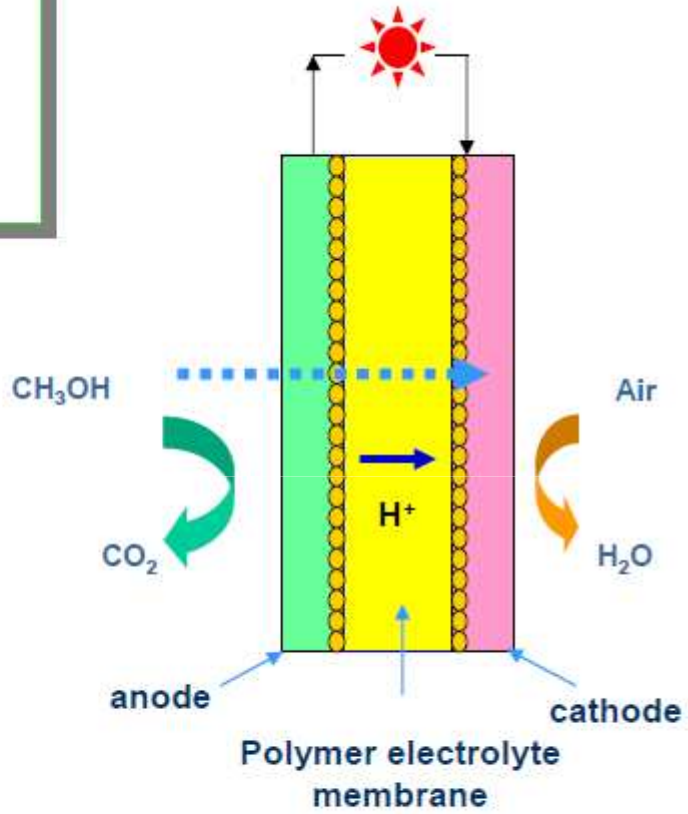

Decrease cell performance

Nano-Silica Layered Membranes

- **Strategies & objective**
  - To reduce methanol crossover by depositing a silica layer on the surface of Nafion membrane
- **Experimental**
  - PECVD of silica with silicon ethoxide in the chamber at 1- 500 mtorr with a 10-500W RF power at room temp.

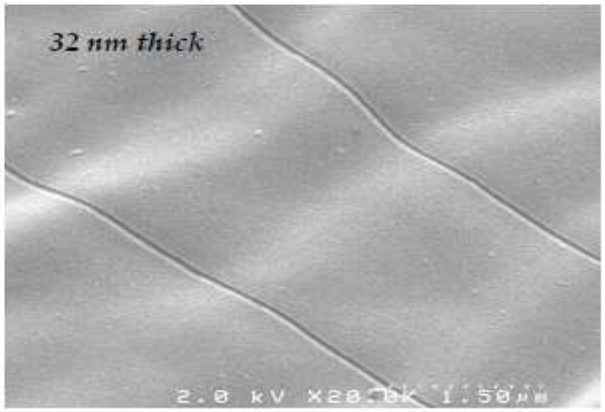

	Selectivity	Ion conductivity (S/cm)	Methanol permeability (cm^2/sec)
Nafion 115	35	0.098 (100%)	2.77×10^{-6} (100%)
10 nm	54	0.091 (92%)	1.68×10^{-6} (61%)
32 nm	83	0.076 (78%)	9.09×10^{-7} (33%)
68 nm	83	0.077 (79%)	9.21×10^{-7} (33%)

CF = characteristic factor = IC/MP * 10^3

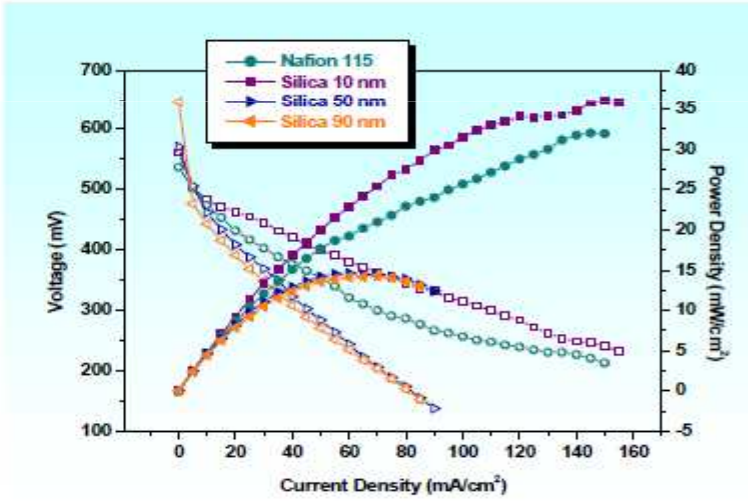

Ion conductivity of the 10 nm-Nafion/silica composite membrane was similar to the unmodified Nafion membrane, but its methanol permeability was reduced by about 40%. And performance of the cell with silica composite membrane was higher than that of the Nafion membrane.

SEM Pictures 1 (Surface)

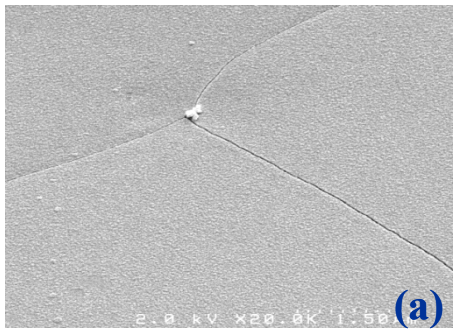

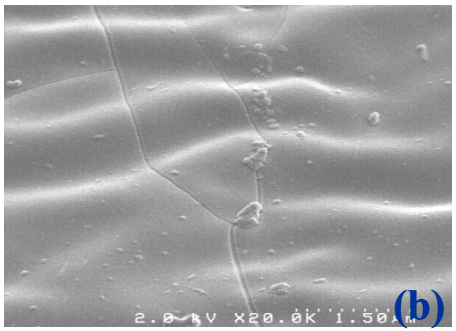

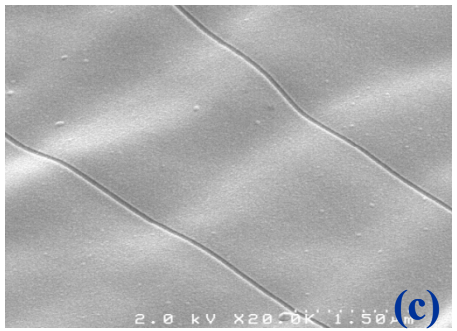

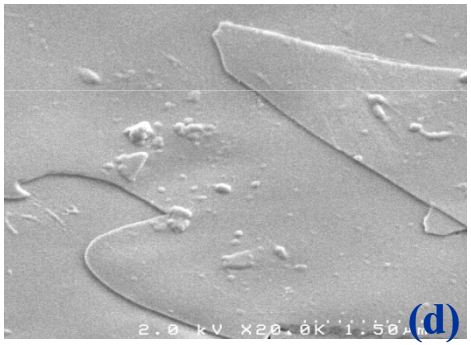

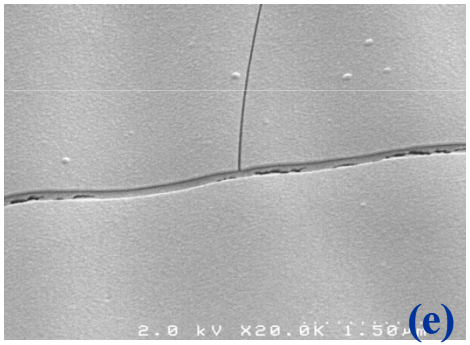

SEM images(×20,000) of the surface of the Nafion/silica composite membranes

(a) Silica-10 nm (b) Silica-30 nm (c) Silica-50 nm (d) Silica-70 nm (e) Silica-90 nm

SEM Pictures 2 (Cross Section)

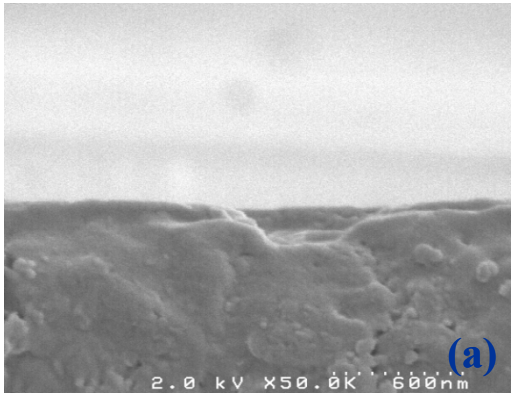

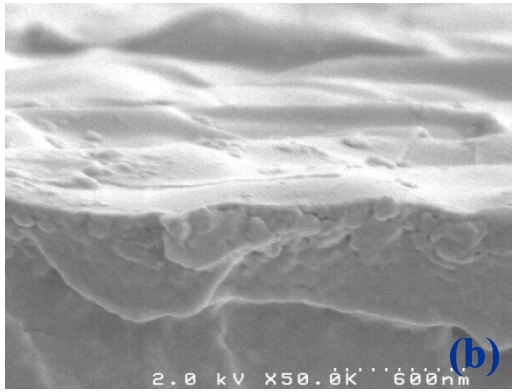

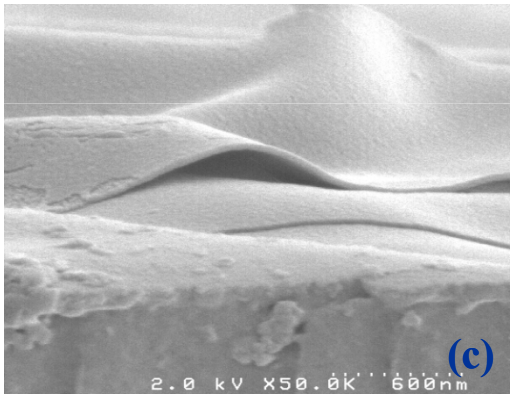

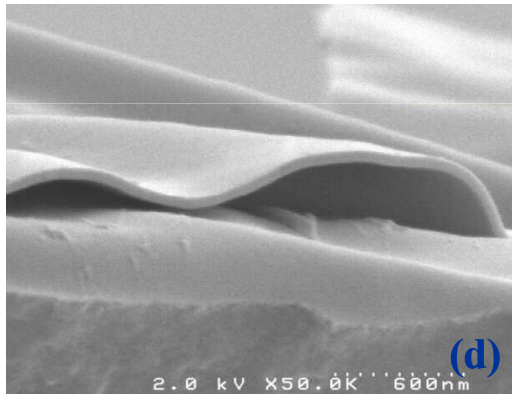

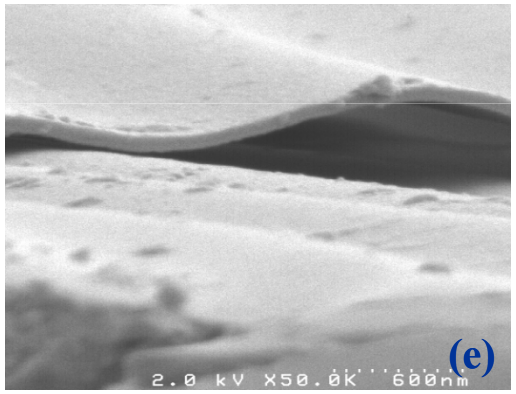

SEM images(×50,000) of the cross section of the Nafion/silica composite membranes

(a) Silica-10 nm (b) Silica-30 nm (c) Silica-50 nm (d) Silica-70 nm (e) Silica-90 nm

Durability of DMFC

- Loss of active electrocatalyst surface area by poisoning or sintering
- Loss of hydrophobic properties of gas diffusion electrodes
- Ruthenium crossover from anode to cathode through the membrane
- Loss of interfacial properties of membrane/electrode (or delamination)
- Loss of cathode activity due to surface oxide formation

Focus of this Study

1. Investigation of the degradation phenomena in DMFC
2. Investigation of the effects of operating conditions
3. Exploration on the recovery techniques

Int. J. Hydrogen. Energy, 34 (2009) 2043-2051

Experimental – Life Time Study

- **Catalyst, Membrane and MEA**
  - Anode = Pt-Ru (1:1), Johnson-Matthey
  - Cathode = Pt , Johnson-Matthey
  - Nafion 115
  - MEA = 3mg/cm^2 Pt-Ru/3mg/cm^2-Pt, 10.9cm^2

- **Operation condition**

  Cell temperature 80 ^{o}C, 1 atm

  Anode: 0.5M methanol solution

  Cathode: dry air 500sccm

- **Characterization**
  - ✓ AC impedance - frequency range 50m-5K Hz;
  - ✓ Excitation potential 5mV (IM6, Zahner)
  - ✓ Half Cell test
  - ✓ Methanol conc with Gas Chromatograph
  - ✓ CO_2 analyzer from Vaisala

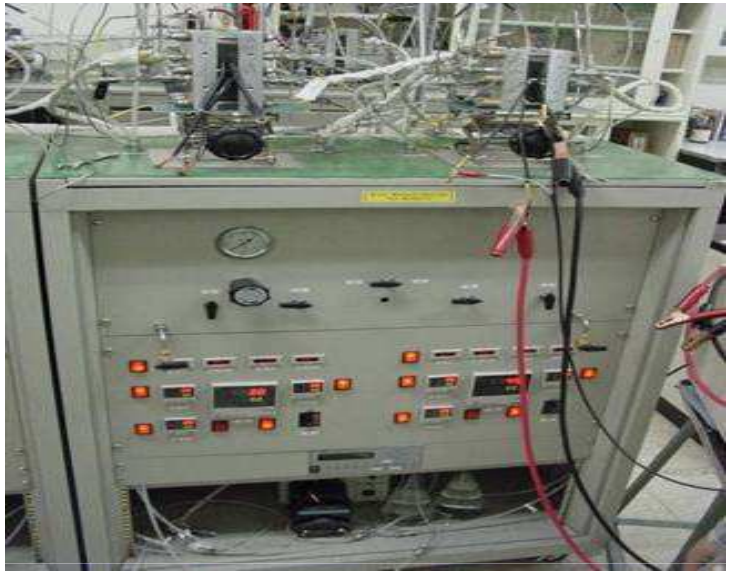

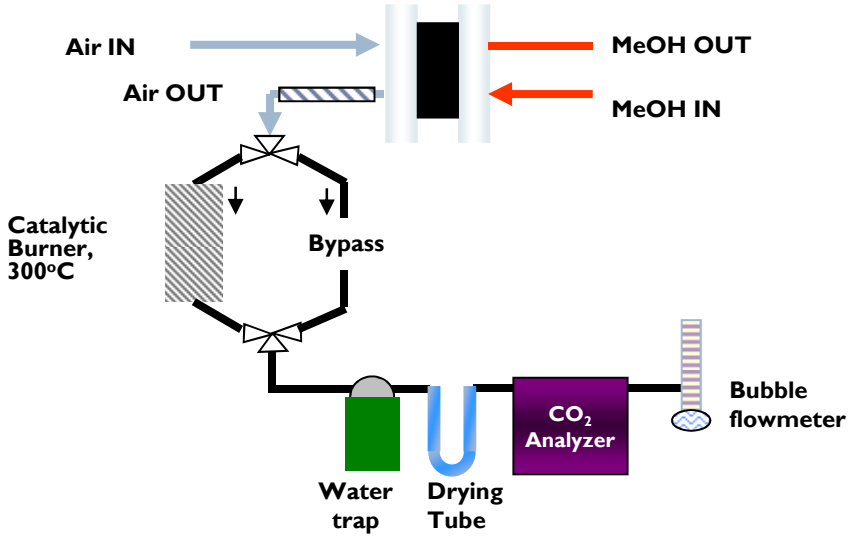

Degradation of DMFC Performance

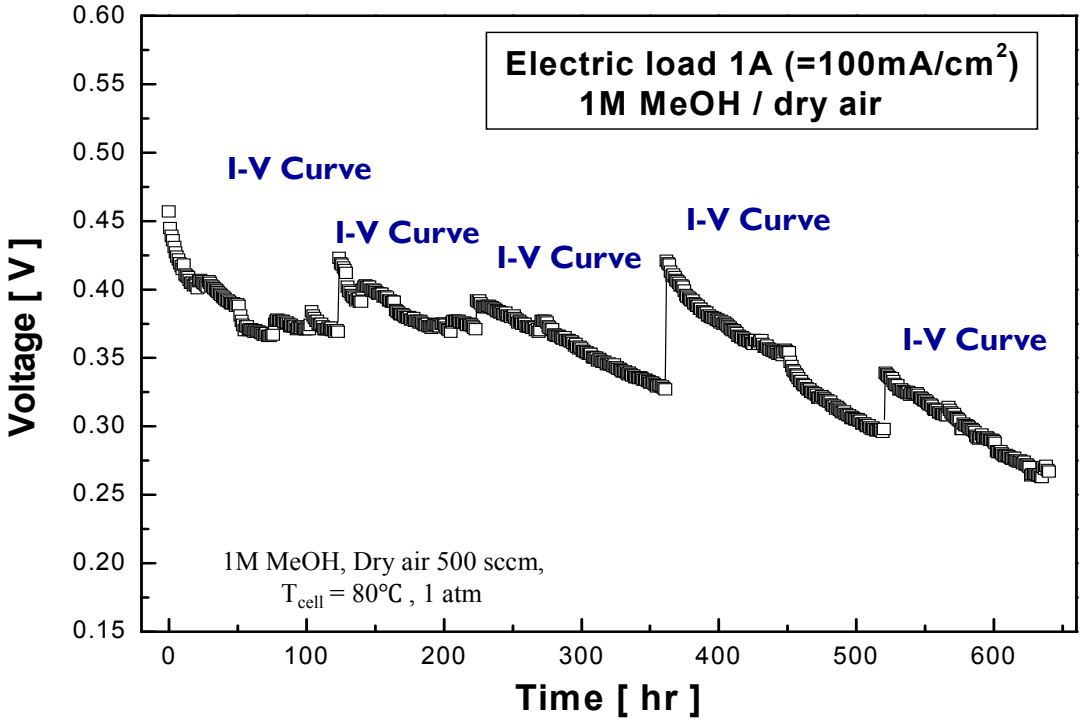

- DMFC performance decreases with increasing operation time.
- Intermittent on-off and changes in operating conditions help to restore the cell performance

Time Dependence of Cell Performance

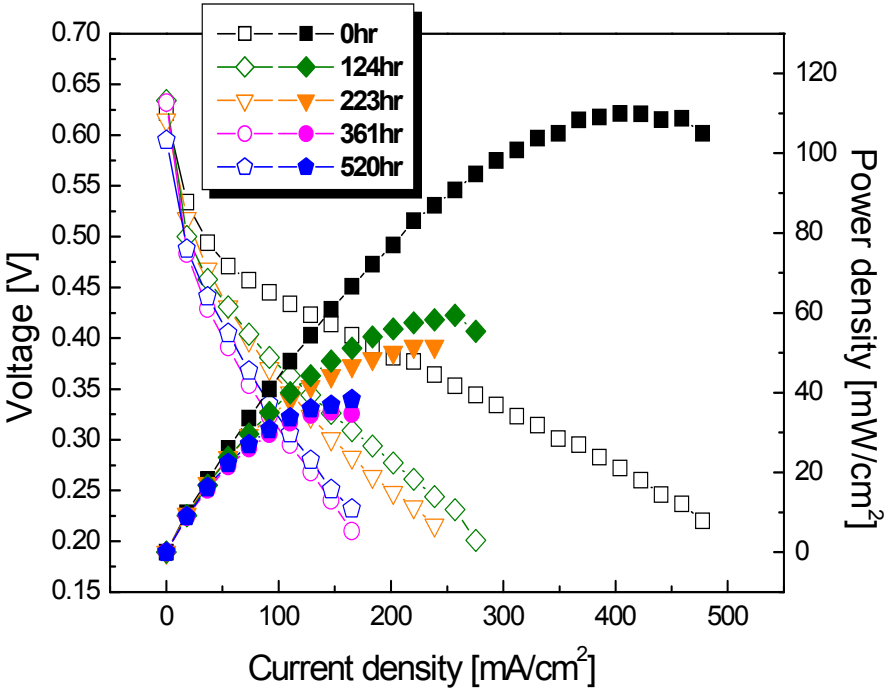

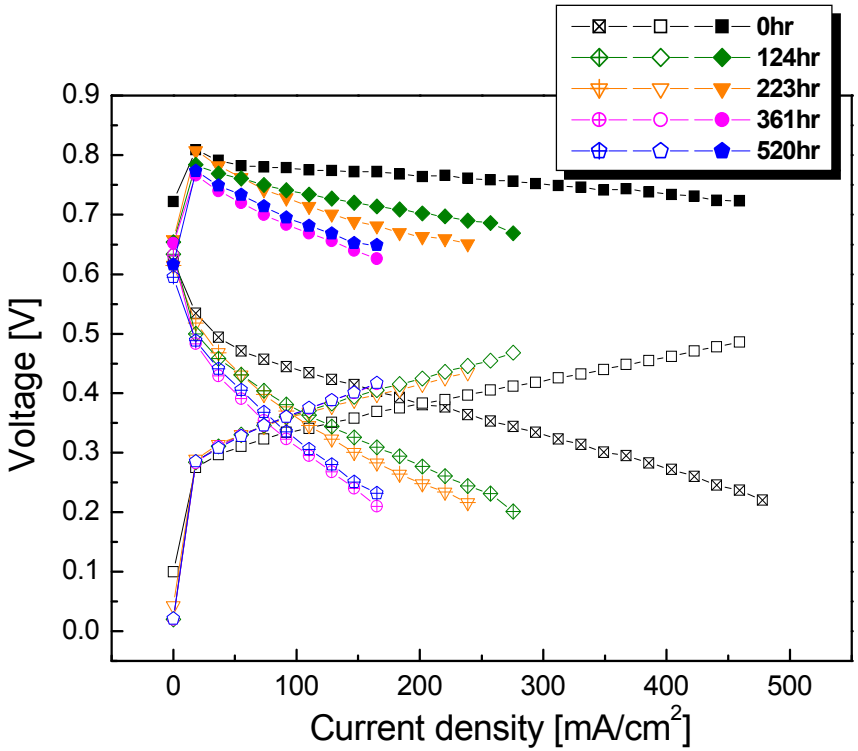

- Cell performance decreases with time
- Degradation is more prominent in the cathode than in the anode

Time Dependence of Impedance

Nyquist plot . Galvano static mode. current = 1A

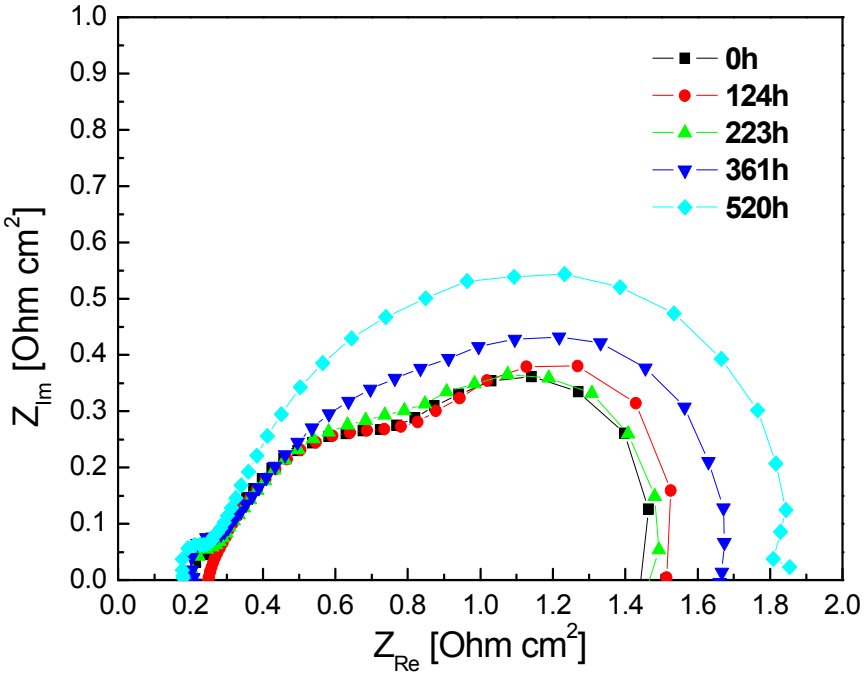

[Fuel cell impedance]

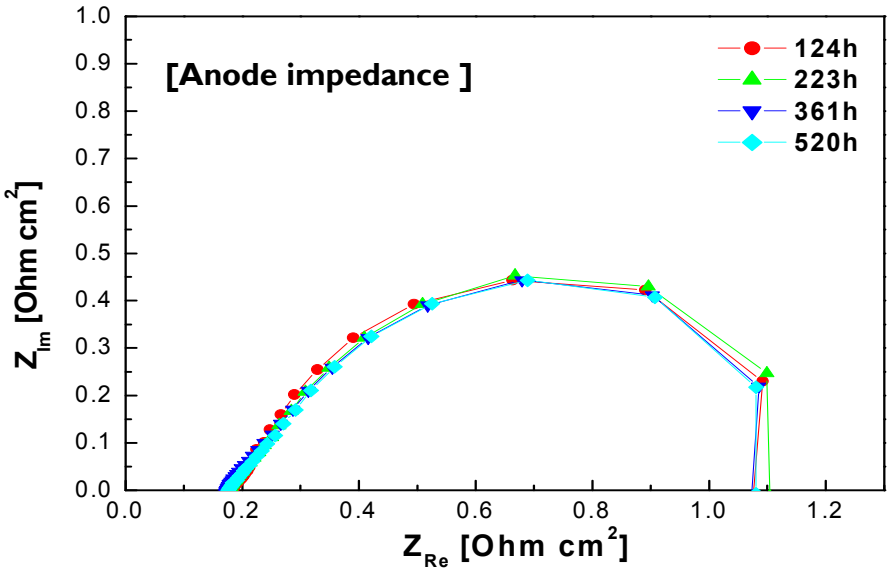

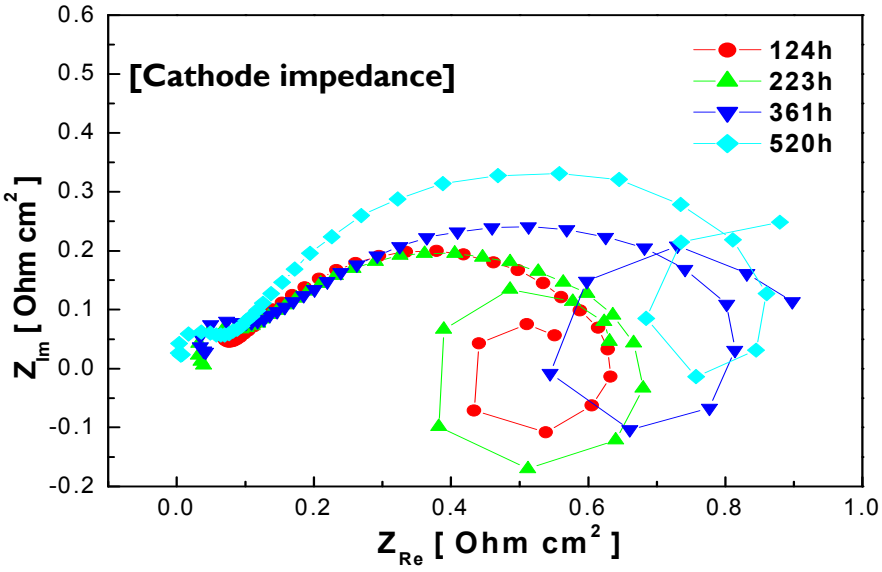

[Half cell: anode 1M MeOH / cathode wet H_2 200sccm]

Clear evidence that the internal resistance of

- **The overall cell increases as time goes on.**
- **Same is the case with cathode.**

SEM Analysis

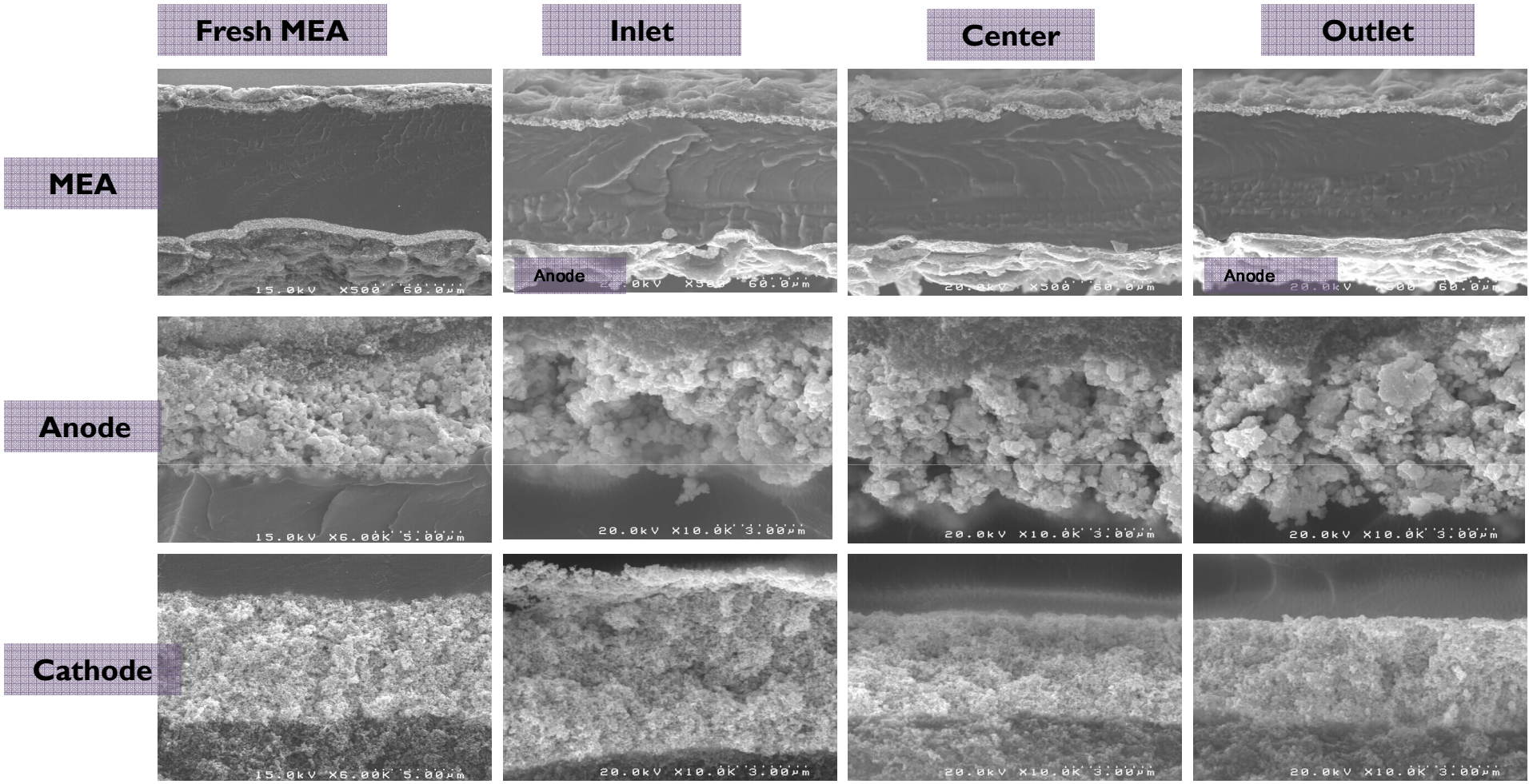

- There is no big change in the cathode layer
- There are appreciable change in the anode structure, the change appears severe at the anode outlet

TEM Pictures

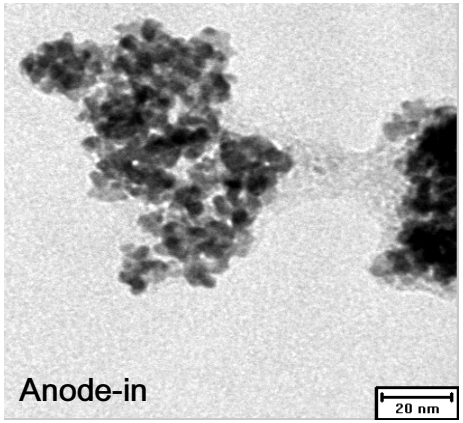

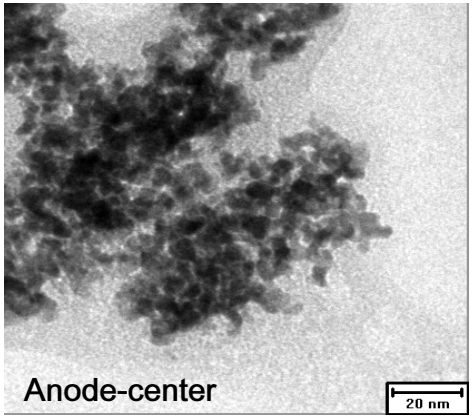

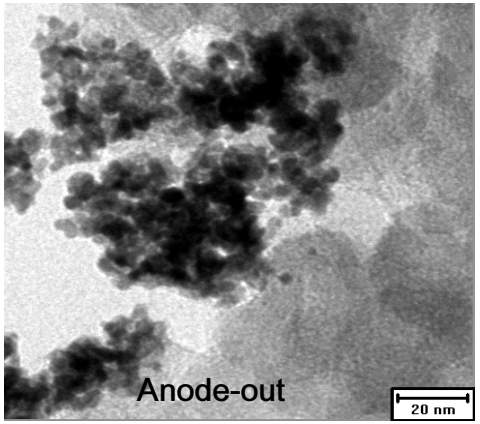

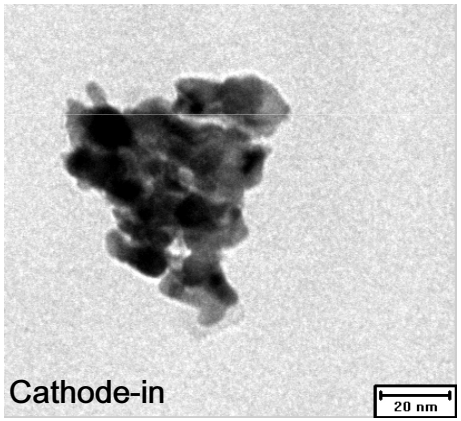

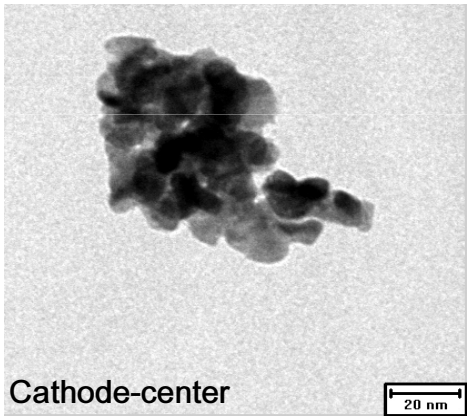

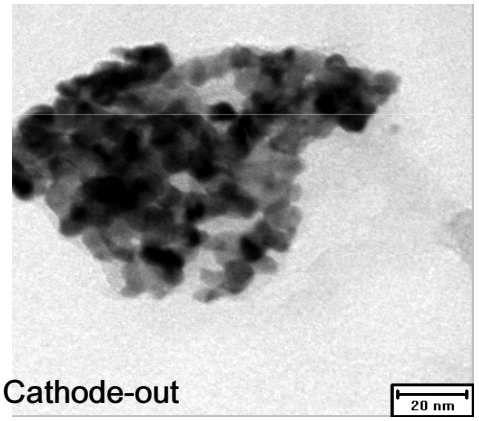

The particle size is higher at the outlet regions

	Anode (nm)	Cathode (nm)
Fresh	2.5	6.6
IN	3.0	7.0
Center	3.3	7.1
OUT	3.6	7.5

Hydrophobicity of the GDL

✓ Pristine Carbon Paper (with GDL)
142.4°

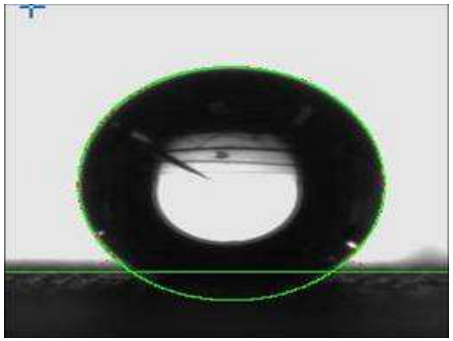

After 300 hrs

✓ Anode In (300 hr)
141.75°

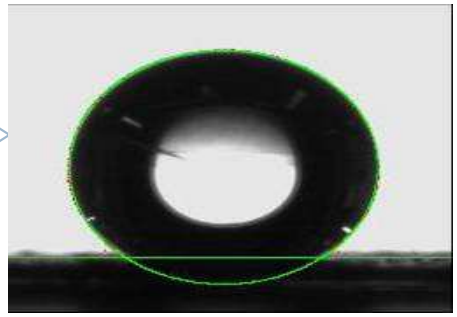

✓ Anode Out (300 hr)
124.4°

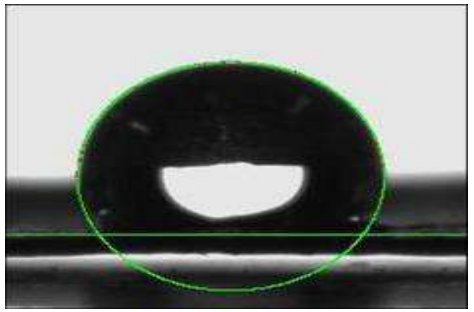

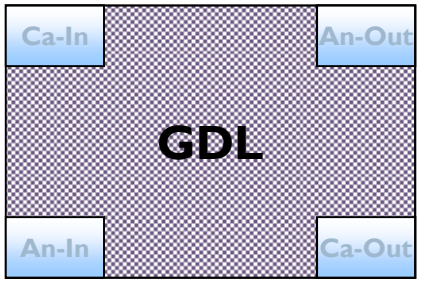

✓ Cathode In (300 hr)
144.6°

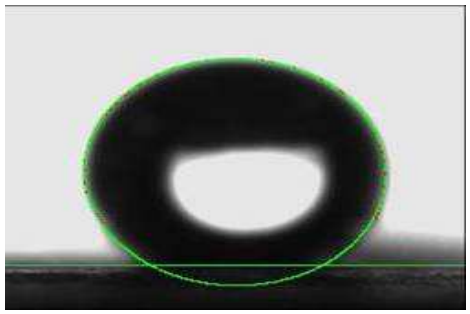

✓ Cathode Out (300 hr)
125.8°

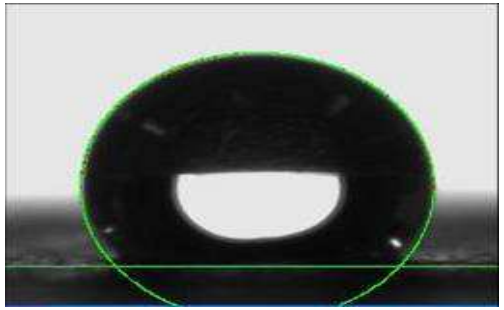

- The extent of the change in the contact angle of the used GDL depends on the positions
- The outlet GDL for both anode & cathode experienced an appreciable decrease in the contact angle by 15°.
- The contact angle of the inlet GDLs remained unchanged

MeOH in Cathode Effluent

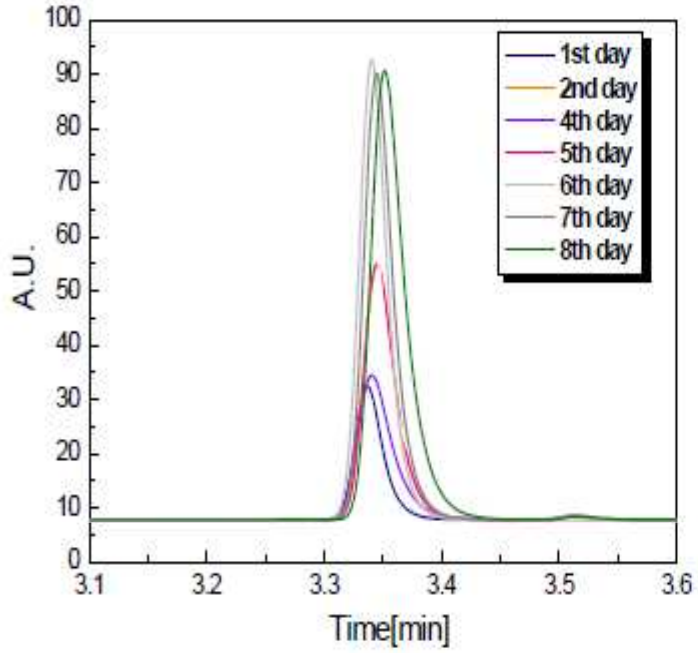

GC chromatograms of methanol in the cathode effluent

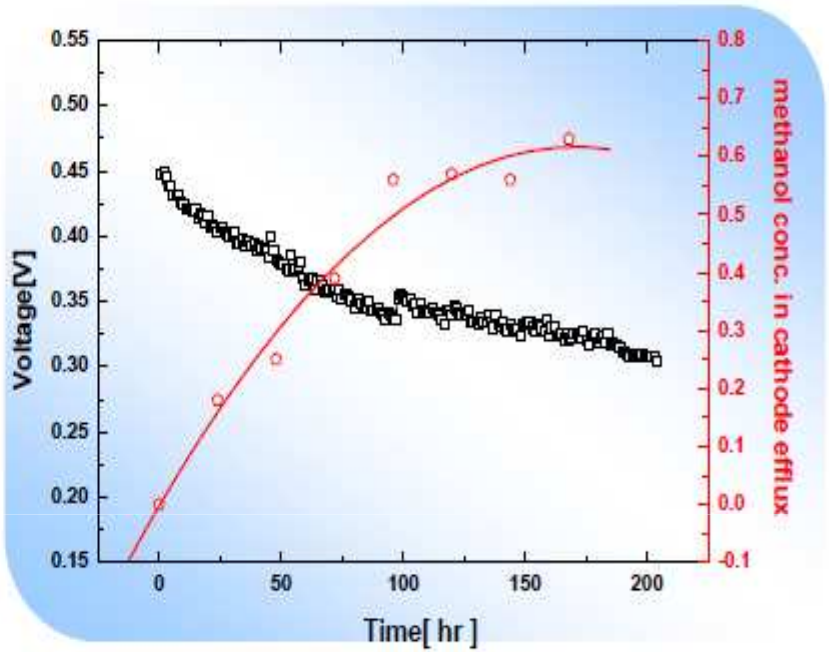

An : 1M MeOH 5 cc/min

- Ca : Dry air 500 sccm

➢ As time goes on, the unreacted MeOH at the cathode increases, probably because of deactivation of cathode catalysts

CO_2 Mass Balance in the anode and cathode

Operating time (hr)	CO_2 Flux (10^{-7} mol/sec/cm^2)			
	Anode outlet	Cathode outlet	An + Ca	CO_2 Flux through the membrane
0	0.948	0.700	1.648	0.097
70	1.182	0.431	1.613	0.105
Remark	Increase	Decrease	constant	Increase

<Test conditions>

- 0.5M MeOH 3cc/min, Dry air 100sccm , Electric load 100mA/cm^2

- As time elapses, CO_2 con. in the cathode stream decreases, but the CO_2 in anode stream increases
- The total amount of CO2 in the anode and cathode streams remains constant

Effect of Operating Voltage

Current variation at constant voltages in the PEMFC conditions

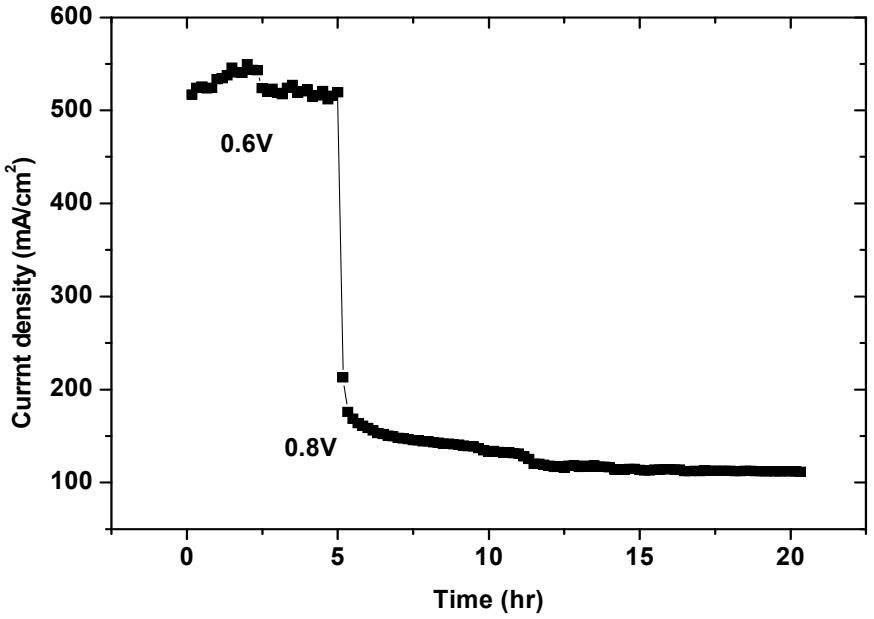

Long-term test at constant voltages of 0.3V and 0.5V, respectively

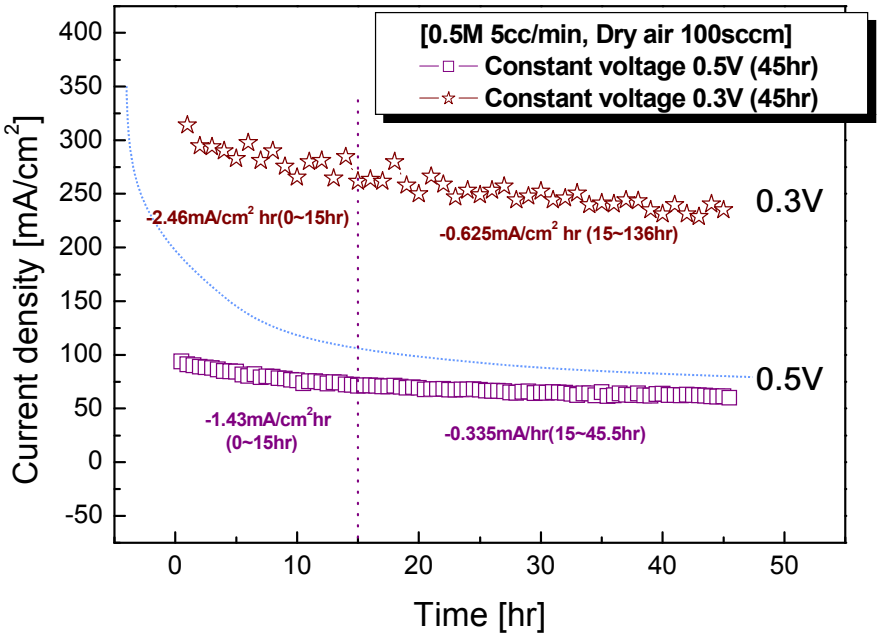

Cell : 80℃, 11 cm^2

3 mg/cm^2 PtRu, Humidified H_2, / 3 mg/cm^2 Pt, Humidified Air

At 0.8V, the decay rate is higher than at 0.6V due to cathode Pt oxidation

Op. Voltage (V)	Decay Rate (mA/cm^2/hr)	
	0-15	15-46
0.3V	2.46	0.625
0.5V	1.43	0.335

The durability at 0.3V is worse than that at 0.5V: due to flooding at lower voltage(?)

Performance Recovery

Degradation Routes

1. **Permanent degradation**
   - Catalyst particle sintering
   - Catalyst CO poisioning
   - MEA delamination
   - Membrane degradation

2. **Recoverable degradation**
   - Oxidation of cathode Pt catalyst
   - Water flooding in the cathode
   - Adsorption of methanol intermediates
   - CO_2 accumulation in the anode

Performance Recovery Techniques

1) Repeated on-off, 2) Voltage swing, 3) Air break

On-Off Operation

30 min-on and 30 sec-off

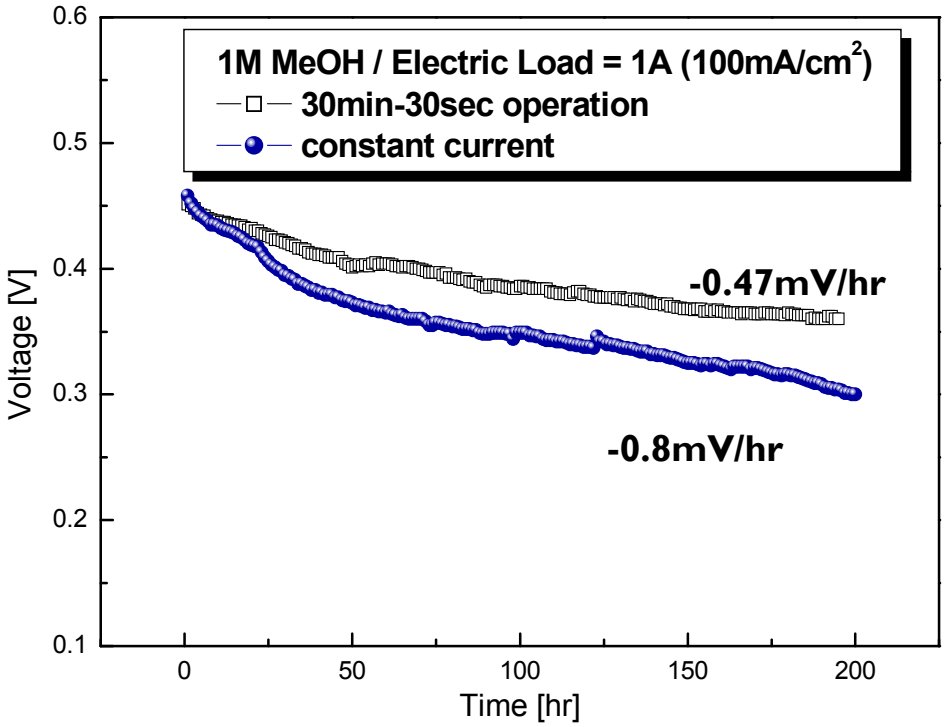

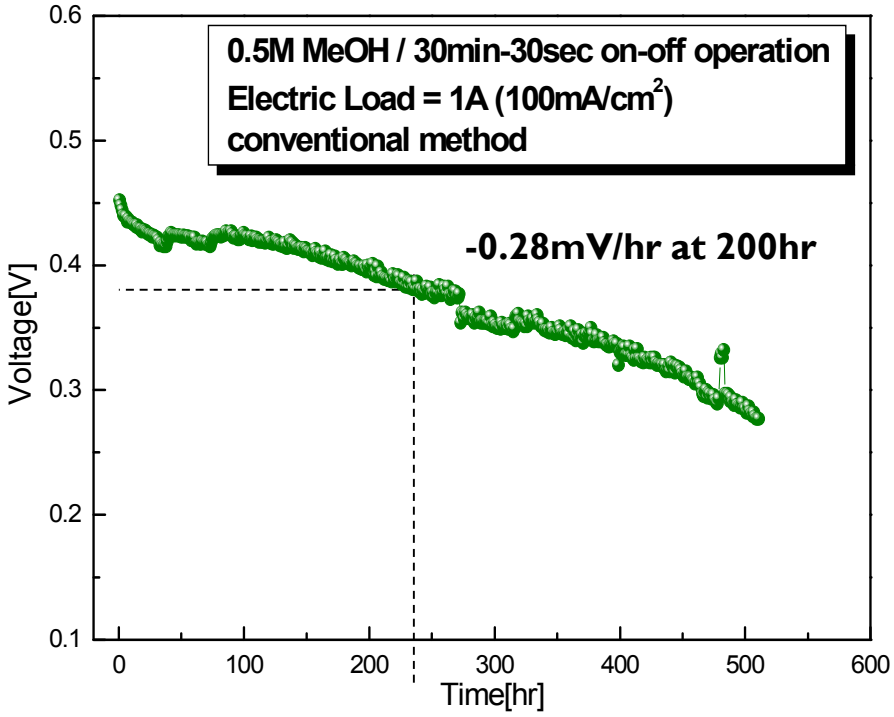

- Deactivation rate is reduced by repeated on-off operation
- It is affected by methanol concentration

Air Break at Constant Currents

Air interruption : 100 sec ON -- 3 sec OFF

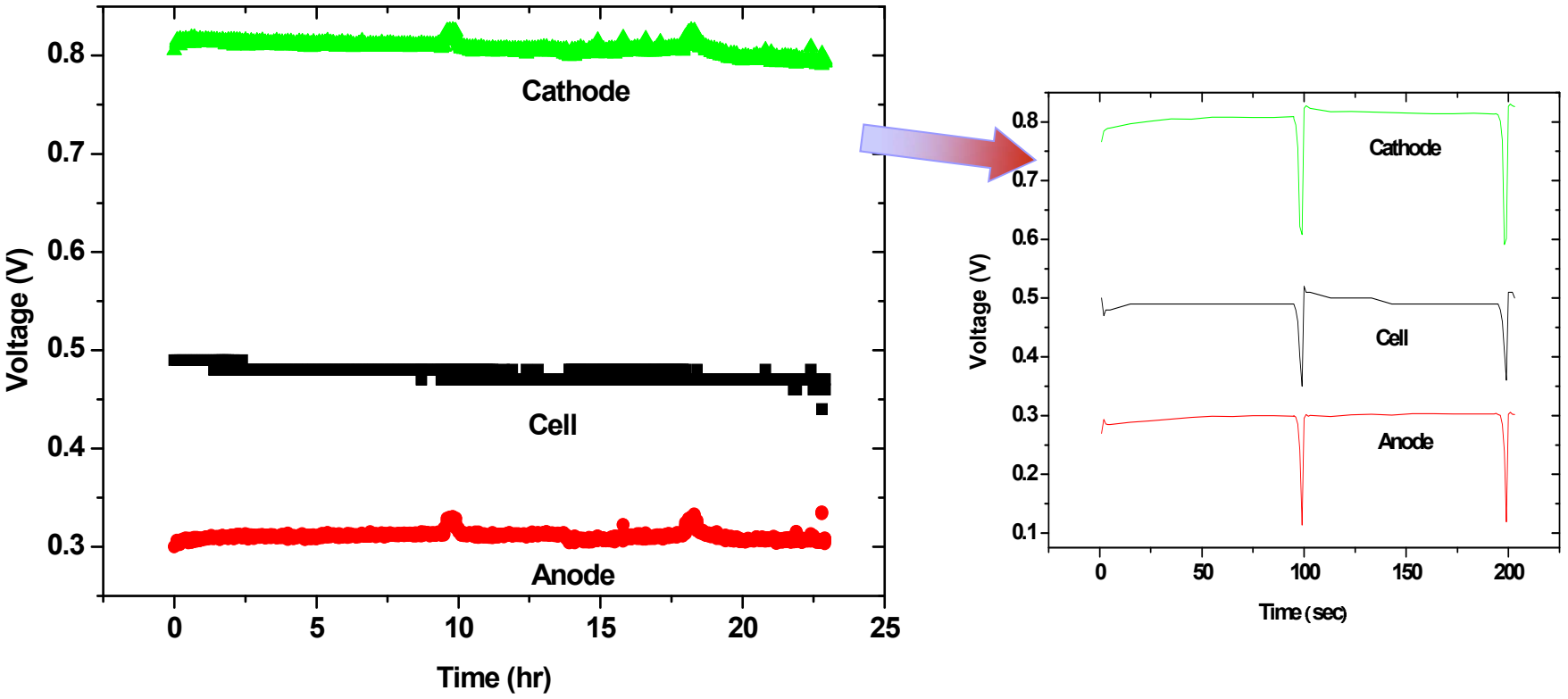

- **Air interruption lowers the cathode potential to 0.5V & helps to preserve the performance**
- **Degradation : Total = 0.87mV/hr**

Voltage Swing

Full Cell

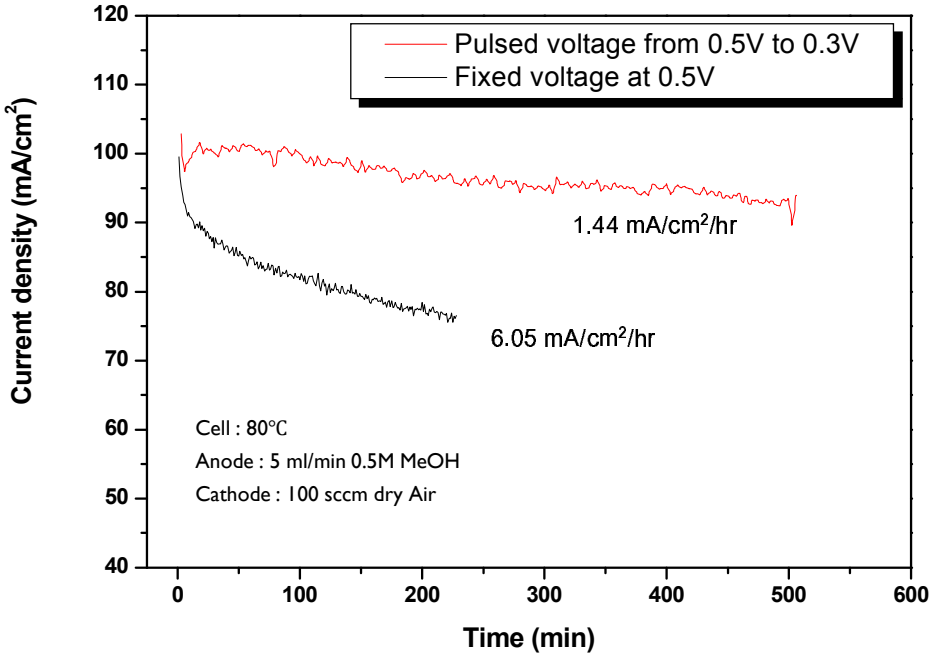

Half Cell

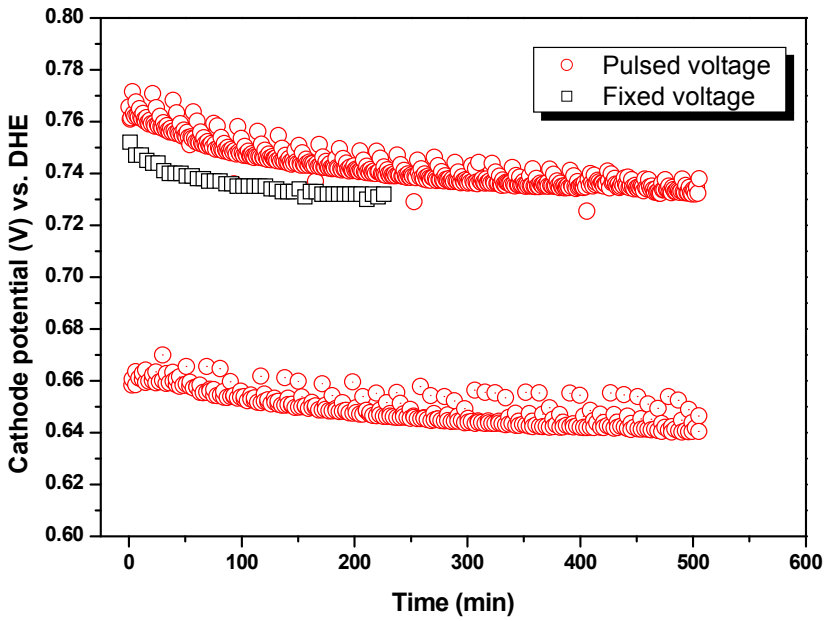

- **Pulsed voltage : 170 s at 0.5 V - 10s at 0.3 V**
- **Fixed voltage : 0.5V**

❖ **Sustainable performance can be obtained by voltage swing method while in case of the fixed voltage operation current dropped dramatically from the beginning.**

❖ **With respect to the anode side, the adsorbed dehydrogenation products such as CO or methyl formate can be cleaned (oxidized) during the voltage swing.**

Life Test Study of DMFC – Our Findings

1. **The DMFC looses its performance during the long term operation, and the loss is more in the cathode than in the anode**
   - ✓ **Internal resistance increases (Impedance results)**
   - ✓ **Loss of GDL hydrophobicity is severe in the outlet regions than in the inlet ones.**
2. **At the cathode outlet, the CO_2 concentration decreases and the unreacted methanol concentration increases as time goes on**
3. **The variation in the operating condition by repeated on-off, voltage swing and air break help to mitigate performance degradation.**
   - ❖ **The air break method shows the best result**

Passive & Air-breathing DMFCs

To apply for micro powers less than 10W

To minimize the system volume

To increase the energy density

To eliminate parasite power losses to pumps and blowers

A passive DMFC for a MP3 player

Completely or semi passive designs

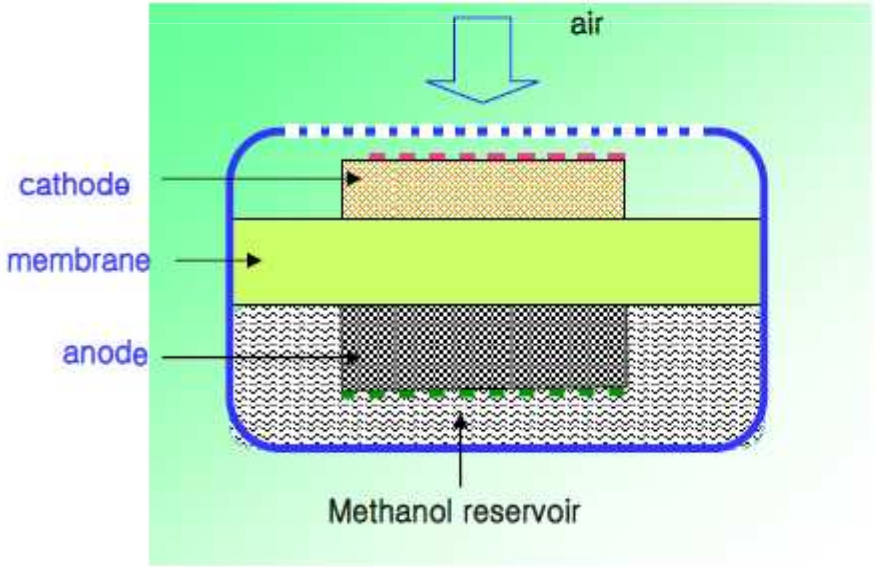

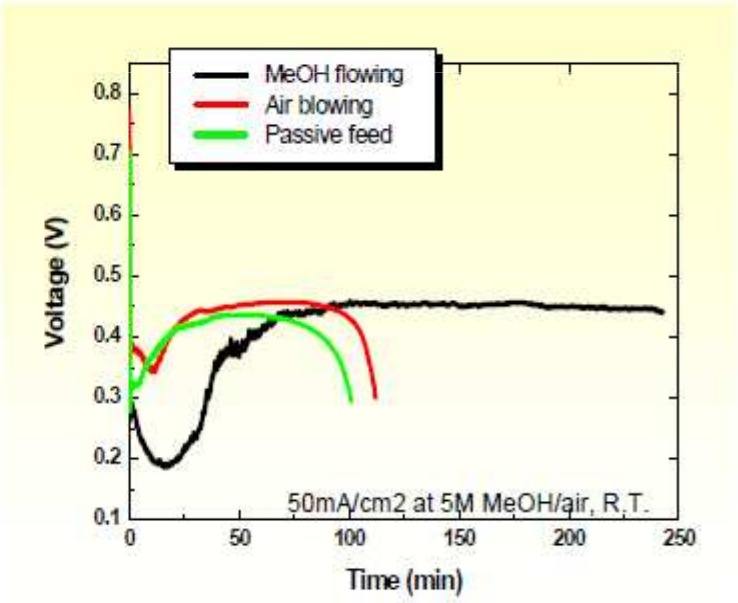

Methanol supply is more important than air supply

Monopolar Stacks

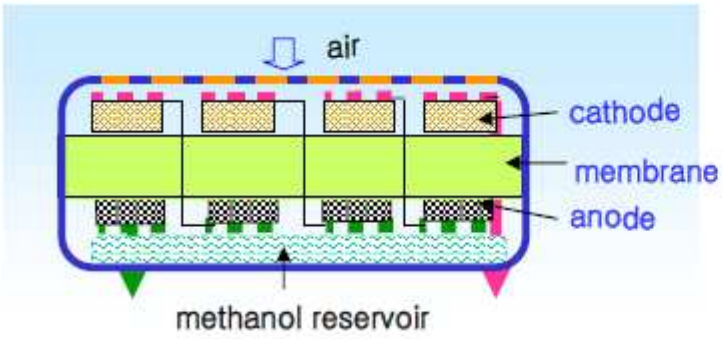

Monopolar MEA

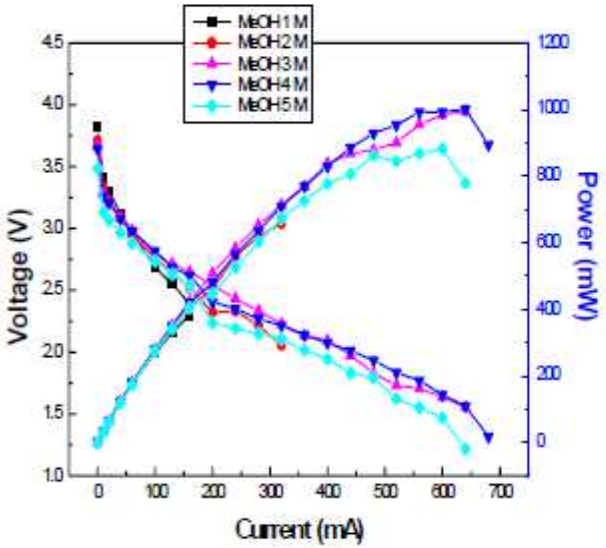

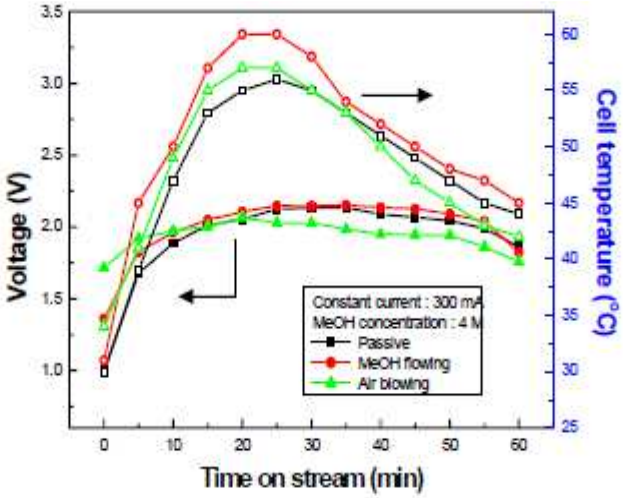

Radiophone (1100mW), 2001

J Power Sources., 157 (2006) 253-259

Research in Fuel Cell – DMFC – Bird's Eye View

1. **Catalysts**

- Modification of various carbon supports with ionomer – To Enhance 3 - Phase boundary
- Anode catalyst - Pt-CeO_2 - Activity/Durability/Cost
- Cathode catalyst – Pt-CeO_2 - Air Utilization, Pt-CeO_2 + Sm - MeOH Tolerant ORR Activity

2. **Membrane/ Methanol Cross over**

- Surface modification by Silica layers
- Consequences of MeOH crossover – Fundamental Study

3. **Membrane Electrode Assembly**

- Optimization of electrode structure
- Durability test and Recovery measures
- Simulation of flow fields

4. **Stacks**

- Passive monopolar stacks – Design & Fabrication
- Active bipolar stacks: 20, 50, 500W stacks

Facet-Selective Platinum Electrodeposition at Freestanding Polycrystalline Boron-doped Diamond Films

XRD of the BDD films

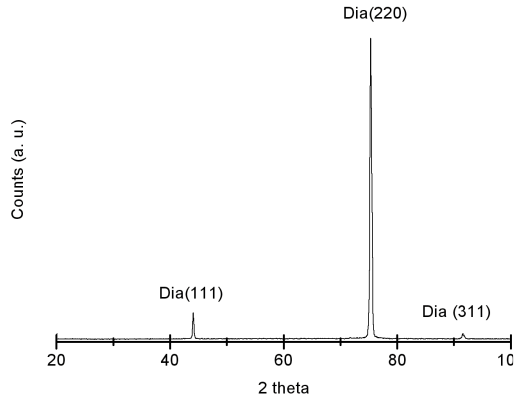

Raman spectrum of the BDD films

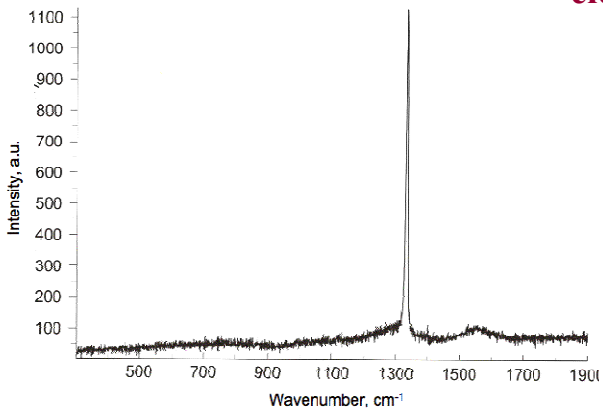

CV of BDD film after sequential Pt catalyst electrodeposition in 0.05 M H_2SO_4 at 500 mV/s

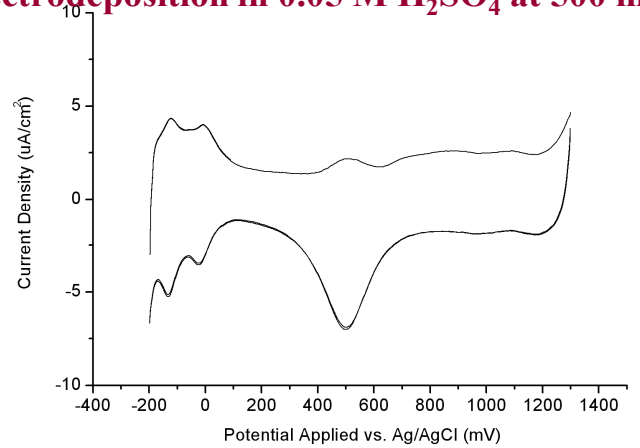

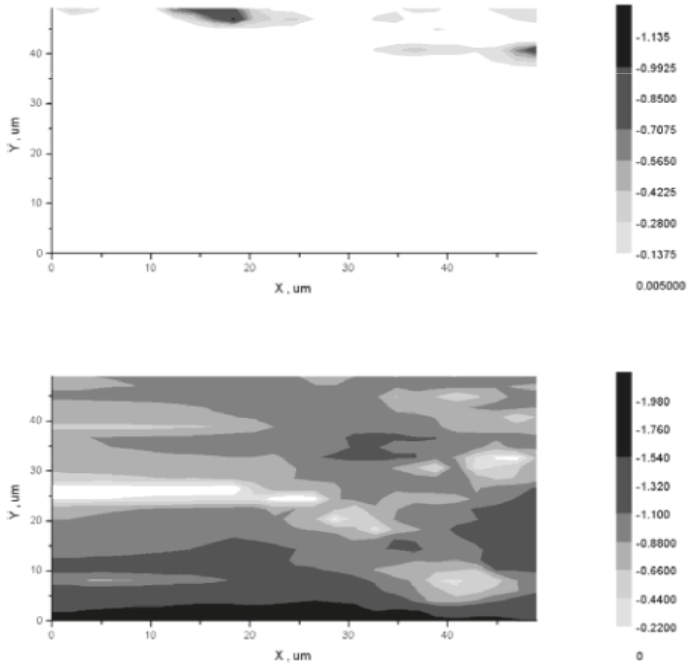

Figure 2. (upper) Scanning electrochemical microscopy of a freestanding boron-doped diamond in a 0.5 M H_2SO_4 solution with a Pt tip potential 800 mV vs Ag/AgCl and a Pt wire as counter electrode. (lower) Comparison of scanning electrochemical microscopy of a freestanding boron-doped diamond in a 0.5 M H_2SO_4 solution with a Pt tip potential 800 mV vs Ag/AgCl and a Pt wire as counter electrode and −500 mV vs Ag/AgCl potential applied to BDD film.

Langmuir 25 (17) (2009) 10329-10336

SEM

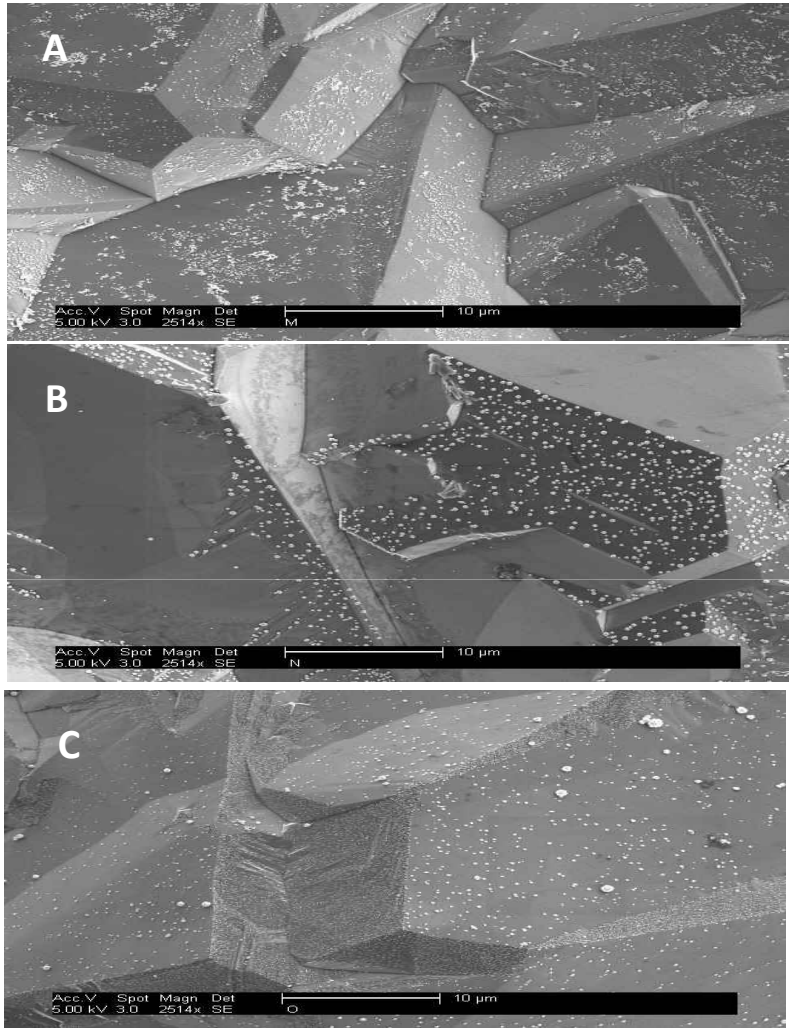

Polycrystalline free standing BDD films after Pt deposition in a 1 mM K_2PtCl_6/0.5 H_2SO_4 by CV at different scan rates (mV/s): (A) 100 (B) 250 (C) 500

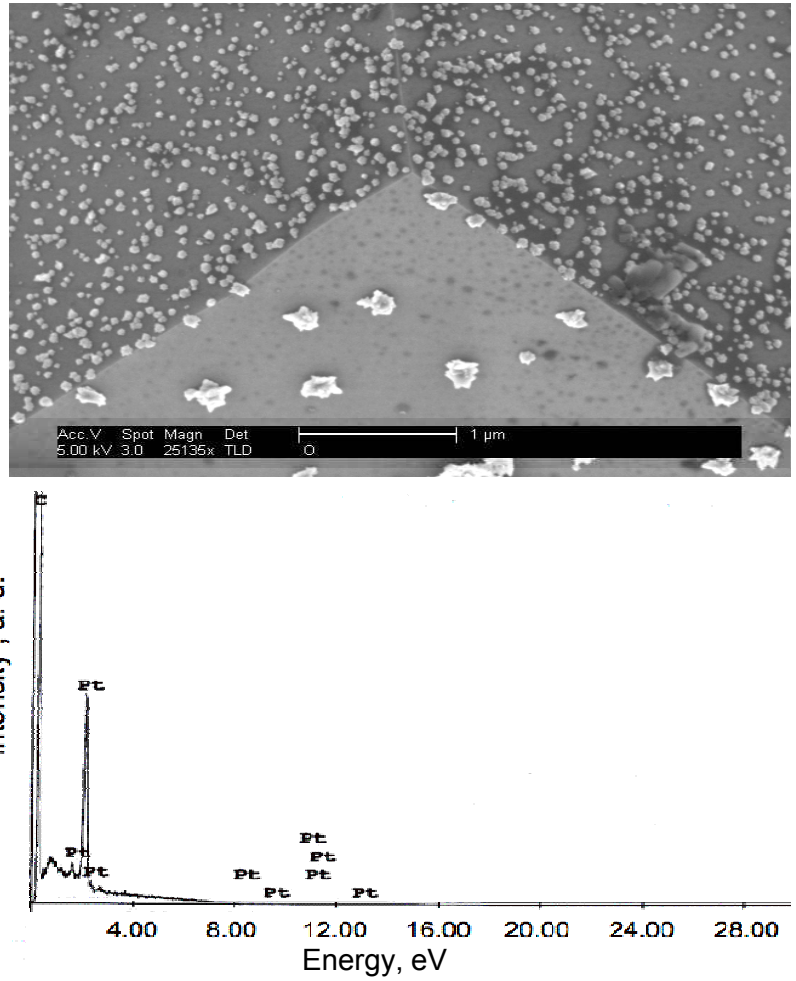

Sample (C) showing edge lines of facets (111) with intersection angle 60º &120º and the corresponding EDS of platinum particle on BDD film

XPS

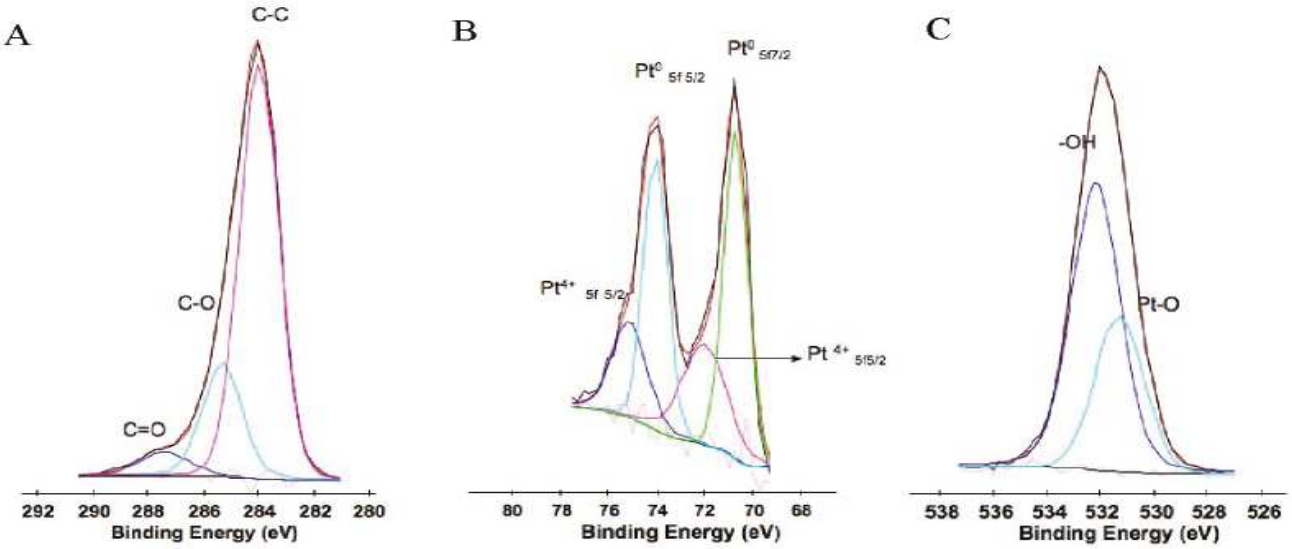

Figure 3. High resolution X-ray photoelectron spectra of the Pt particle decorated boron-doped diamond film. (A) C 1s, (B) Pt 4f, and (C) O 1s binding energy regions.

	Carbon Region, 1s CO/C=O			**Oxygen Region, 1s (O-H) / Metal Oxides**		
	(A)	**(B)**	**(C)**	**(A)**	**(B)**	**(C)**
BDD	2.4	4.59	5.82	6.05	3.64	16.48
Pt-BDD	1.40	2.67	2.81	1.39	2.57	6.68

Histogram of the ferret diameter of the Pt particles deposited

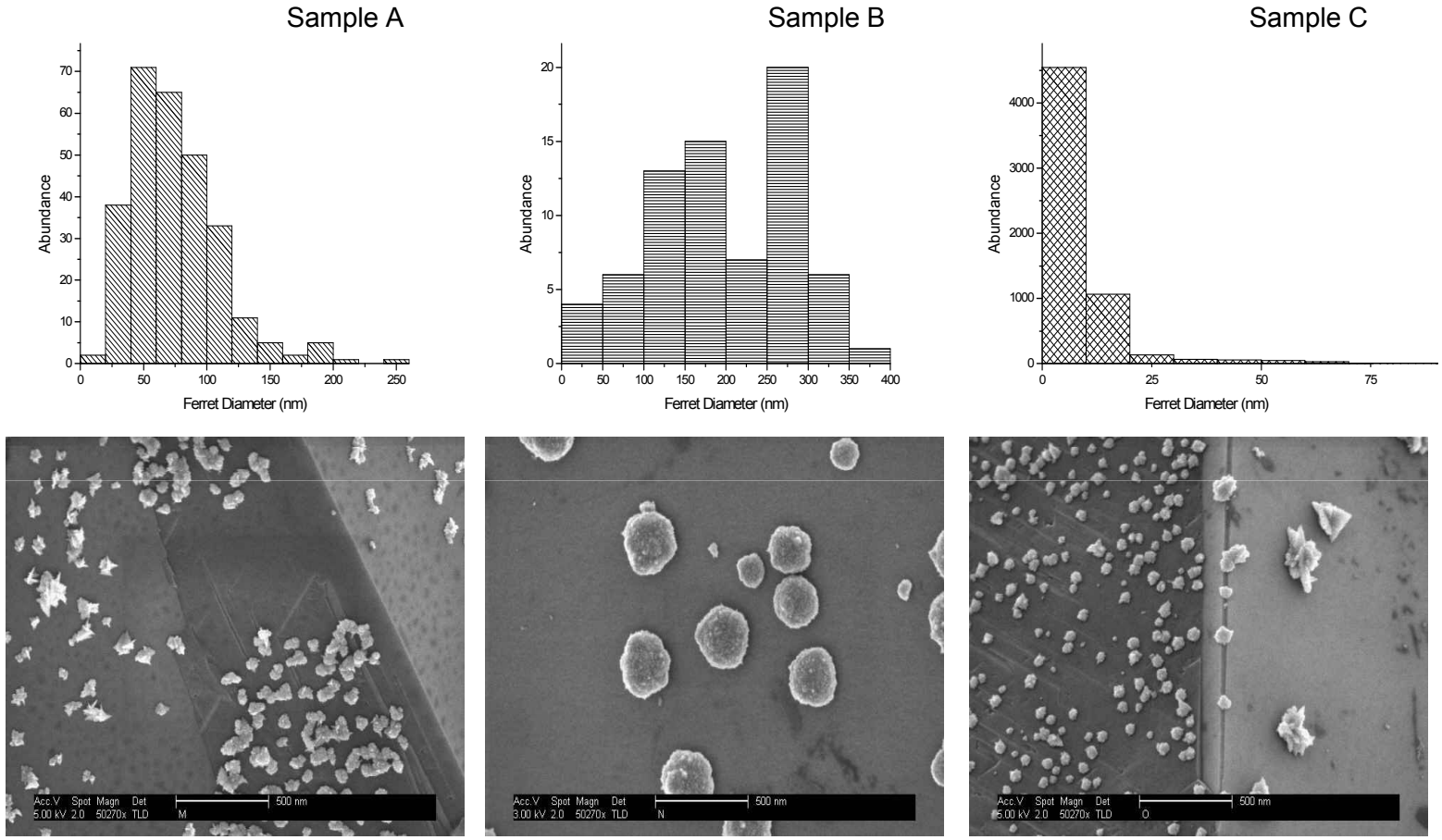

SEM - Polycrystalline free standing BDD films after Pt deposition by CV in 1 mM K_2PtCl_6/0.5 H_2SO_4 at (A) 100 (B) 250 and (C) 500 mV/s

Langmuir 25 (17) (2009) 10329-10336

CV on 0.5 M CH_3OH/ 0.5 M H_2SO_4 Pt particles deposited on BDD films

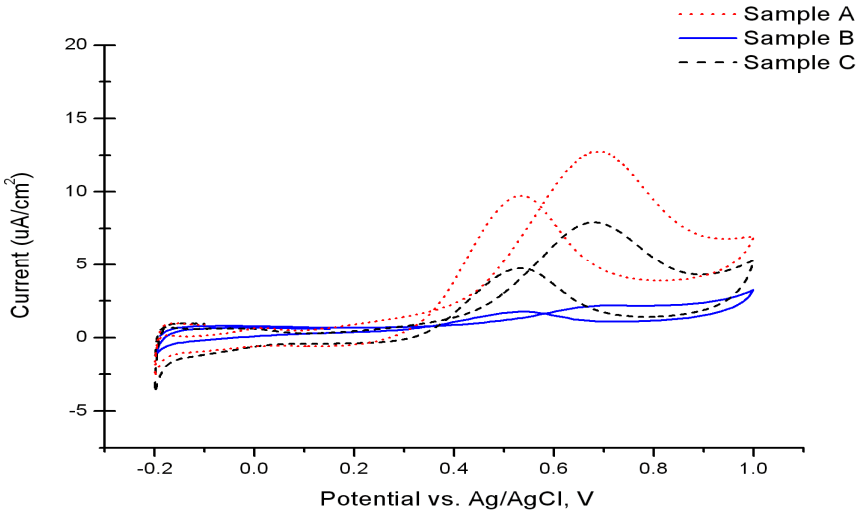

Chronoamperometry at 400 mV vs.Ag/AgCl of Pt on BDD films by CV on 0.5 M CH_3OH/ 0.5 M H_2SO_4

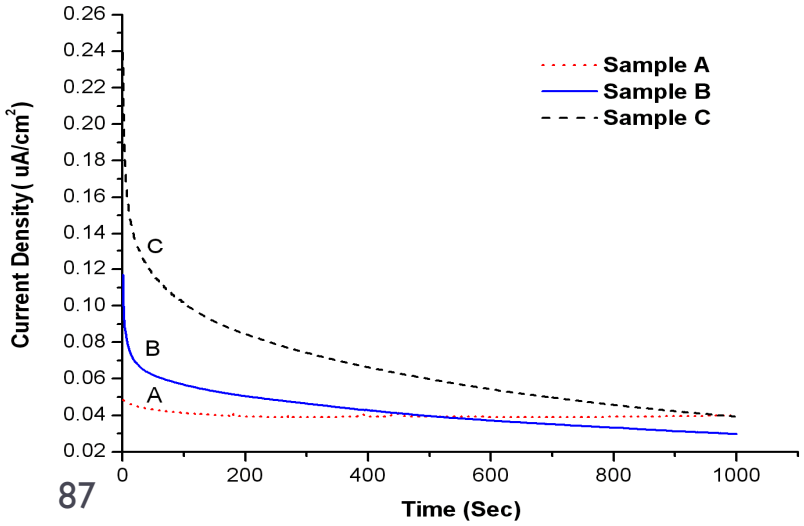

SEM of Pt/BDD film after methanol oxidation measurements

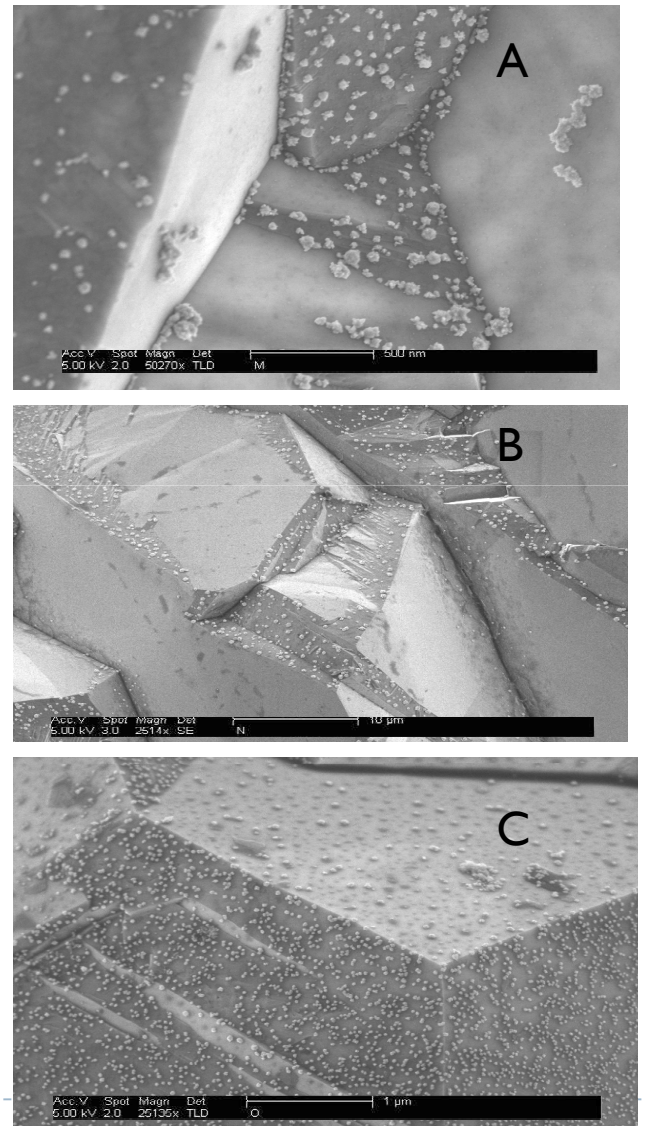

Modulation of Electron Transfer Activity at Diamond Films by Dissolved Oxygen in Aqueous Solution

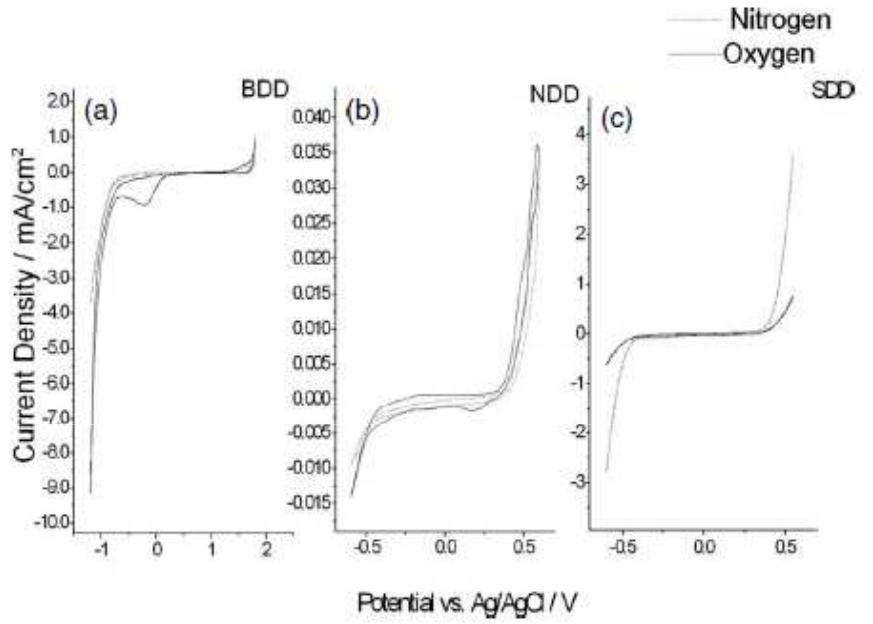

Figure 1. Cyclic voltammetry curves for (a) BDD, (b) UDD, and (c) SDD (5% sulfur) samples in N_2-sparged (solid line) and O_2-sparged (dashed line) 0.5 M H_2SO_4 at 50 mV s^{-1}.

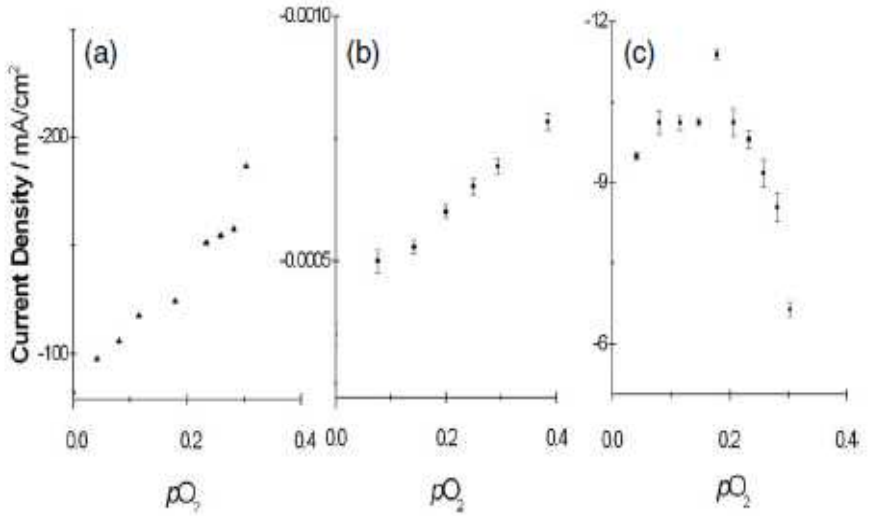

Figure 2. (a) Current density at an applied potential of −0.90 V vs Ag/AgCl for a BDD sample; (b) −0.60 V vs Ag/AgCl for a UDD sample; and (c) −0.60 V vs Ag/AgCl for an SDD (3% sulfur) sample; all were measured in 0.5 M H_2SO_4 at various $O_2/(O_2 + N_2)$ ratios (O_2 partial pressure) sparged through the electrolyte solution.

J. Electrochem. Soc., 156 6 J152-J157 2009

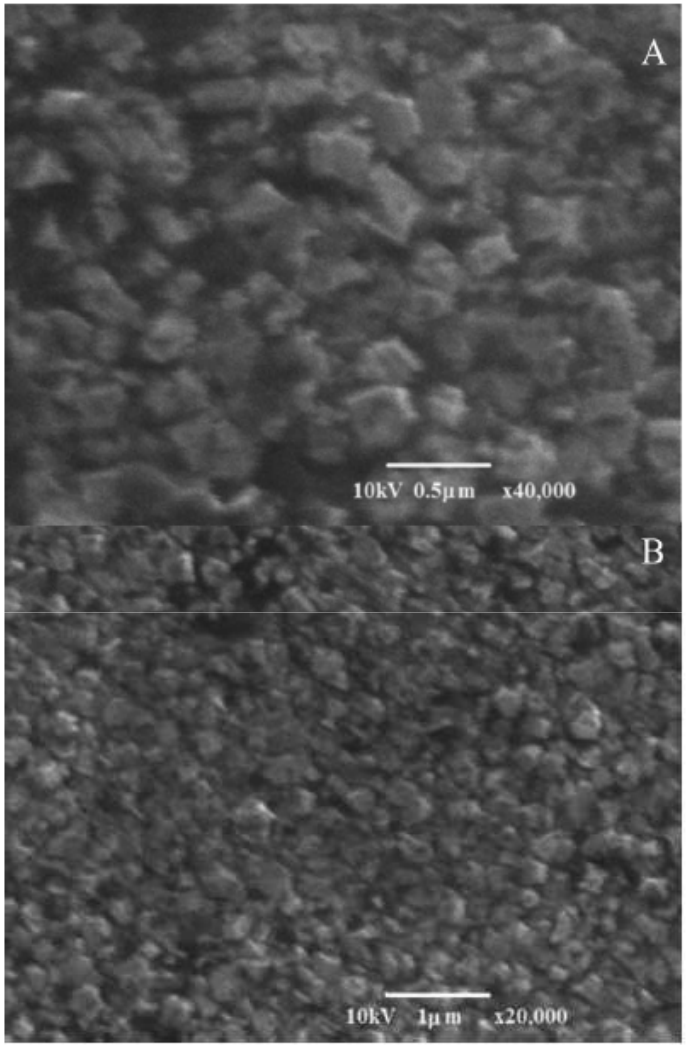

Figure 3. SEM of an SDD film deposited on a molybdenum substrate at different magnifications: (a) 40,000× and (b) 20,000×.

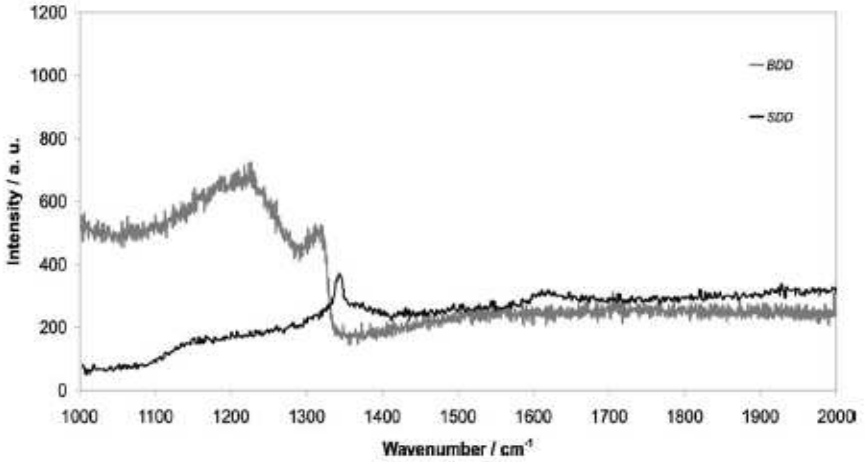

Figure 4. Raman spectra of SDD (3% sulfur) (gray curve) and BDD (black curve) films deposited on a molybdenum substrate and a silicon wafer, respectively.

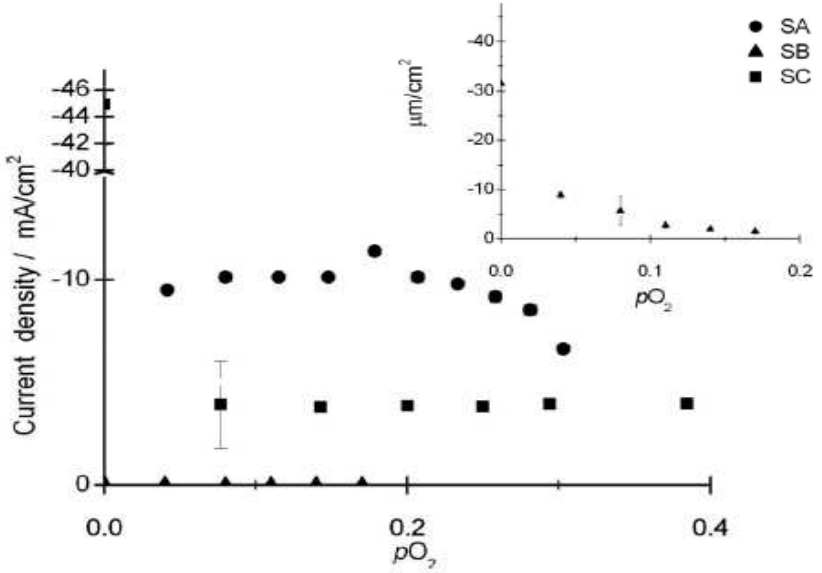

Figure 5. Current density at −0.60 V vs Ag/AgCl for several SDD samples in 0.5 M H_2SO_4 at various $O_2/(O_2 + N_2)$ ratios (O_2 partial pressure) sparged through the electrolyte solution: ● (SA: 3% sulfur), σ (SB: 5% sulfur), and ◆ (SC: 9% sulfur).

Table I. Characteristic results from Raman spectroscopy, XPS, and electrochemical measurements on the UDD films.

Sample	Diamond/carbon[a] by Raman	Sulfur by XPS (atom %)	O/C proportion by XPS	Calibration curve slope (mA/% O_2)
NA	0.056	0.001	0.34	−2
NB	0.0072	0.001	0.20	−0.5
NC	0.038	0.001	0.13	−0.3
ND	0.080	0.001	0.12	−0.1

[a] sp^3/sp^2 form the D/G band ratio.

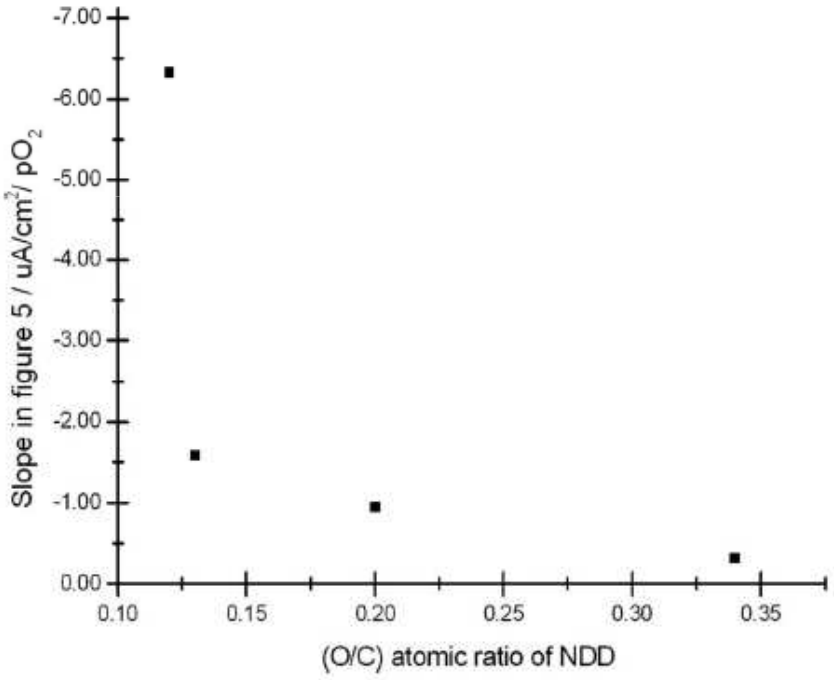

Figure 7. Relationship between the oxygen sensitivity and the surface composition of the UDD films as determined by XPS.

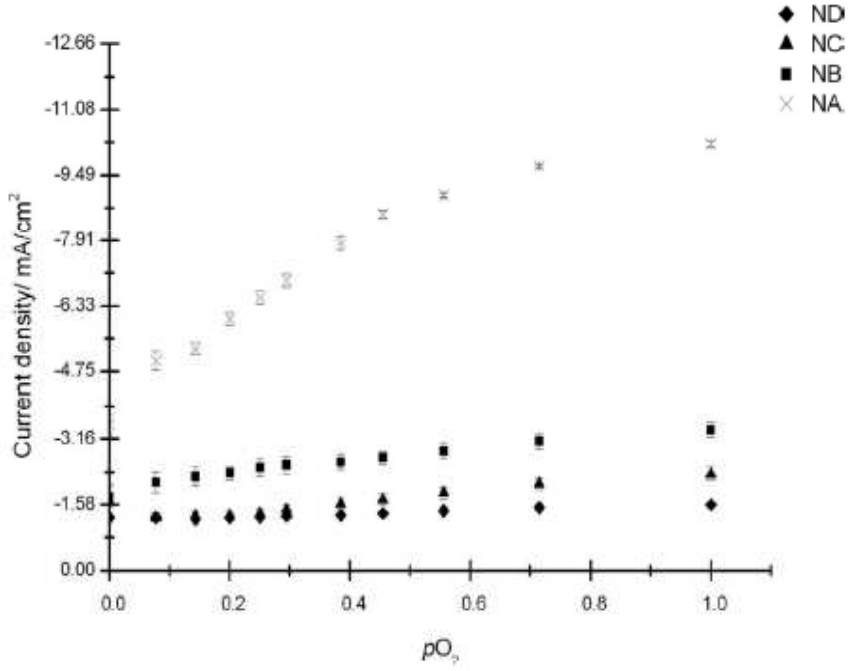

Figure 6. Current density at −0.60 V vs Ag/AgCl for several UDD samples in 0.5 M H_2SO_4 at various $O_2/(O_2 + N_2)$ ratios (O_2 partial pressure) sparged through the solution: × (NA), ■ (NB), ▲ (NC), and ◆ (ND).

Electrodeposition of Pt onto electrophoretically fabricated diamond nanoparticle layers for methanol oxidation

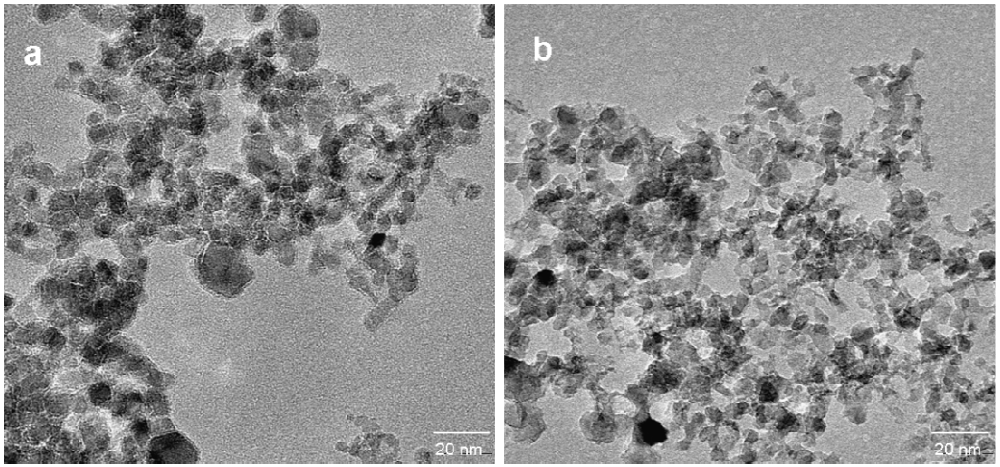

TEM – DNP before (a) and after (b) chemical pretreatment

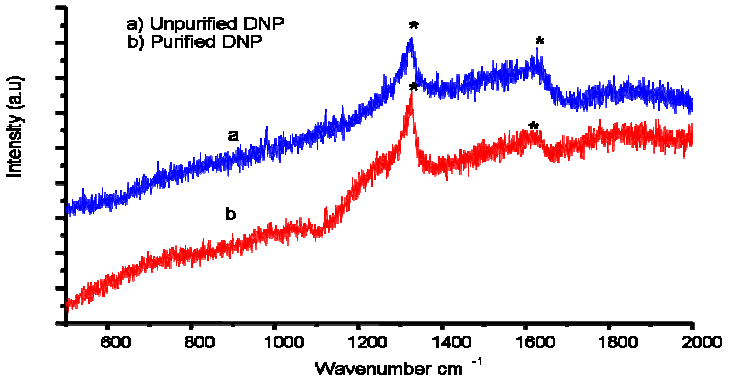

Raman Spectra - DNP before (a) after (b) chemical pretreatment

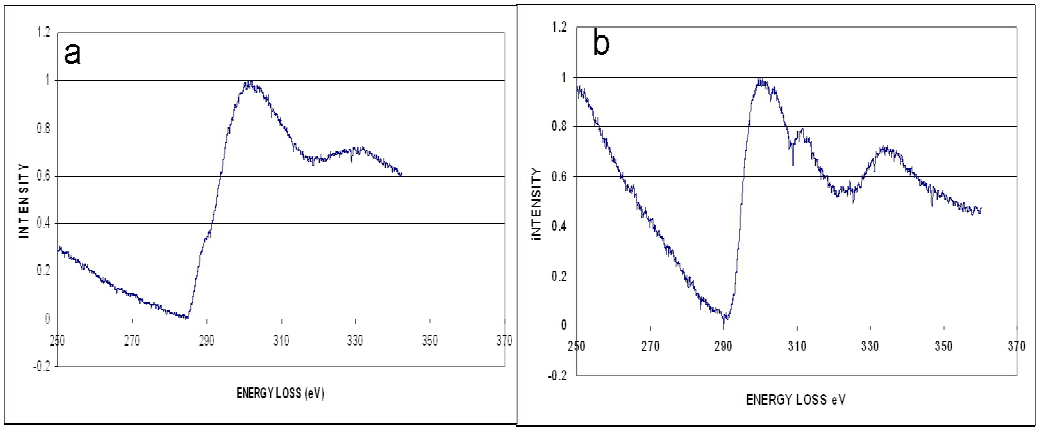

Electron Energy Loss Spectra - DNP before (a) after (b) chemical pretreatment

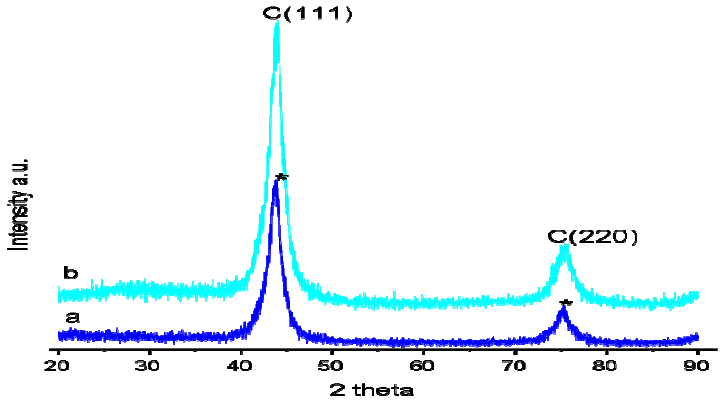

XRD of unpurified (a), purified (b) DNP by HNO_3 reflux process.

J Electrochem Soc., 157 (6), 2010, B831-836.

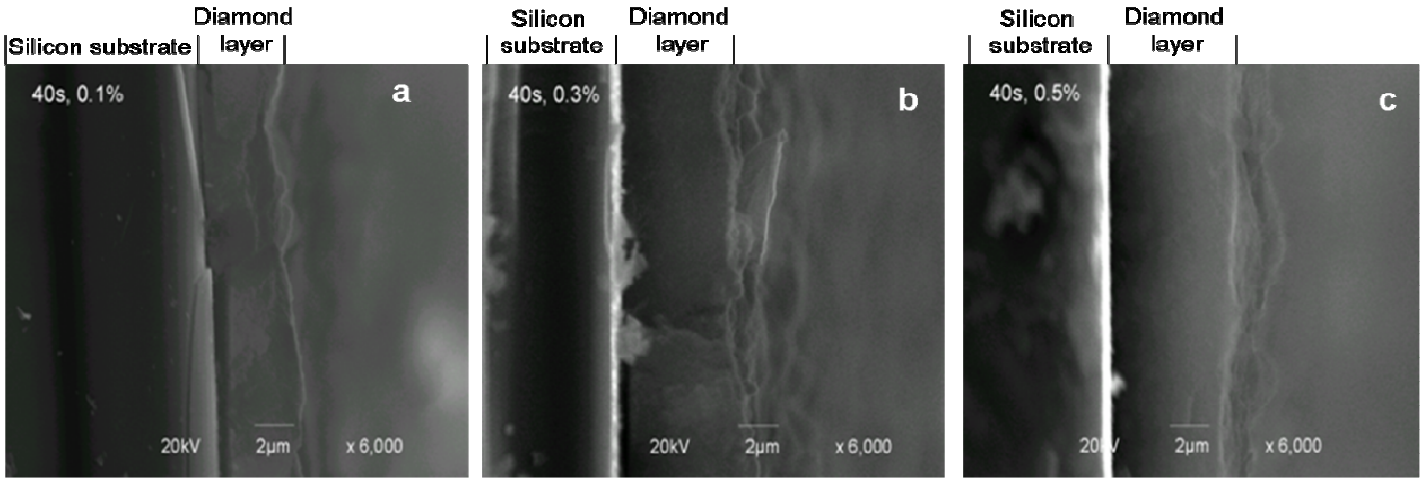

SEM -Electrophoretically deposited layers of DNP onto Si wafers for 40 s, At 260 V, with different suspension concentrations 0.1% (a), 0.3% (b) and 0.5% (c).

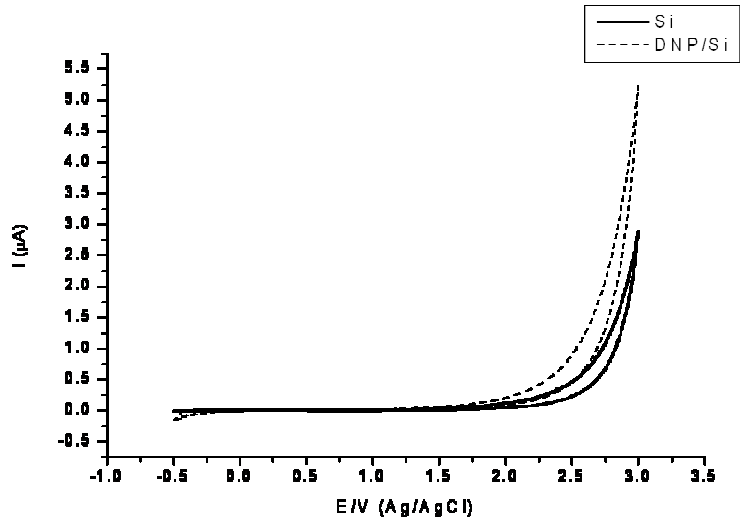

CV of Si wafer & electrophoretically deposited DNP

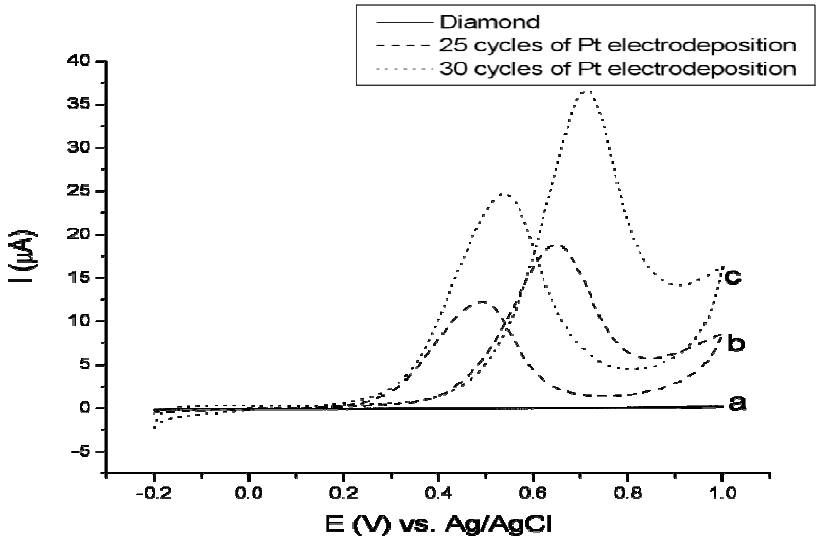

CV of methanol 1.0 M in H_2SO_4 0.5 M at 20 mV/s

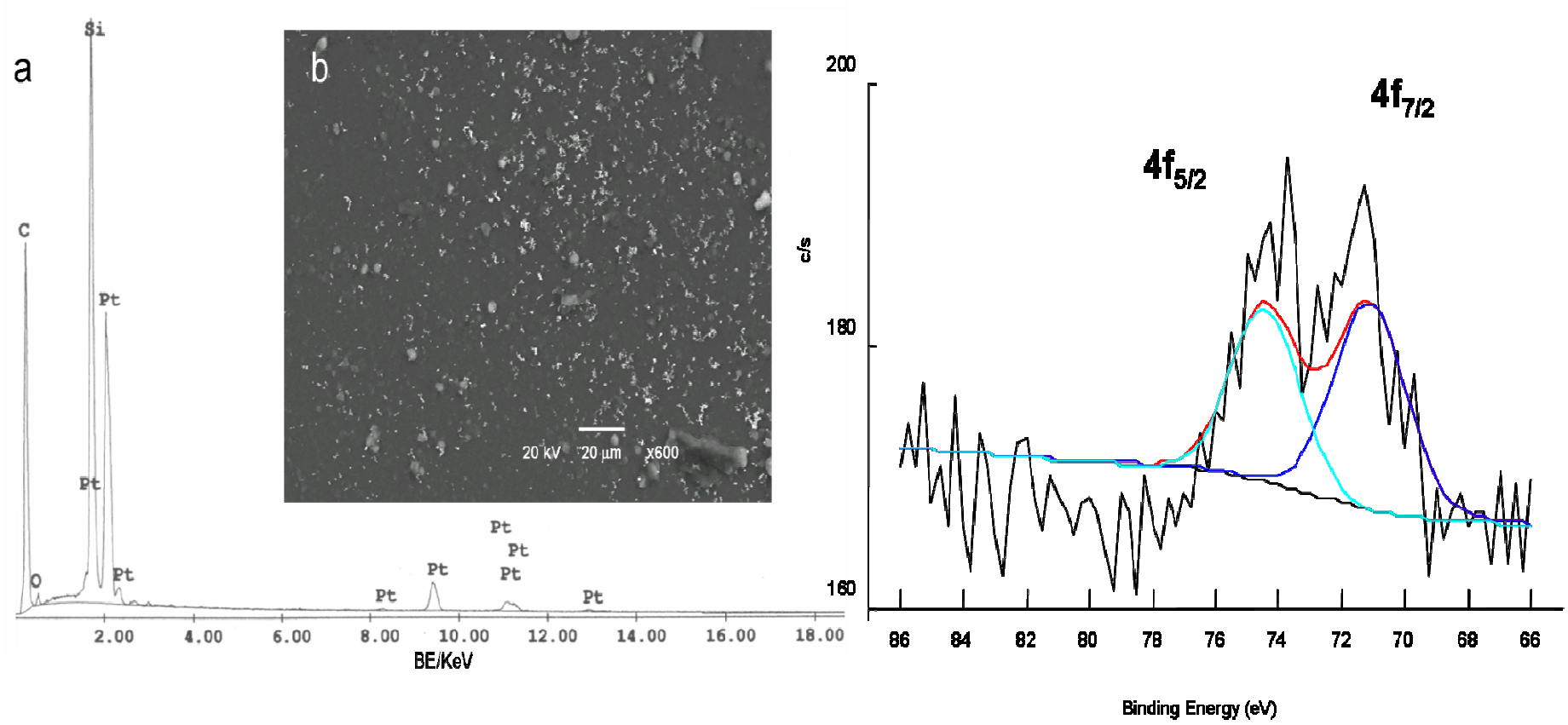

(a) EDS - Pt on electrophoretically deposited DNP

(b) SEM - Various sizes of Pt particles

XPS- Pt in metallic state on DNP

Facile synthesis of Pt & PtRu nanocatalysts on undoped & boron doped diamond nanoparticles via chemical reduction route

XRD

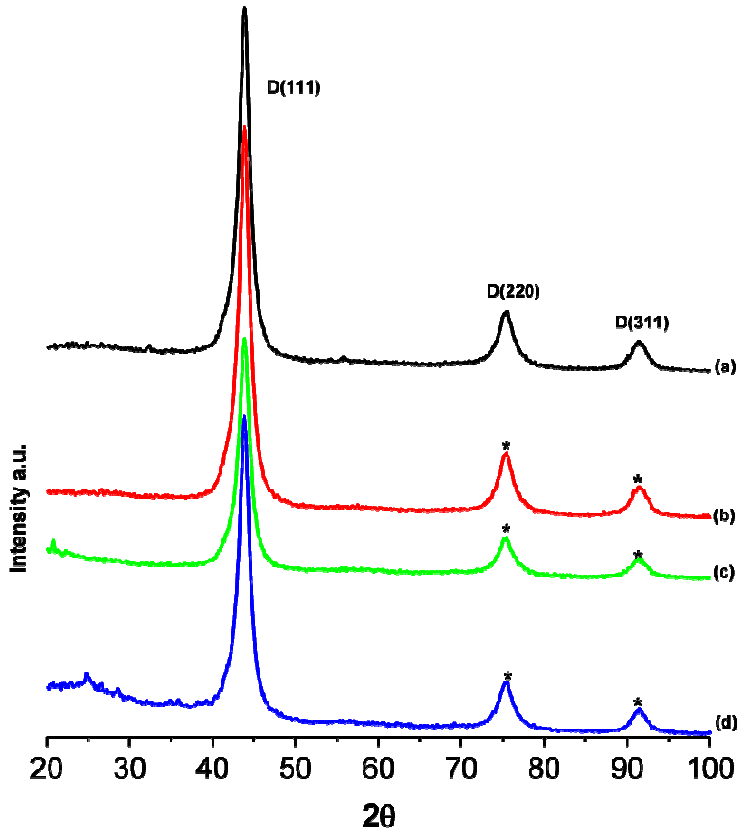

Unpurified (a), purified (b) DNP HNO_3 reflux purification reduced ($NaBH_4$) DNP (c), boron doped diamond nanoparticles (d)

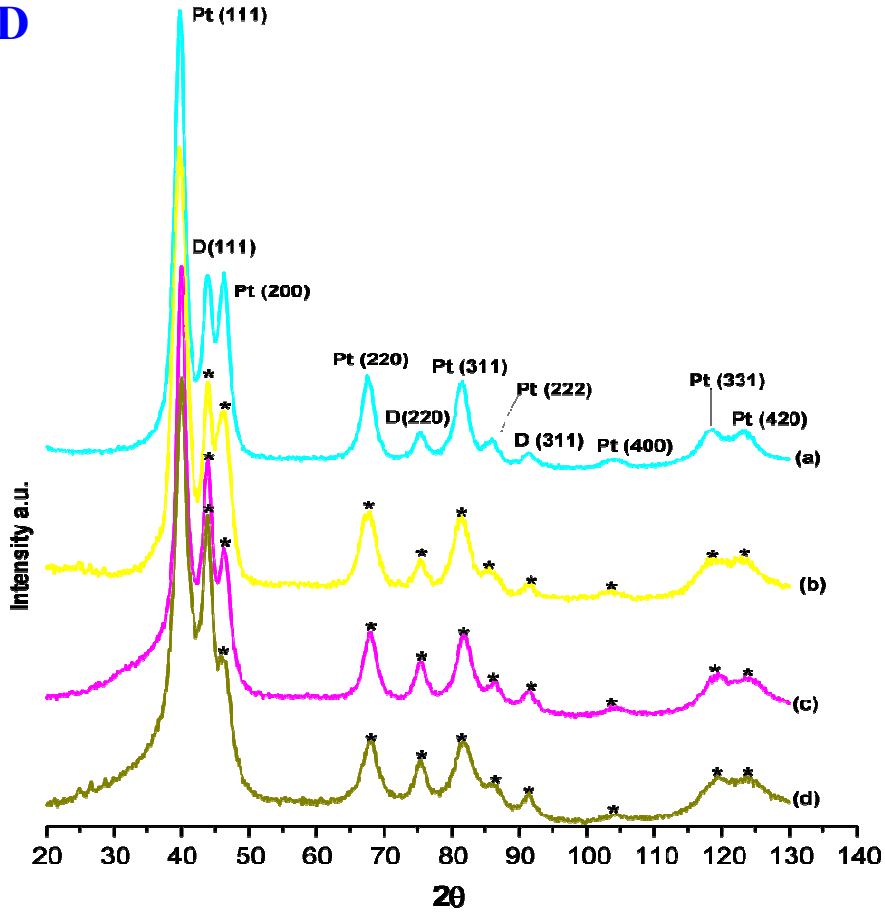

Pt (a), Pt-Ru nanoparticles supported on purified (concentrated HNO_3) DNP surface, Pt (c), and Pt-Ru nanoparticles on BDD nanoparticles

XPS

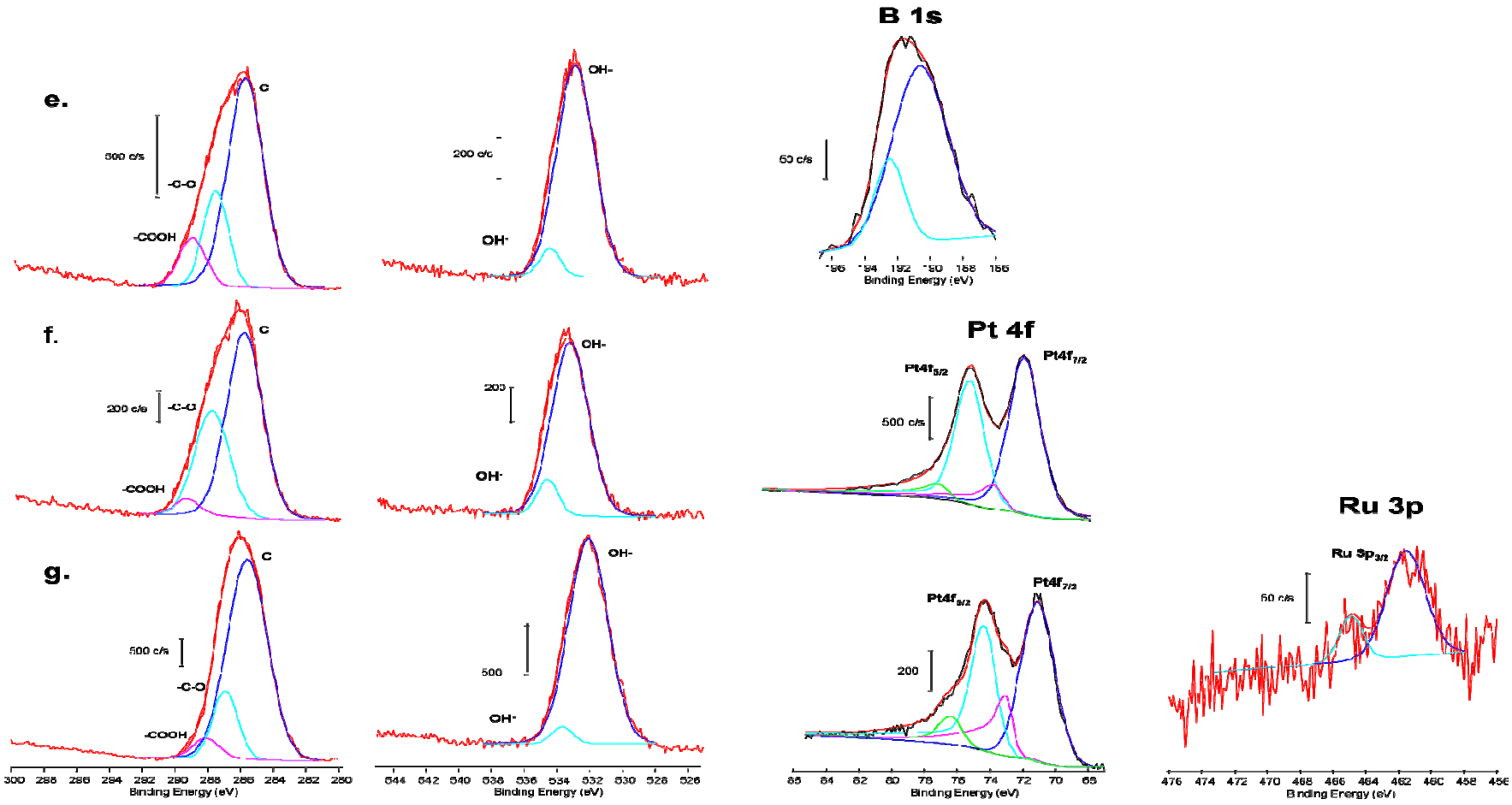

e) C_{1s}, O_{1s} and B_{1s} of BDD nanoparticles cleaned in HNO_3 , f) C_{1s}, O_{1s} and Pt_{4f} of BDD nanoparticles cleaned in HNO_3 with chemically reduced Pt, and g) C_{1s}, O_{1s}, Pt_{4f}, and Ru_{3p} of purified BDD nanoparticles in HNO_3 with chemically reduced Pt and Ru.

FT-IR spectra

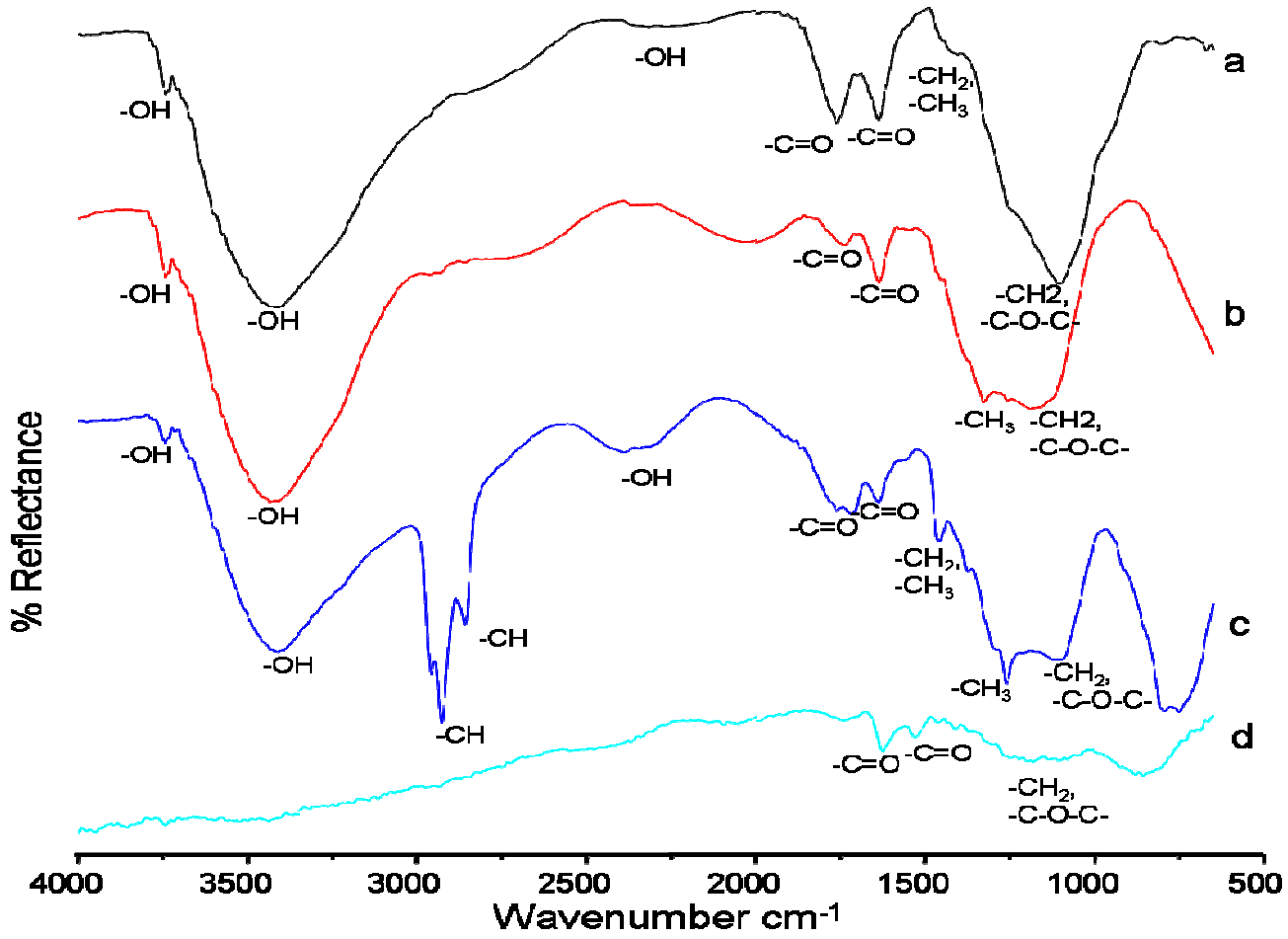

a) Unpurified DNP, b) purified DNP in Con. HNO_3, c) DNP in reaction with reducing agent $NaBH_4$, and d) DNP decorated with metallic Pt by chemical reduction using reducing agent ($NaBH_4$)

Platinum Electrodeposition at Vulcan-XC-72R Using a Rotating Disk-Slurry Electrode Technique

Catalysts preparation by electrodeposition (RoDSE)

- Consists of a disk at the end of an insulated shaft
- Hydrodynamic convection
- Potential Control
- RoDSE allows for bulk preparation

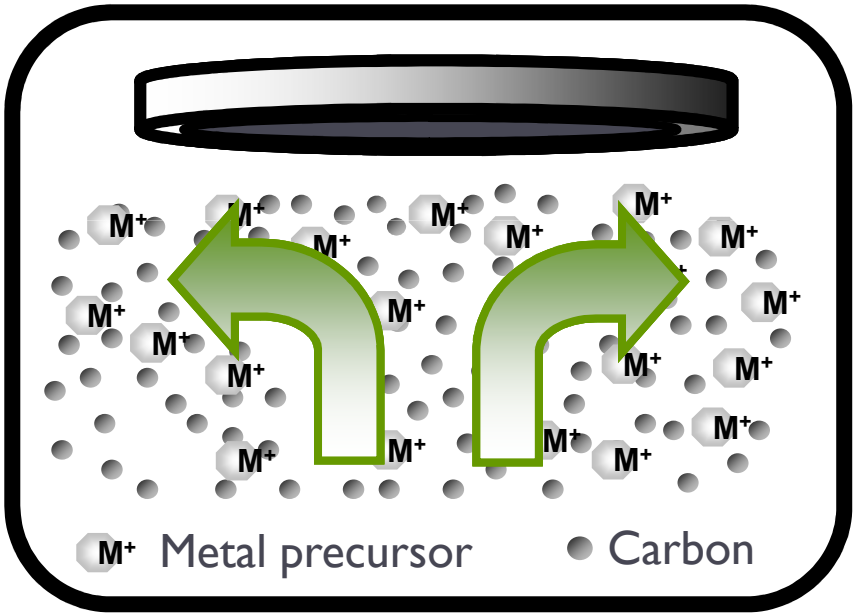

XPS

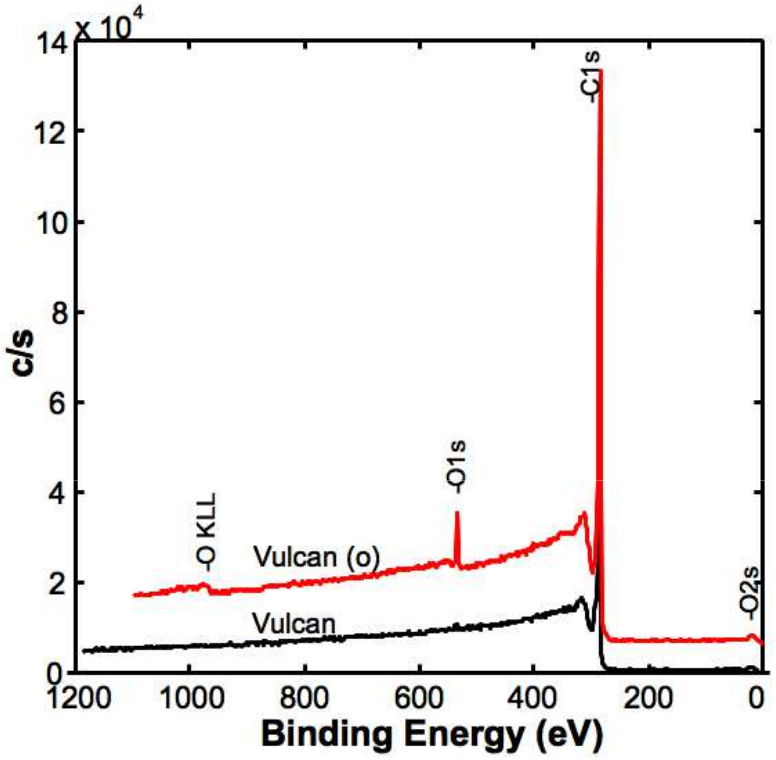

As-received Vulcan XC-72R (Vulcan) & acid-treated Vulcan XC-72R (Vulcan (o))

TEM

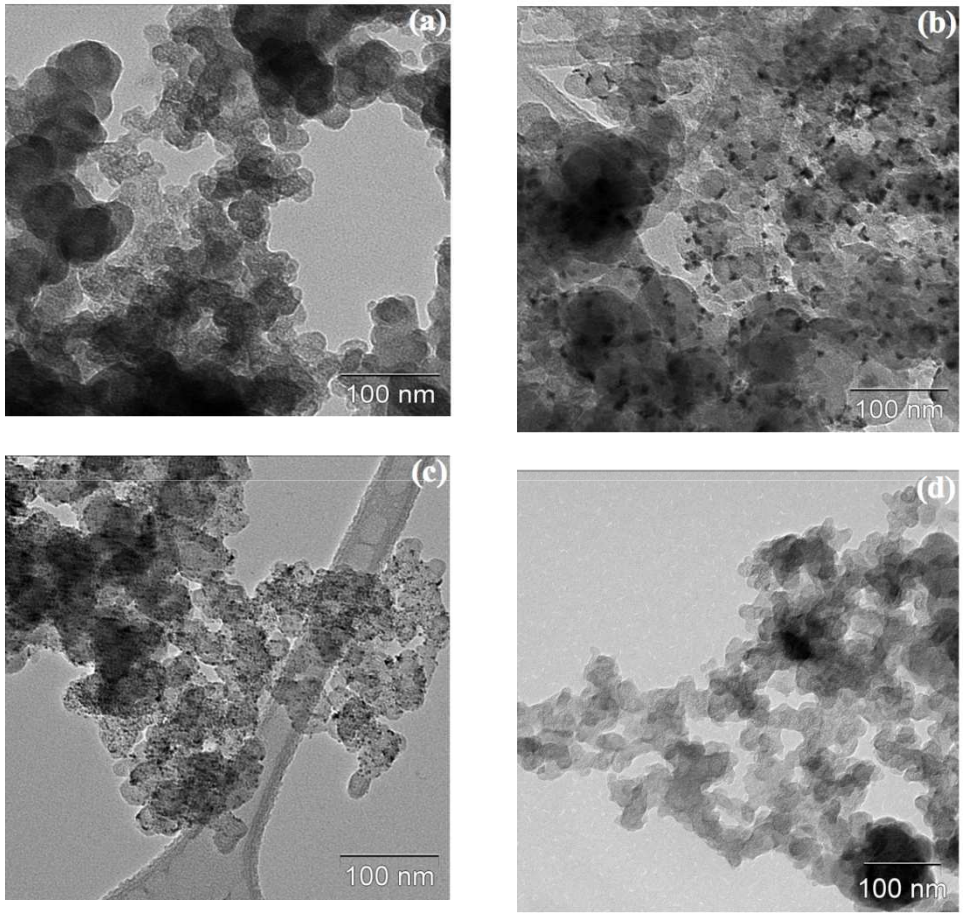

(a) Vulcan (o), (b) RoDSE Pt/VXC (A), (c) ETEK Pt/VXC, and (d) RoDSE Pt/VXC (B)

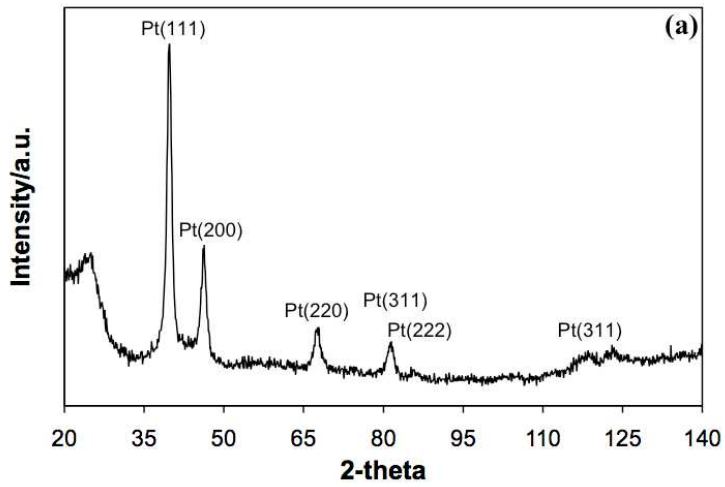

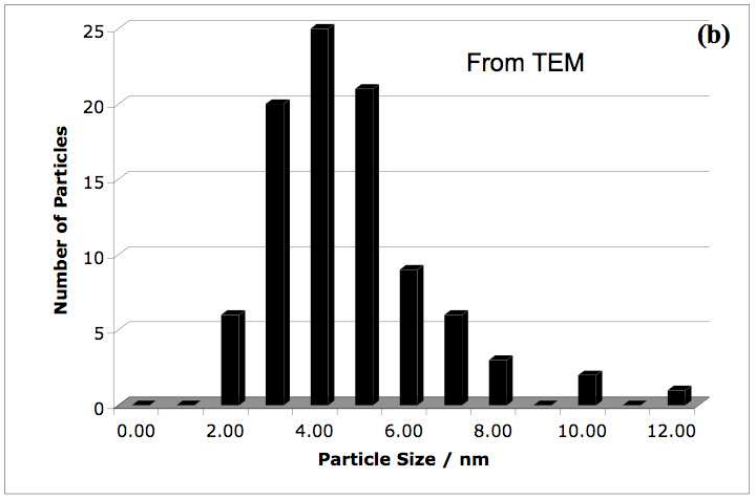

XRD of RoDSE Pt/VXC (A) sample (a), & particle size histogram from TEM for RoDSE Pt/VXC (A) sample (b)

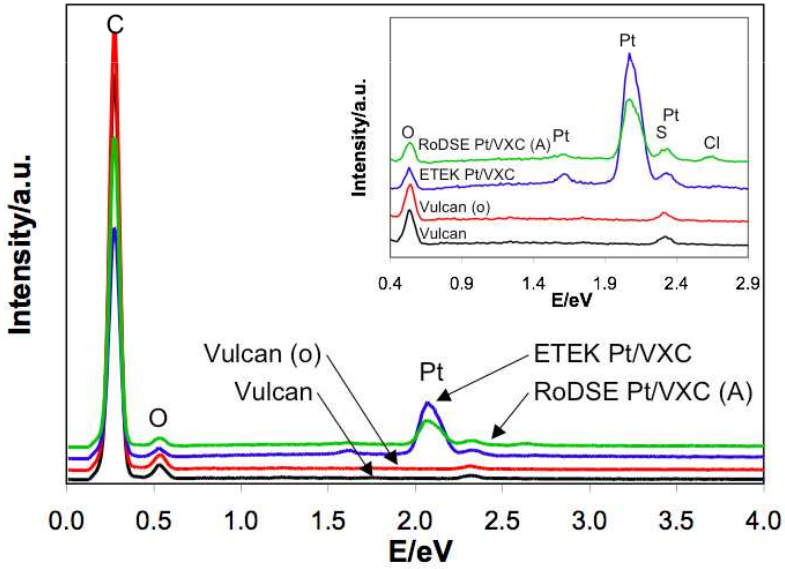

X-ray fluorescence energy dispersive spectra of Vulcan, Vulcan (o), RoDSE Pt/VXC (A) and ETEK Pt/VXC

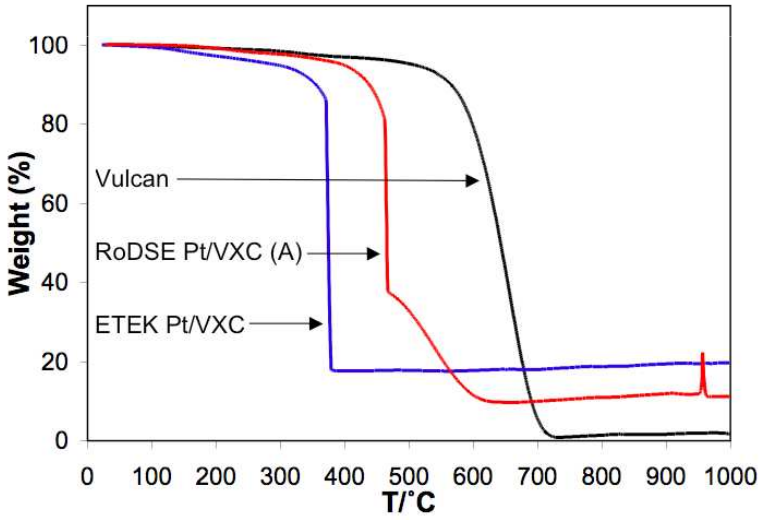

Thermal gravimetric analysis (TGA) traces of Vulcan, RoDSE Pt/VXC (A) and ETEK Pt/VXC catalysts

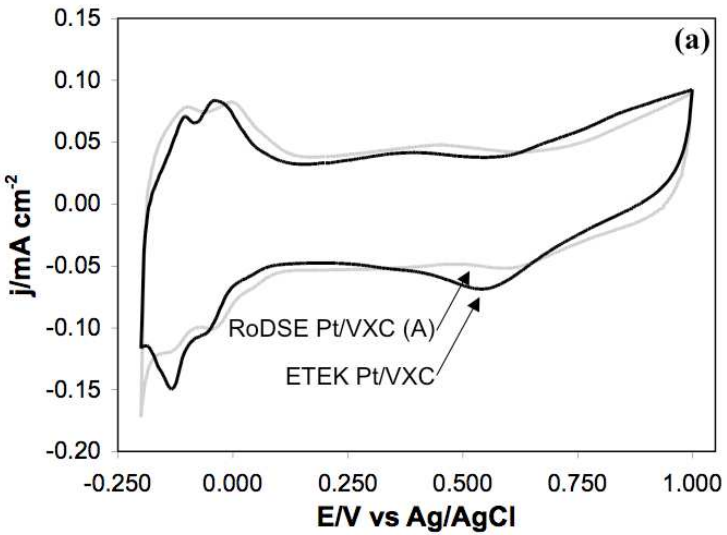

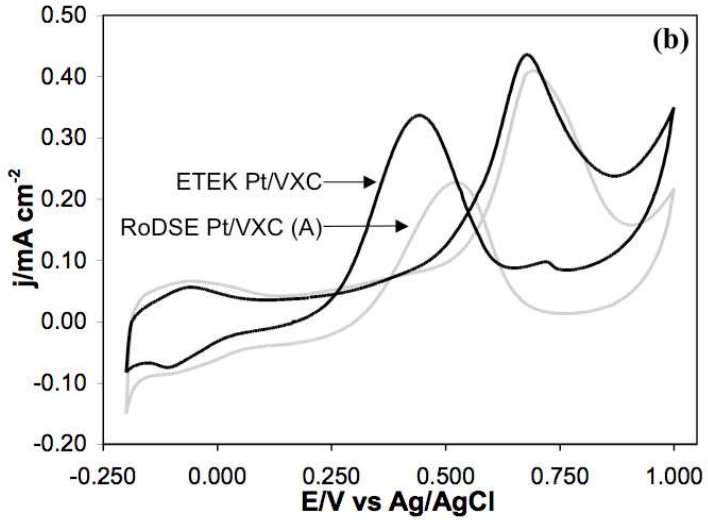

RoDSE Pt/VXC (A) and ETEK Pt/VXC catalysts (a) CV in 0.5 M H_2SO_4 at 50 mV s^{-1}, (b) 1 M CH_3OH / 0.5 M H_2SO_4 at 50 mV s^{-1}, and (c) CA of 1 h in 1 M CH_3OH / 0.5 M H_2SO_4 at 0.500 V vs. Ag/AgCl

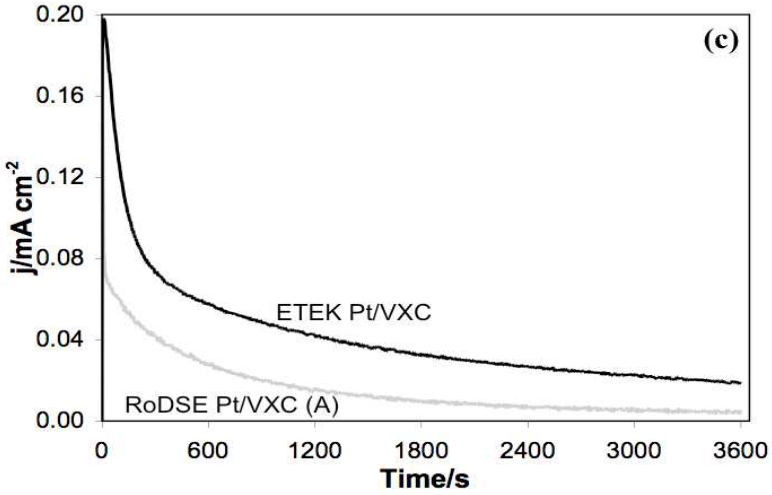

Self-assembled monolayers of L-cysteine on Pd electrodes

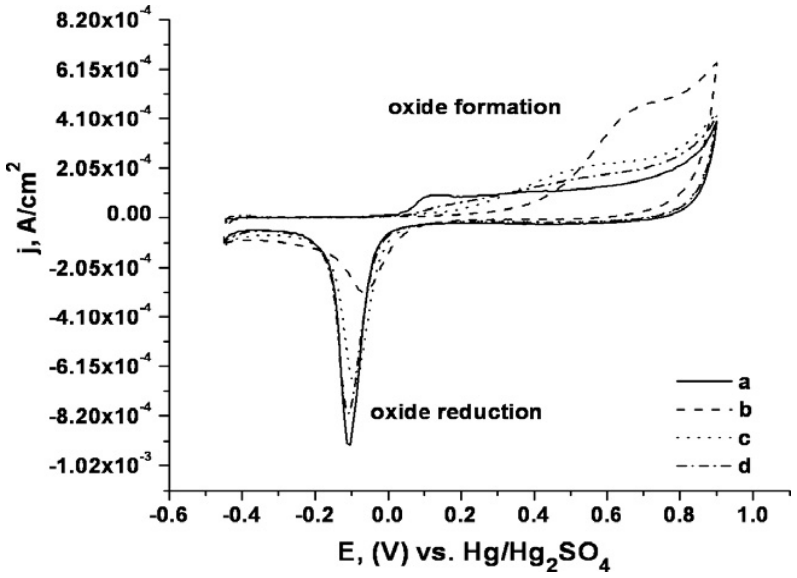

CV for bare Pd (a) and first (b) second (c) third cycle (d) to L-cysteine modified Pd in 0.1 M H2SO4 at 100 mV/s.

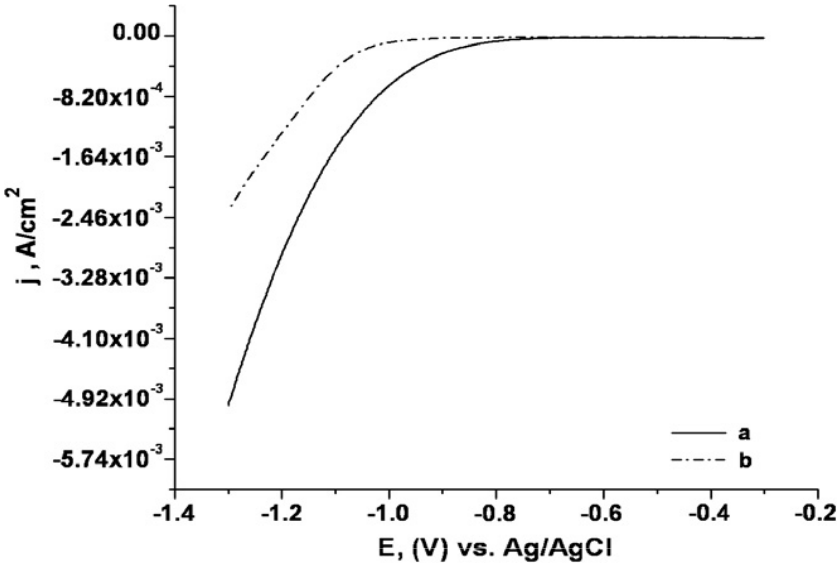

LSV for bare Pd(a) and L-cysteine modified Pd (b) in 0.1 M KOH at 20 mV/s, showing reductive desorption of L-cysteine monolayer on Pd electrode.

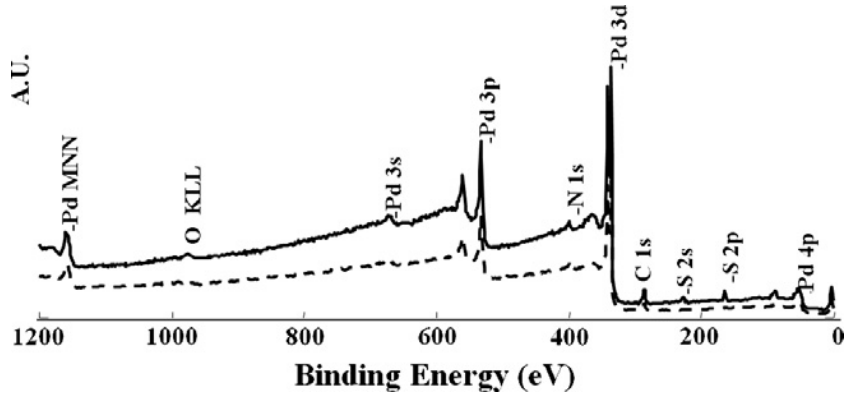

XPS for unmodified Pd surface (dash line) and L-cysteine modified Pd surface (solid line) after of a period of 24 h of immobilization.

Single-wall CNT chemical attachment at Pt electrodes

Raman Spectra

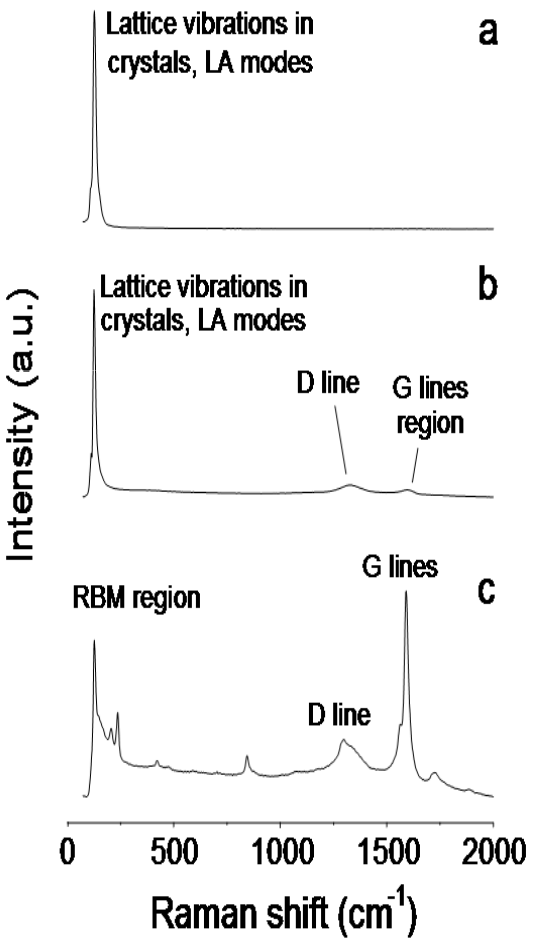

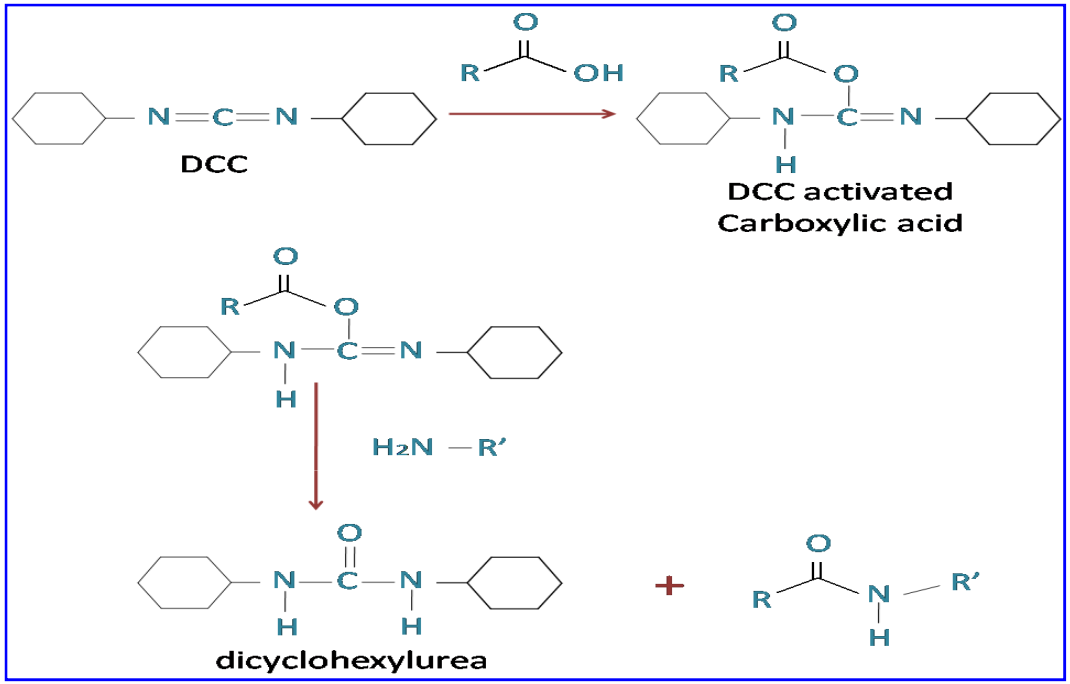

Sample	Crystal lattice vibration / cm^{-1}	RBM region / cm^{-1}	D line / cm^{-1}	G lines / cm^{-1}
Clean Pt	127	-	-	-
Ethanol / SWCNTs Pt	125	-	1330	1597
4-ATP/ SWCNTs Pt		100-300	1300	1561,1590

Appl. Surf. Science 257 (2010) 340–353

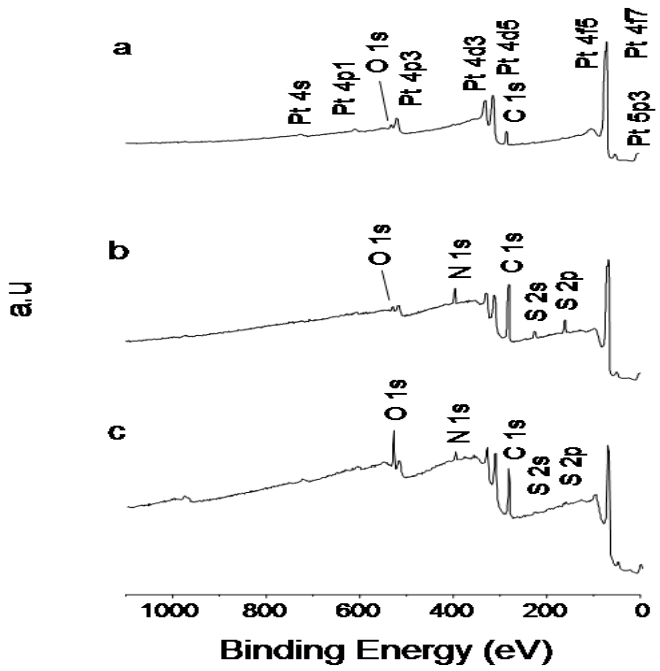

XPS of (a) a clean, (b) a 4-ATP modified (c) SWCNT modified Pt electrode

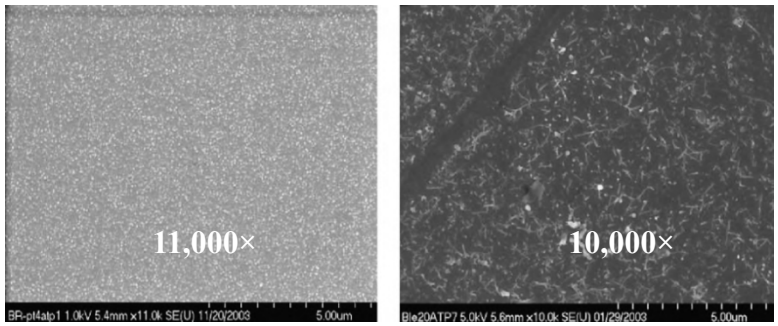

SEM - (a) 4-ATP modified Pt electrode (b) 4-ATP/SWCNT modified Pt electrode

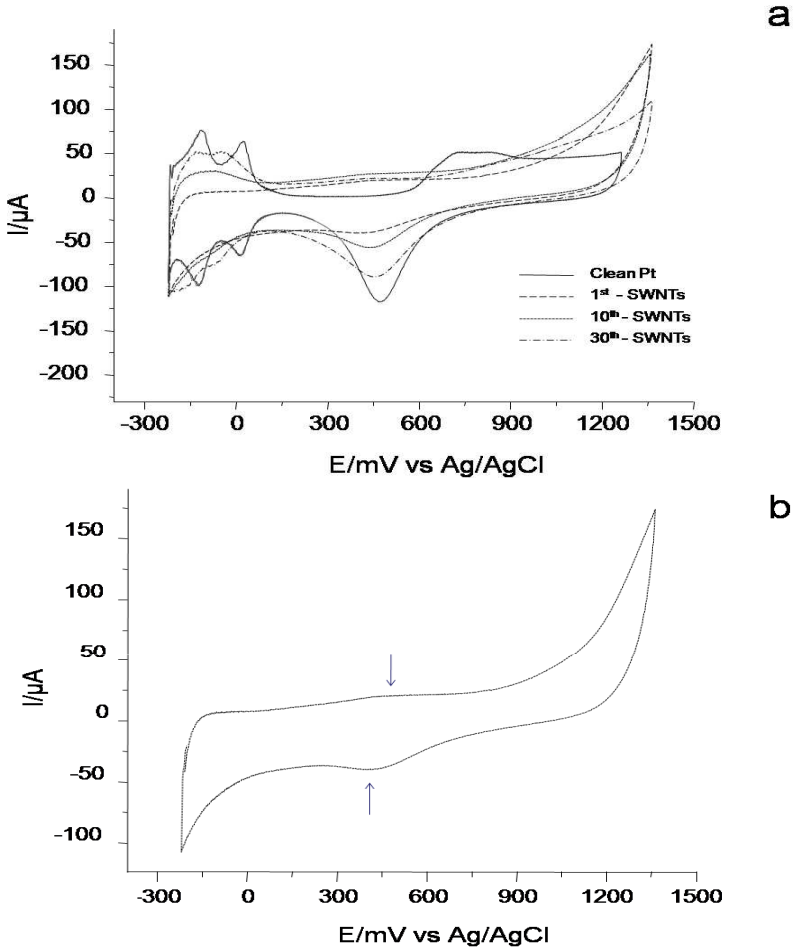

CV in H2SO4 0.5M (a) for (—) bare Pt electrode; (- - -) first (· · · · · · · · ·) tenth (-· -· -·) 30th cycles of 4-ATP/SWCNT modified Pt surface, (b) first cycle of 4-ATP/SWCNT modified Pt surface.

AFM

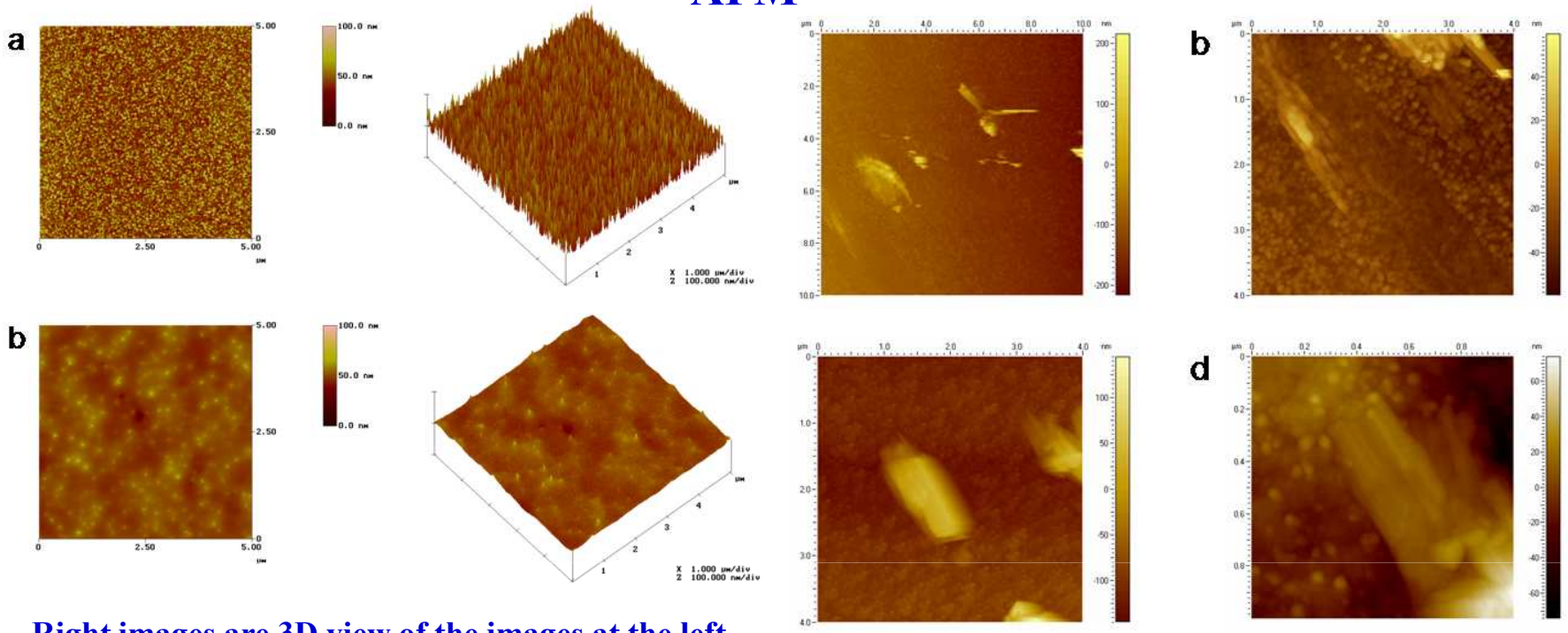

Right images are 3D view of the images at the left.

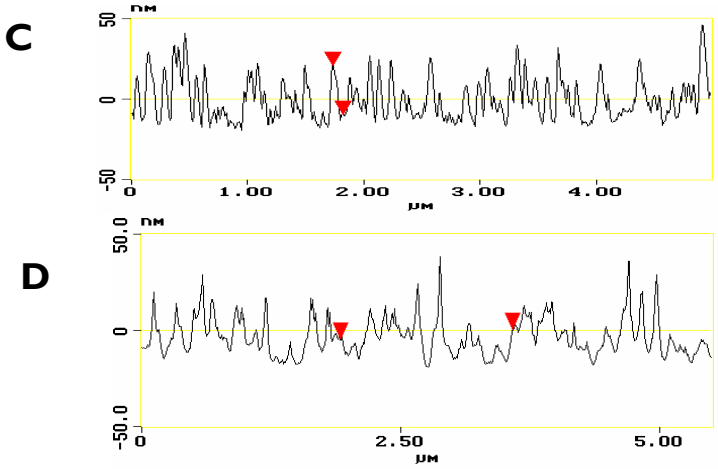

AFM for SWCNTs deposited over clean Pt electrodes from an ethanol suspension at scan size of (a) 10.0m (b and c) 4.0m, and (d) 1.0m.

AFM (a) bare (b) 4-ATP modified Pt.
Scan size : 5.00m & Z scale at 100 nm.
Cross-section analysis : (c) bare (d) 4-ATP modified Pt.

Energy Generation

Ideal Energy Cycle Involving Hydrogen

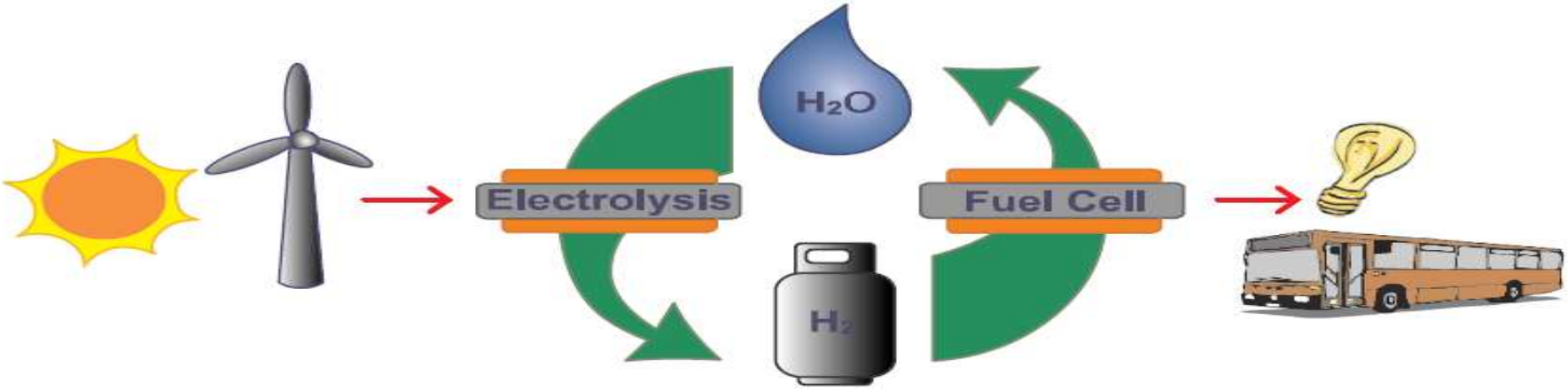

Regenerative fuel cell (RFC)

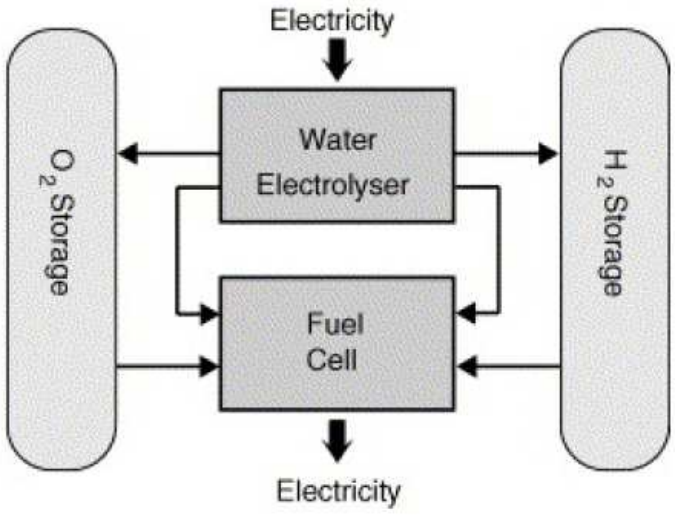

Unitised regenerative fuel cell (URFC)

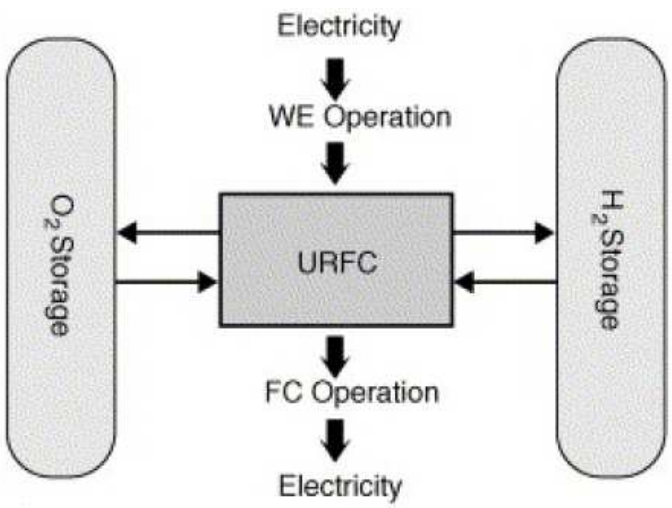

Water Electrolysis Using PEM – Relevance & Importance

Why Water Electrolysis?

- An obvious way of producing Hydrogen
- Water is plentiful & product hydroger is pure
- Most practical & efficient route
- Reaction is endothermic – Simplest way – Electrochemical splitting

Cathode: $4H^+ + e^- \rightarrow 2H_2$

Anode: $2H_2O \rightarrow O_2 + 4H^+ + e^-$

Total: $2H_2O \rightarrow O_2 + 2H_2$

PEM Electrolysis Cell

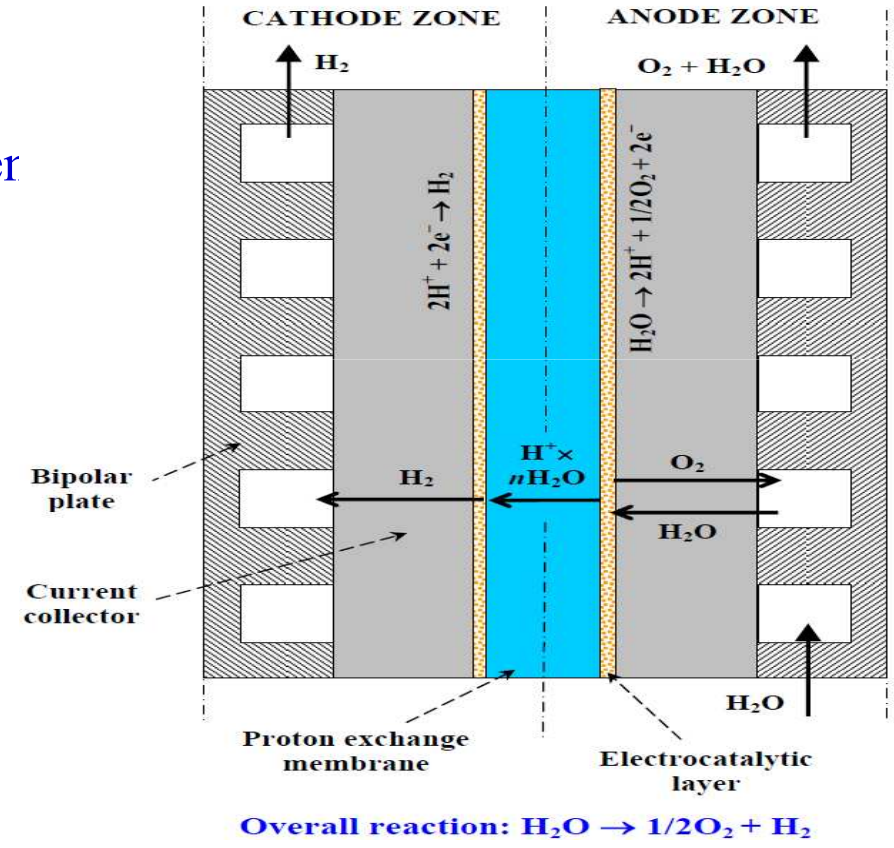

Inherent gas separation by membrane electrolyte

Ref: Deschamps et al, WHEC 16 / 13-16 June 2006 – Lyon France

Water Electrolysis – Associated Advantages

Advantages

- Environment – No carbon emissions
- Very pure hydrogen (no CO poisoning of fuel cell catalysts)
- Pure oxygen as a by-product
- No dependence on hydrocarbon sources
- *Scalable Architectures*
  Small scale / real time hydrogen supply is simple
- Utilises renewable primary energy sources
- Reduce / eliminate mechanical compression

Distributed Energy System Models

Ref: http://www.chewonkih2.org/docs/PEM%20vs%20Alkaline.pdf

Modern Water Electrolyzers – Types

• PEM - electrolyzer • Alkaline - electrolyzer • SOE - electrolyzer

PEM - electrolyzer

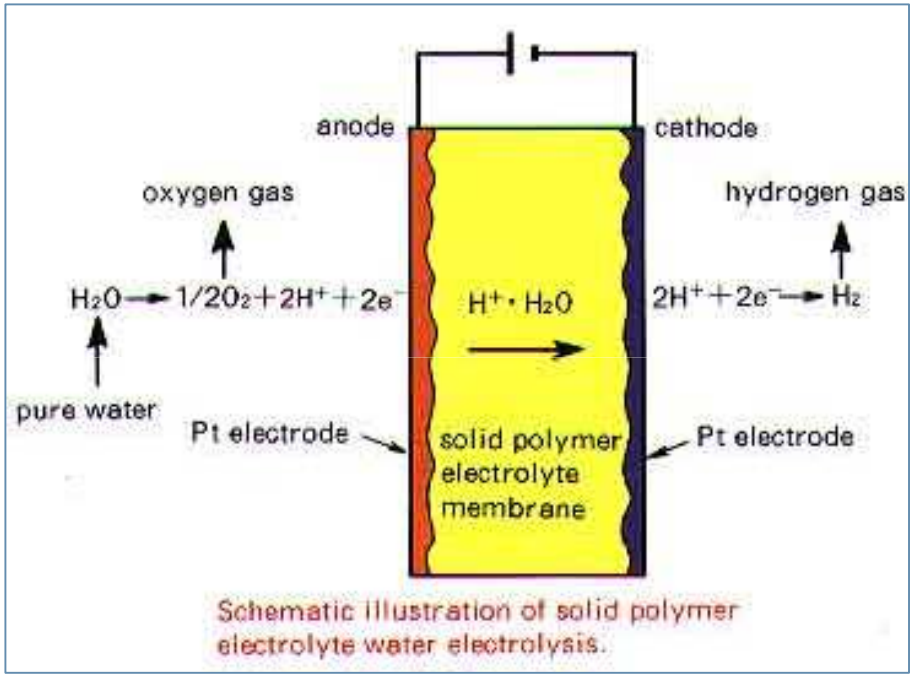

Schematic illustration of solid polymer electrolyte water electrolysis.

Proton conducting membrane: **s**olid **p**olymer **e**lectrolyte,
e.g. Nafion® (acidity ~20% sulfuric acid);
zero gap: electrodes attached to the membrane;
acid or de-ionized water
high-pressure operation (< 200 bar)

Alkaline- electrolyzer

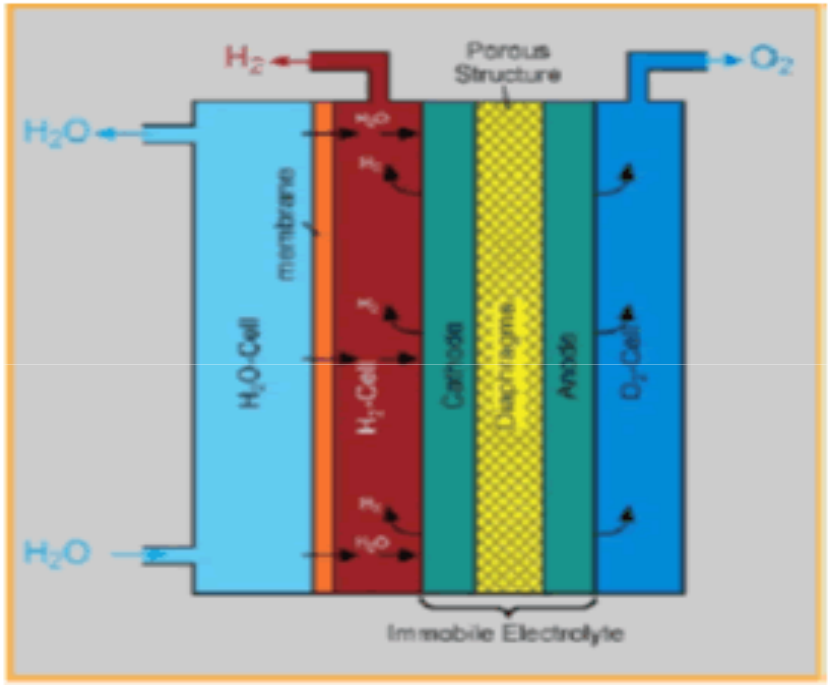

Diaphragm: NiO, polysulfone;
20 - 40% KOH;
high-pressure operation (7 - 30 bar)

PEM *Vs* Alkaline *Vs* High Temperature Water Electrolyzer

PEM electrolyzer	Alkaline electrolyzer	SOEC solid oxide electrolyzer cell
temperature: 70 – 80°C;	temperature: 70 – 90°C;	Diaphragm: yttria stabilized zirconia Y_2O_3 / ZrO_3 (YSZ);
current density: 600 – 1000 mA/cm^2	current density: 200 – 400 mA/cm^2	steam;
H_2-generation capacity:	H_2-generation capacity: 1 – 760 Nm^3/h	cathode: Ni/ZrO_2;
100 Nml/min – 10 Nm^3/h		anode: $LaMnO_3$;
electrical power: 100 W – 50 kW	electrical power: 5 kW – 3.4 MW	temperature: 850 – 1000°C;
still a matter of research	established technique	current density: 300 mA/cm^2

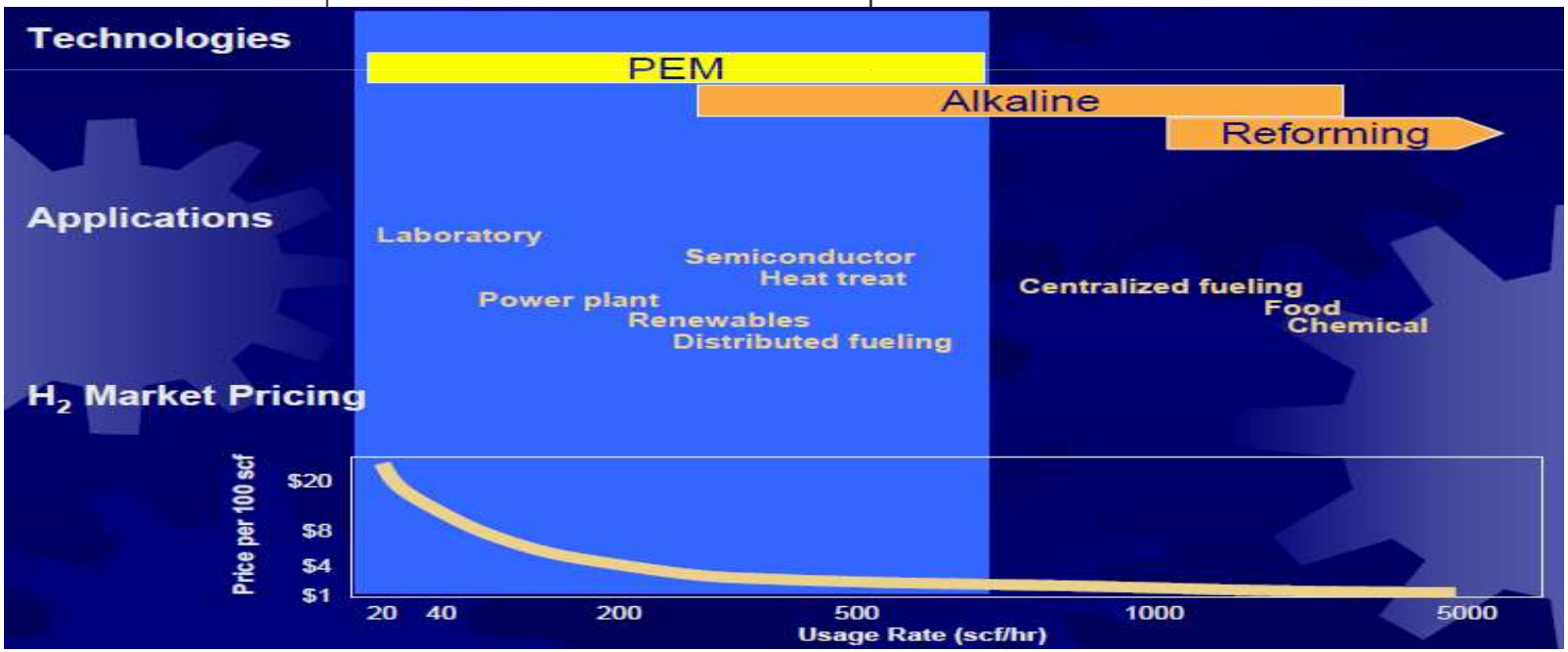

Ref: http://www.chewonkih2.org/docs/PEM%20vs%20Alkaline.pdf

PEM *Vs* Alkaline System Comparison

Characteristic	PEM Water Electrolysis	Alkaline Water Electrolysis
Stack Configuration/Cost	- More conducive to cost reduction through mass manufacturing techniques - Capable of very high current densities, stack can be highly compact with fewer cells - Capable of high differential pressure- safer design	- Alkaline environment generally allows for use of less costly materials, but not mass manufacturing - Typical current densities are low, limiting ability to reduce the package size. - Difficult to scale down in size
System Configuration/Cost	- Low pressure oxygen reduces material costs - Scaleable from 50 ccm up to 50 Nm^3/h -Ultra compact systems available	- Balanced pressure complicates system design - Limited ability to scale package size down -Nitrogen purge and explosion-proof fixtures may be required
System Reliability	- Proven for high-reliability life support in submarines - Proven in over 40,000 laboratory scale systems since 1980 -More than 400 HOGEN systems worldwide	-Proven commercial designs, relatively robust -Potential KOH contamination of piping

Ref: http://www.chewonkih2.org/docs/PEM%20vs%20Alkaline.pdf

PEM *Vs* Alkaline: Safety

Pressure

Characteristic	PEM Electrolysis **Differential Pressure**	Alkaline Electrolysis **Balanced Pressure**
Hydrogen/Oxygen Pressure	-Up to 3,000 psi differential pressure demonstrated -Hydrogen released safely via normally open valves at shutdown or power failure -Impossible for oxygen to enter hydrogen stream	- Very small differential pressure tolerated -Difficult to shut down safely. Requires special controls and backup power to avoid possible catastrophic rupture and mixture of H2 and O2 -Oxygen can flow into product hydrogen in failure mode.

Hazardous Materials

Characteristic	PEM Electrolysis	Alkaline Electrolysis
Hazardous materials	-NONE - System uses clean water only -No special safety equipment requirements -No hazardous waste -Surgical gloves required to keep contaminants from *entering* system	- KOH (potassium Hydroxide). -Extremely corrosive, especially at 60C operating temperature -May require eyewash station or full-body shower -Special hazardous waste disposal rules may apply -Special protective gear required for service

Ref: http://www.chewonkih2.org/docs/PEM%20vs%20Alkaline.pdf

Electrolysis of Water

Anode: $2H_2O \rightarrow O_2 + 4H^+ + e^-$

Cathode: $4H^+ + e^- \rightarrow 2H_2$

Total: $2H_2O \rightarrow O_2 + 2H_2$

Hydrogen Evolution Reaction HER

Mechanisms:

$M + H_3O^+ + e^- \rightarrow M\text{-}H_{ad} + H_2O$ Volmer reaction

$2\ M\text{-}H_{ad} \rightarrow 2\ M + H_2$ Tafel reaction

$M\text{-}H_{ad} + H_3O^+ + e^- \rightarrow M + H_2 + H_2O$ Heyrowsky reaction

M metal atom at the surface

Catalyst: Pt, Ni, steel

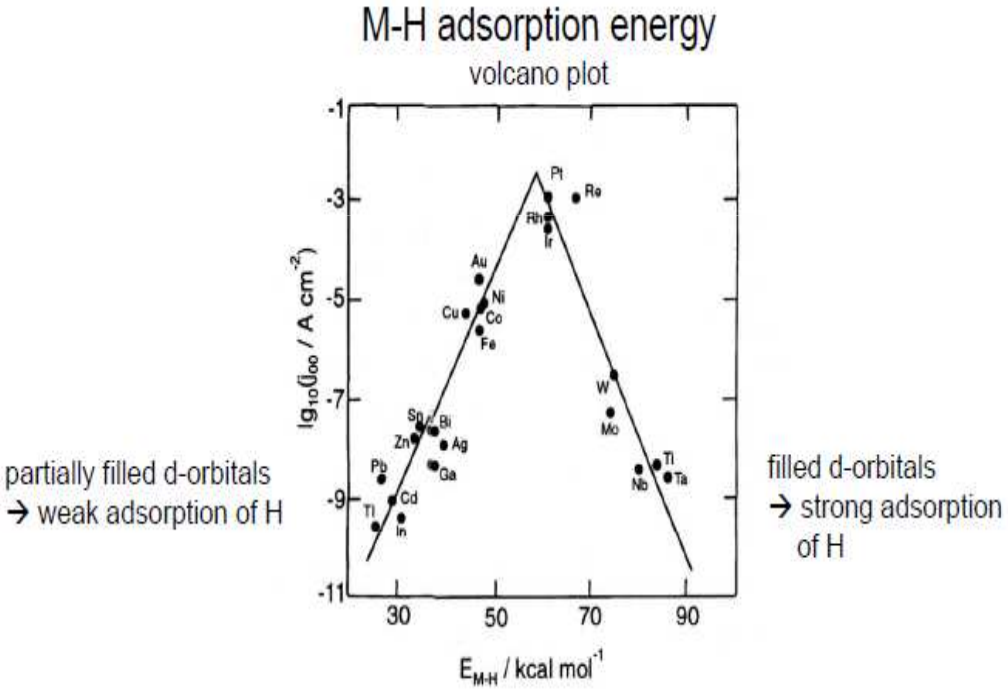

Oxygen Evolution Reaction OER

Mechanism

$4\ H_2O \rightarrow 4\ OH_{ad} + 4\ H^+ + 4\ e^-$

$4\ OH_{ad} \rightarrow 2\ H_2O + 2\ O_{ad}$

$2\ O_{ad} \rightarrow O_2$

Adsorption at metal oxide surface layer

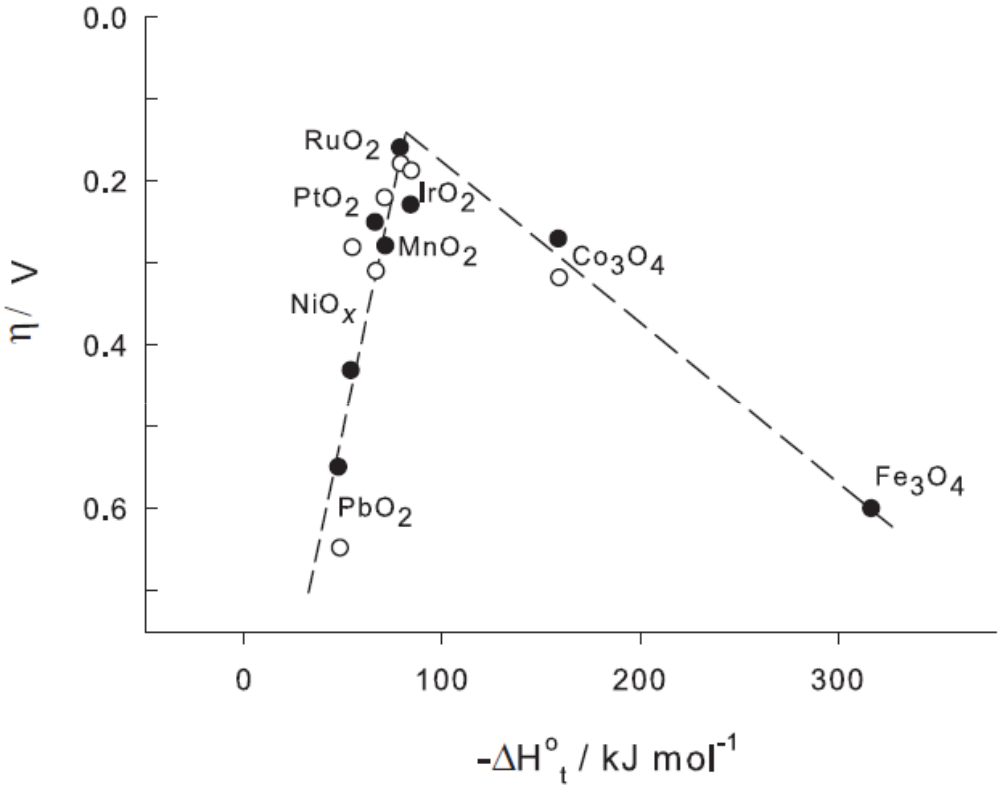

OER Electrocatalytic activity of various oxides
As a function of enthalpy of lower → higher
oxide transition in acid (o) & alkaline (•) solutions

Typical Parameters of HER & OER

HER (Pt; 1 M H_2SO_4) exchange current density: 10^{-3} A/cm^2

OER (Pt; 1 M H_2SO_4) exchange current density: 10^{-6} A/cm^2

HER (Ni; 1 mA/cm^2; 0.4 M NaOH) overpotential: 0.3 V

OER (Ni; 1 A/cm^2; 1 M KOH) overpotential: 1.05 V

The Oxygen electrode is the main factor related to energy efficiency

Critical Issues for Research

Hydrogen Cathode

- Pt is the natural choice. Very low over potential at low CDs
- Problems: decreased loading, lateral resistance is high at high CDs

Oxygen Anode

- Oxides of noble metals (Ir, Ru) mixed with non-noble metal oxides (Sn, Ti, Ta) based on knowledge from DSA- technology
- Problems: Catalytic activity, electrical conductivity and stability related to composition and loading

The Oxygen electrode is the main factor related to energy efficiency

We have given this part priority

Abundance of Elements of Catalytic Interests

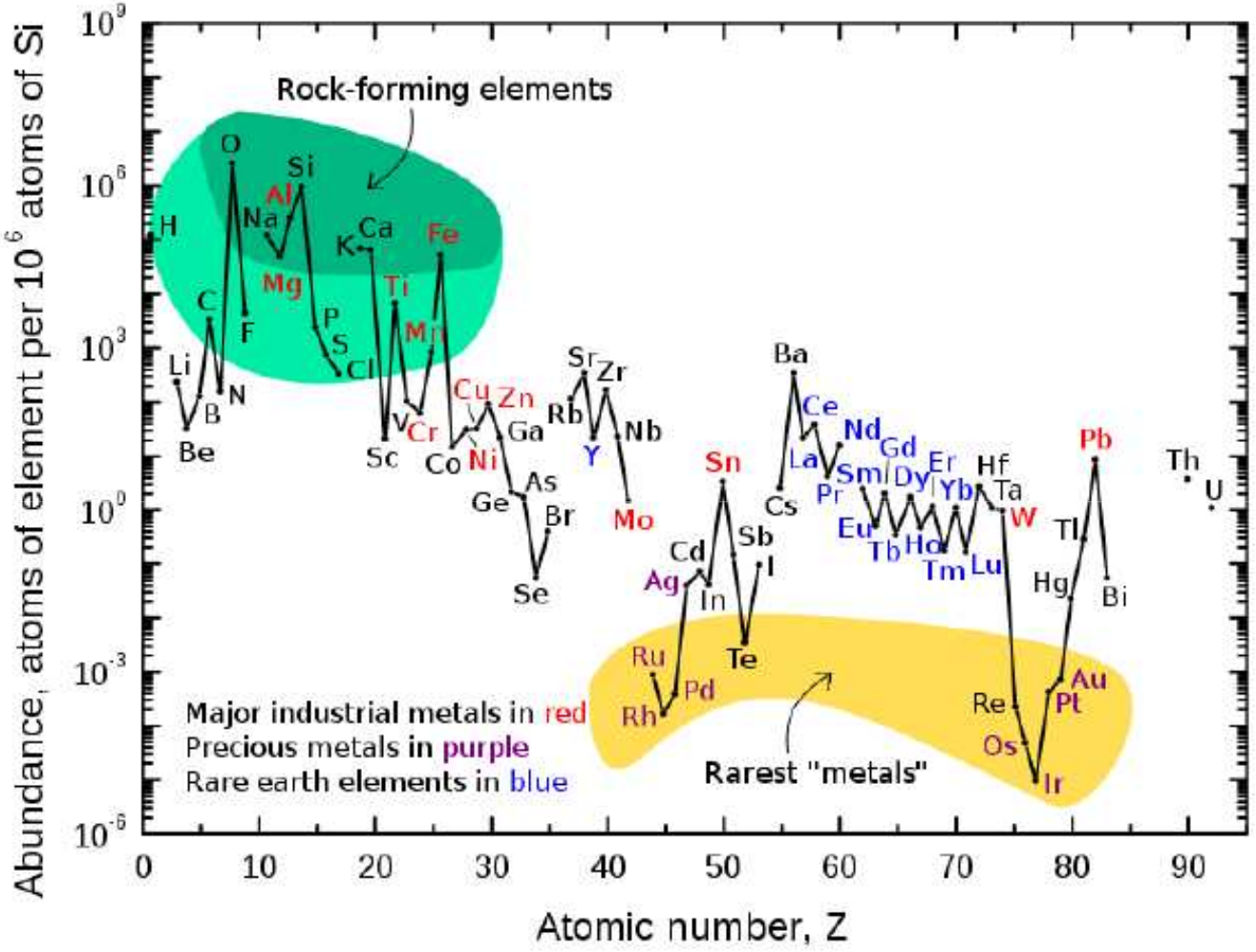

Pt-group metals (Pt, Ir, Pd, Rh, Ru) are expensive and limited in supply

Needs of Pt in Catalysis and Electrocatalysis

- *Demand in Heterogeneous Catalysis:*

  Pt catalysts are used in many chemical and refining processes

- *Demand in Emerging Clean Energy Technologies:*

  Pt electrocatalysts are required in low-temperature fuel cells, electrolyzers, and photoelectrochemical cells in significant amounts

- *Research Efforts in Solving "Pt Challenge":*

  I. Replace Pt with alternative materials with similar activity and stability
  II. Reduce loading of Pt using monolayer catalysts and electrocatalysts

Reduce Pt Loading with Monolayer (ML) Pt

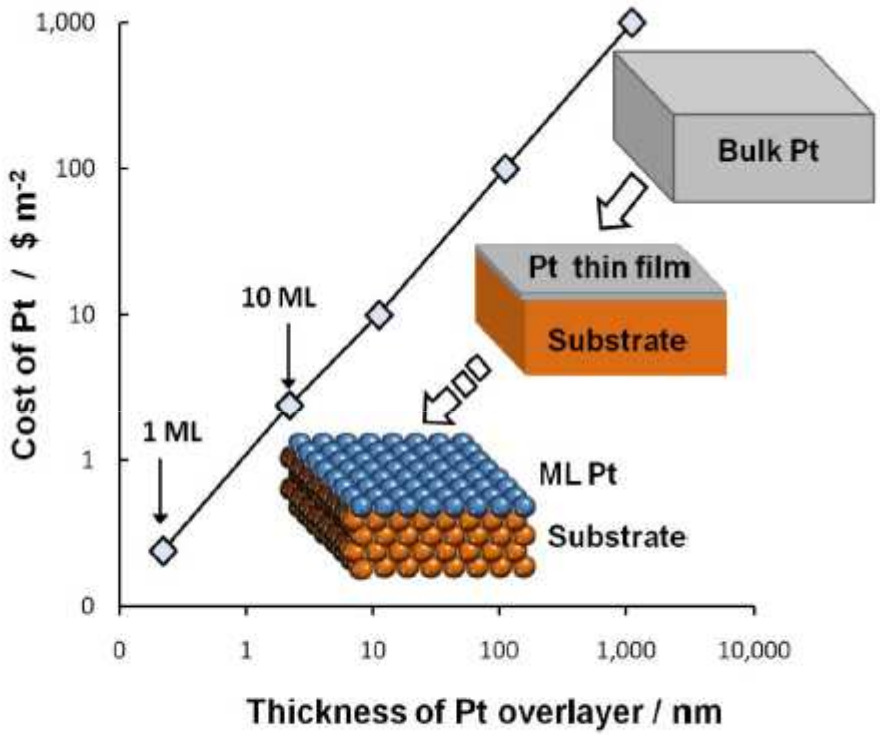

Challenge: Identify substrates with Pt-like bulk properties

Graphene - Mother of all graphitic forms

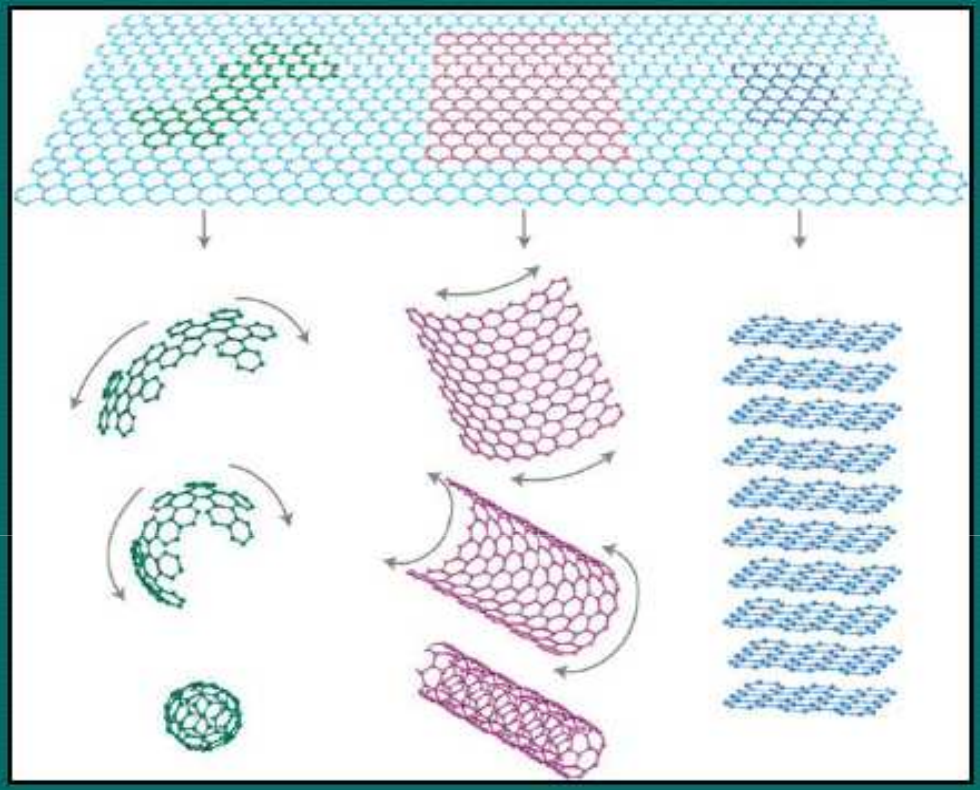

Graphitic family: 0-dimensional fullerene, 1-dimensional carbon nanotube, 2-dimensional graphene, 3-dimensional graphite

Courtesy: A. K. Geim and K. S. Novoselov, Nature Mater., 2007, 6, 183

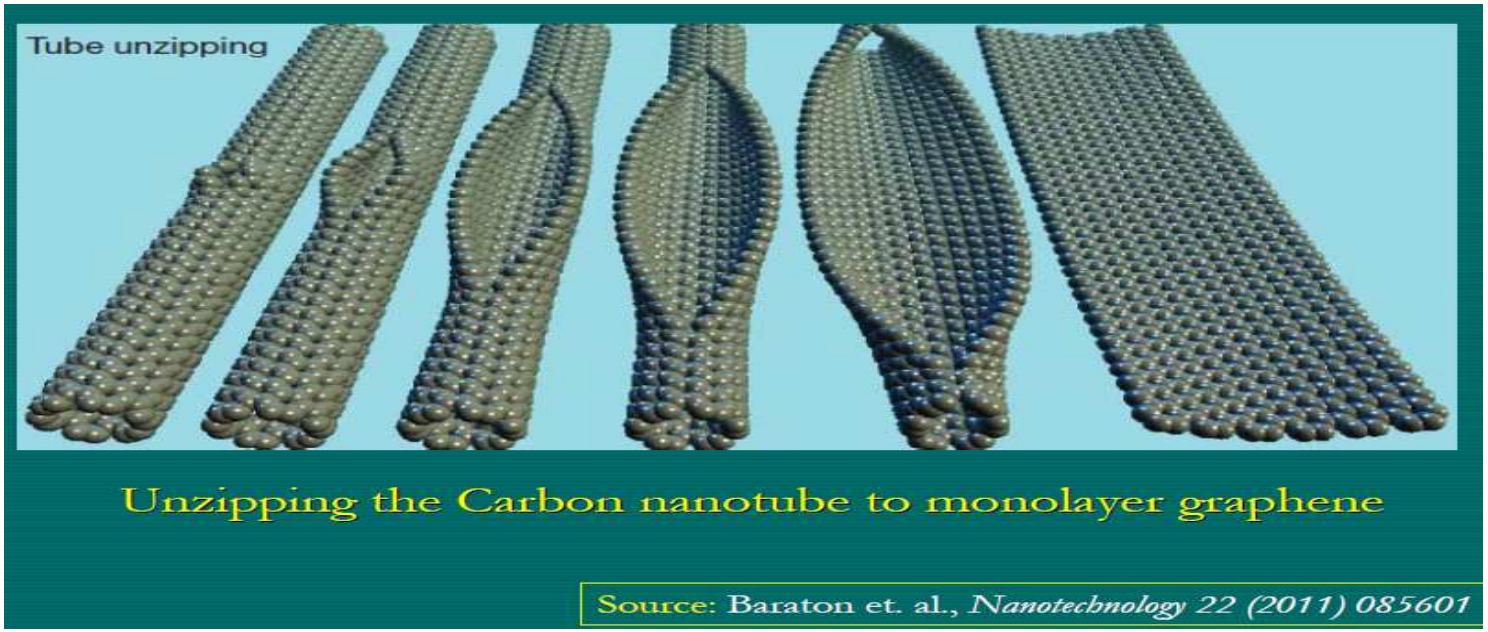
Tube unzipping
Unzipping the Carbon nanotube to monolayer graphene
Source: Baraton et. al., Nanotechnology 22 (2011) 085601

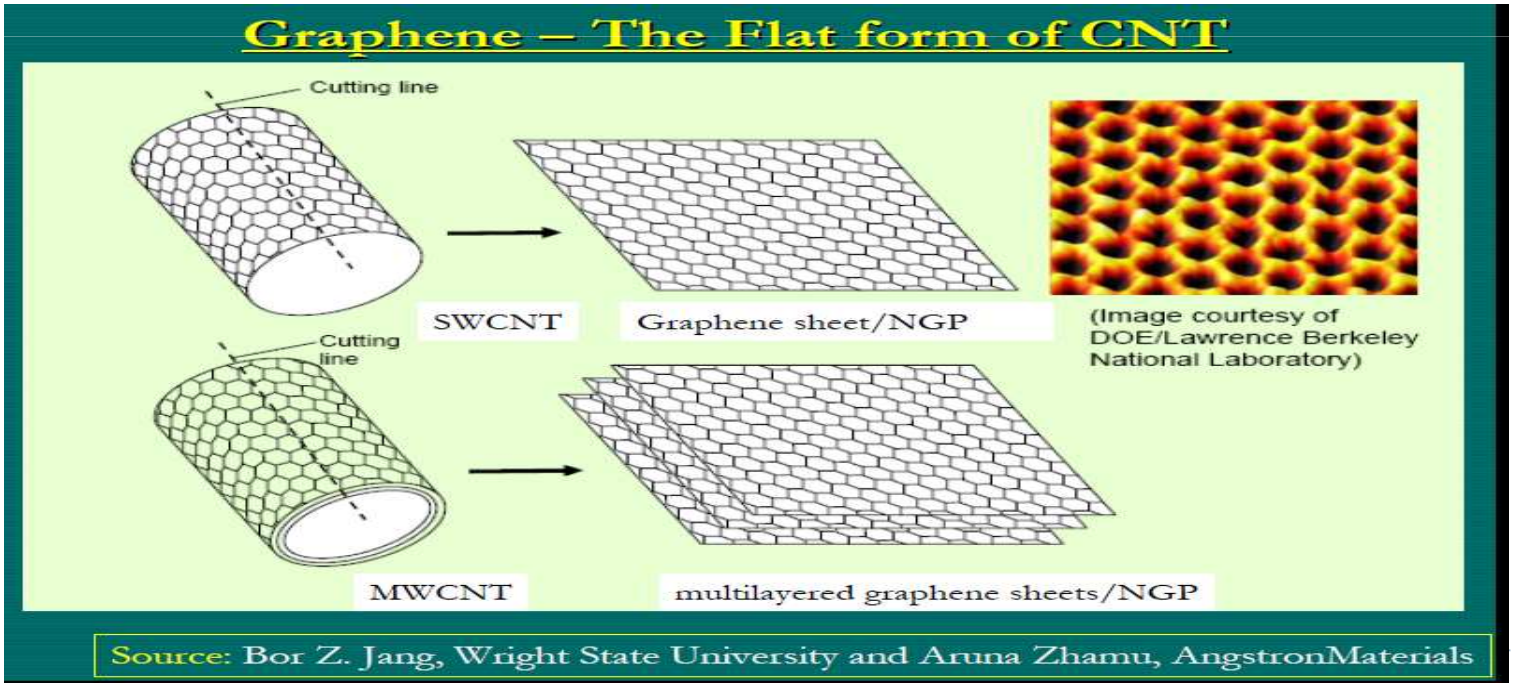
Graphene – The Flat form of CNT
Cutting line
SWCNT
Graphene sheet/NGP
(Image courtesy of DOE/Lawrence Berkeley National Laboratory)
Cutting line
MWCNT
multilayered graphene sheets/NGP
Source: Bor Z. Jang, Wright State University and Aruna Zhamu, AngstronMaterials

Characteristics of graphene

- ✓ thinnest possible material that is ever feasible
- ✓ Highest thermal conductivity (up to ~5,300 W/m-K), five times that of copper – faster thermal dissipation
- ✓ Electrical conductivity similar to Cu, yet its density is four time lower than Cu – lighter weight components
- ✓ Ultra-high Yong's modulus (approximately 1,000 GPa) and highest intrinsic strength (~130 GPa)
- ✓ High specific surface area (up to~ 2,675 m^2/g)
- ✓ Outstanding resistance to gas permeation
- ✓ ~200 times stronger than steel
- ✓ "It would take an elephant, balanced on a pencil, to break through a sheet of graphene the thickness of Saran Wrap." – *Researchers at Columbia University's Fu Foundation School of Engineering*
- ✓ Readily surface-functionalizable
- ✓ Dispersible in many polymers and solvents
- ✓ High loading in nanocomposites

Methods of preparing graphene

- Top-down approaches
  - ✓ scotch tape stripping
  - ✓ ion sputtering
  - ✓ pulsed laser deposition
  - ✓ ball milling
  - ✓ arc discharge
- Bottom-up approaches
  - ✓ chemical vapour deposition (CVD)
  - ✓ wet chemistry
  - ✓ ion implantation
  - ✓ pyrolysis

Exfoliation of graphite

- ✓ Chemical exfoliation
- ✓ Chemical and thermal exfoliation
- ✓ Electrochemical exfoliation
- ❖ These methods assume significance
  - ❖ ability to prepare graphene in large quantities
  - ❖ cost-effective

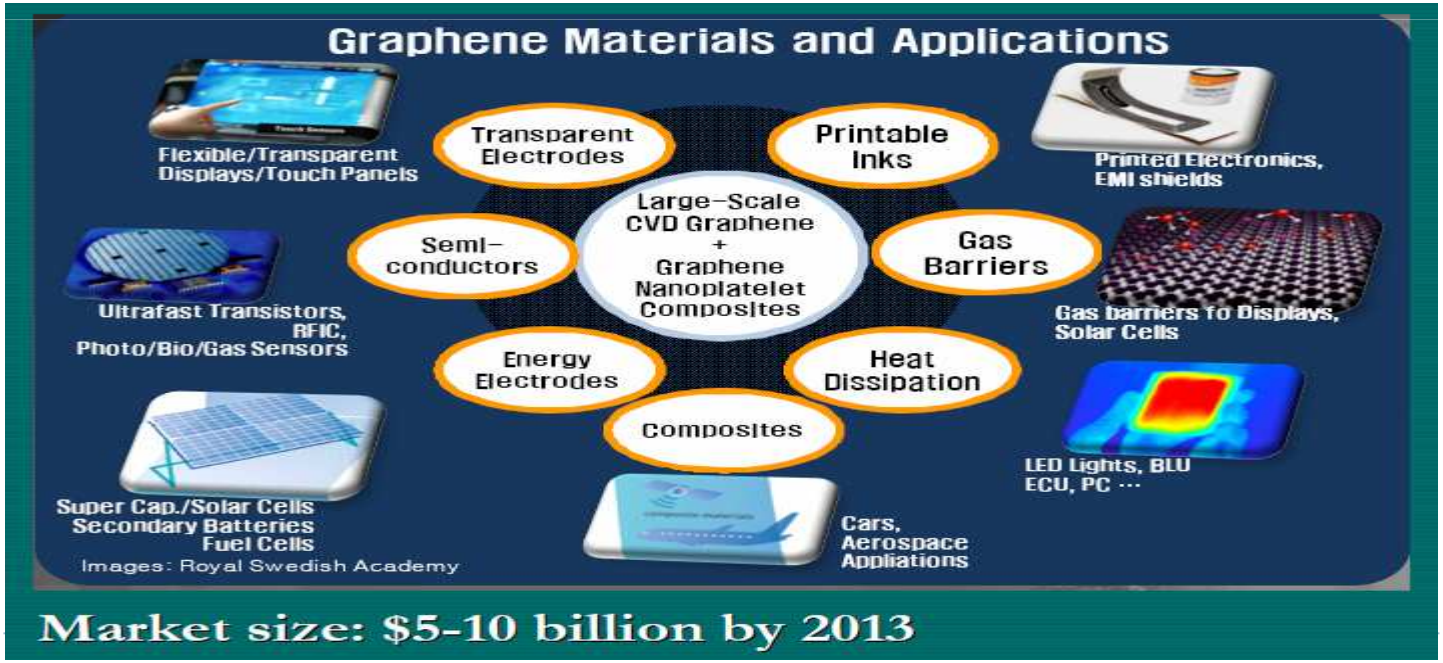

Role of graphene in fuel cells

- Graphene – good electrical conductivity and large specific surface area – how we can use it?

Schematic route for anchoring of Pt/Pt-Ru nanoparticles on graphene to prepare Pt/Pt-Ru-graphene nanocomposites

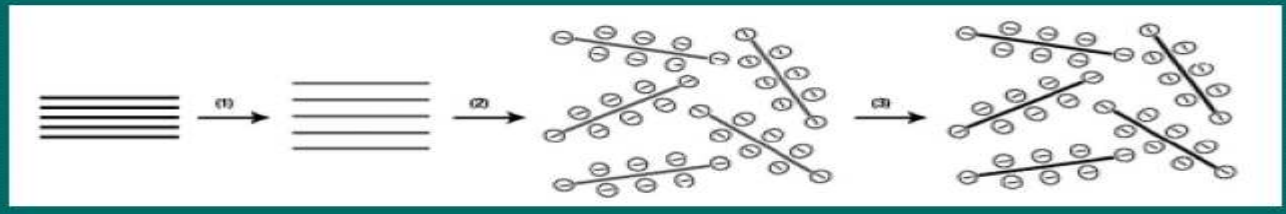

- Water-ethylene glycol is used as the medium
- oxidation of graphite to graphite oxide (GO);
- exfoliation of GO to graphene oxide sheets by sonication in water;
- attachment of Pt/Pt-Ru particles on the graphene oxide sheets;
- chemical reduction of graphene oxide sheets

Source: *Xu et al., J. Phys. Chem. C 112, (2008) 19841-19845*

- Nitrogen-doped graphene - metal-free electrode
  - Offers enhanced electro-catalytic activity
  - long-term operation stability
  - tolerance to crossover effect than Pt for ORR oxygen reduction via a four-electron pathway in alkaline solutions producing water as a product

Role of graphene in fuel cells

- In proton exchange membrane fuel cells (PEMFCs) Pt based electro-catalysts are widely used as anode and cathode electrocatalysts for hydrogen oxidation and for ORR, respectively.
- Graphene nanosheets (GNS) and nitrogen doped-GNSs can serve as the catalyst support for Pt nanoparticles for ORRs in PEMFCs.
- Nitrogen doping
  - creates defects, which could act as anchoring sites for the deposition of Pt nanoparticles
  - increase the electrical conductivity
  - improve carbon-catalyst binding

Gratefully Remembering…

Loyola College, India

University of Madras, India

CLRI, India

IITM, India

KIST, South Korea

NASA-URC, UPRRP, PR, USA

NC State University, USA


thank you!